Università degli Studi di Genova
SCUOLA POLITECNICA
DIME - sez. TEC

Doctoral School in Science and Technology for Engineering

RESEARCH DOCTORATE THESIS IN
MECHANICAL ENGINEERING

CURRICULUM FISICA TECNICA (XXVIII CICLO)
ING-IND 19 – Impianti Nucleari

In collaboration with

SCK•CEN
Belgian Nuclear Research Centre

"The MYRRHA reactor design and the Primary Heat Exchanger (PHX) tube rupture event analysis"

Ph.D candidate: Ing. Diego Castelliti

Tutor: Prof. Ing. Guglielmo Lomonaco
SCK•CEN advisor: Dr. Gert Van den Eynde

Genova, 23 Aprile 2018

Table of Contents

Abstract

Among the different nuclear plant concepts proposed in the frame of Generation IV, the pool-type reactors cooled by Heavy Liquid Metal represent one of the most promising options.

One of the most important challenges, form the point of view of design and safety, consists in optimizing an efficient and compact design. Such requirements often imply the adoption of a lower number of cooling loops in comparison with similar reactor concepts.

The intermediate loop can be eliminated by adopting a secondary fluid entering in a heat exchanger (or steam generator) located in the primary vessel. Pressurized water represents a common choice as secondary cooling fluid.

One of the most safety-relevant events for this reactor concept is indeed represented by the accidental water ingress in the primary vessel, which can trigger a series of consequences potentially jeopardizing the reactor safety functions. The study of this transient implies the analysis of multiphase flow, characterized by several phenomena on different time and spatial scales.

The MYRRHA reactor is a pool-type Material Testing Accelerator Driven System (ADS), cooled by Lead-Bismuth Eutectic (LBE) with the ability to operate also as a critical reactor. Pressurized water is adopted as secondary coolant, removing the power generated in the primary system through the Primary Heat Exchangers (PHX).

The Ph. D. activities should focus on the MYRRHA reactor design and the impact of a PHX Tube Rupture (PHXTR) event on its components: all the analyses foreseen and the experimental campaigns in support of calculations should be aimed at studying the transient in MYRRHA relevant configuration.

The theoretical analysis on the consequences following the moisture release into the primary vessel must be performed in MYRRHA-like conditions, assuming the correct dimensions for the PHX and all the related systems and components in order to be able to predict in the best way the PHXTR accident evolution.

The impact on the reactor internals and the mechanical loads determined by the pressure wave and potential steam explosion should be evaluated according to the real MYRRHA configuration, as well as the pressure build-up in the reactor cover gas and the consequent reactor cover rupture disk break.

The experimental campaign foreseen for MYRRHA PHXTR event, mainly in the framework of EU FP7-MAXSIMA project, have been run in a set of conditions that closely resembles the MYRRHA environment. The purpose is to validate the theoretical models and the numerical simulations towards the experiments in order to obtain suitable calculation tools allowing correct predictions.

The final purpose of the Ph.D. activities consists then in fully covering the evolution of the PHXTR accident in the MYRRHA reactor by the use of suitable and validated computational tools, taking thus into account all the evolution phases and predicting the potential implications caused by the event.

Sommario

Tra tutti i differenti concetti di reattori nucleari proposti nell'ambito della Generation IV, I reattori "pool-type" raffreddati a metallo liquido pesante rappresentano una delle opzioni più promettenti.

Uno dei principali obbiettivi, dal punto di vista progettuale e della sicurezza, consiste nell'ottenere un concetto efficiente e compatto. Tale requisito spesso implica l'adozione di un numero inferiore di circuiti refrigeranti rispetto ad altri reattori simili. La rimozione del circuito intermedio può essere ottenuta tramite l'adozione di un fluido secondario che entri direttamente nello scambiatore di calore (o generatore di vapore) situato nel vessel primario. Per quanto concerne il fluido secondario, una scelta comune è rappresentata dall'acqua in pressione.

Uno degli eventi più rilevanti dal punto di vista dell'analisi di sicurezza applicata a reattori di questa tipologia è rappresentato dall'ingresso accidentale di acqua nel vessel primario, che potrebbe scatenare una serie di conseguenze potenzialmente in grado di mettere a repentaglio la sicurezza del reattore. Lo studio di tale transitorio implica un'analisi multifase dei flussi, caratterizzata da svariate fenomenologie su diverse scale spaziali e temporali.

MYRRHA è un reattore di ricerca pool-type raffreddato da una lega eutettica di piombo e bismuto (LBE). Pur essendo un Accelerator Driven System (ADS), ha la capacità di operare in modalità critica. La potenza generata nel sistema di raffreddamento primario è trasferita, tramite lo Scambiatore di Calore Primario (PHX), nel sistema secondario, per il quale l'acqua in pressione è stata selezionata come refrigerante.

Le attività del Ph.D. si focalizzeranno sul progetto del reattore MYRRHA, con particolare riferimento al PHX. L'incidente di rottura di un tubo dello scambiatore stesso (PHXTR), con le conseguenze sugli altri componenti del reattore, sarà analizzato in una configurazione realistica del reattore tramite specifici modelli di calcolo ed attività sperimentali dedicate.

Le analisi teoriche sulle conseguenze del rilascio di una miscela bifase di acqua-vapore nel vessel primario devono essere eseguite in condizioni rappresentative del reattore MYRRHA: questo comporta una fedele modellazione, in termini geometrici e di processo, dello scambiatore e degli altri componenti, al fine di essere in grado di simulare l'evoluzione dell'incidente nel modo migliore possibile.

L'impatto sui componenti situati all'interno del vessel ed i carichi meccanici generati dall'incidente di rottura del tubo devono essere valutati in base alle reali condizioni d'impianto, così come l'incremento di pressione nel vessel e la conseguente apertura del disco di rottura.

Numerose campagne sperimentali finalizzate all'analisi della rottura di un tubo dello scambiatore primario sono previste nell'ambito del progetto Europeo FP7-MAXSIMA. Tali esperimenti sono stati concepiti per simulare le condizioni operative del reattore MYRRHA nel migliore dei modi, allo scopo di validare i modelli di calcolo. Tali simulazioni numeriche saranno poi utilizzate per estendere le capacità predittive degli esperimenti.

Lo scopo finale del Ph.D. consiste dunque nella finalizzazione del progetto dello scambiatore di calore del reattore MYRRHA, rivolgendo particolare attenzione allo studio dell'incidente di

rottura di un tubo. La programmazione di specifici strumenti di calcolo è prevista al fine di essere in grado di simulare tutte le fasi dell'incidente e le potenziali implicazioni per la sicurezza dell'impianto.

Samenvatting

In het onderzoek naar reactoren van generatie IV worden verschillende concepten voorgesteld. Reactoren van het "pool"-type gekoeld door zware metalen (Heavy Liquid Metal) behoren tot een van de meest belovende opties.

Een van de belangrijkste uitdagingen is het optimaliseren van een efficiënt, compact en veilig ontwerp voor de reactor. De eisen die daarmee gepaard gaan, kunnen bereikt met slechts twee koelsystemen, zonder een tussenlus (die bij Na-gekoelde reactoren gebruikelijk is). De warmtewisselaar (of stoomgenerator) bevindt zich in het reactorvat. Water onder druk is een veelgebruikte keuze als secundaire koelvloeistof.

Een van de meest veiligheidsrelevante gebeurtenissen voor dit reactorconcept is het plotseling binnendringen van water in het reactorvat door een lek of een breuk in de warmtewisselaar. De gevolgen van zo'n lek zouden de veiligheidsfuncties van de reactor in gevaar kunnen brengen. Een lek in een watersysteem op hoge temperatuur en onder druk geeft aanleiding tot faseveranderingen (verdamping). De meerfasestroming wordt gekenmerkt door verschijnselen op verschillende tijds- en ruimtelijke schalen.

De MYRRHA-reactor wordt aangedreven door een deeltjesversneller (Accelerator Driven System of ADS) en gekoeld door lood bismut-eutecticum (LBE). Ook is MYRRHA in staat om als een kritische reactor te werken. Water onder druk wordt gebruikt als secundair koelmiddel waarbij het vermogen, opgewekt in het primaire systeem, wordt afgevoerd door de primaire warmtewisselaars (PHX).

De doctoraatsactiviteiten zijn gericht op het ontwerp van de MYRRHA-reactor en het bepalen van de impact van een stoomgeneratorpijpbreuk (PHX Tube Rupture)(PHXTR) op de reactorcomponenten: alle geplande analyses en de experimentele campagnes ter ondersteuning van de berekeningen zijn gericht op het bestuderen van transienten in de MYRRHA reactor.

De theoretische analyse van de gevolgen van een waterlek in het reactorvat wordt uitgevoerd in MYRRHA-relevante omstandigheden, uitgaande van de juiste afmetingen voor de PHX en alle gerelateerde systemen en componenten om op de beste manier het verloop van het PHXTR ongeval te kunnen voorspellen.

De impact op de inwendige structuren van de reactor en de mechanische belastingen bepaald door de drukgolf en de potentiële stoomexplosie moeten worden beoordeeld volgens de echte MYRRHA-configuratie, evenals de drukopbouw in het gasvolume en de opening van de breekplaat in de reactordeksel.

De experimentele campagne voor het MYRRHA PHXTR ongeval, in het kader van EU FP7-MAXSIMA project, werden gedaan voor een reeks omstandigheden die sterk lijken op de MYRRHA configuratie. Het doel is om de theoretische modellen en de numerieke simulaties voor de experimenten te ontwikkelen en te valideren om zo correcte voorspellingen mogelijk te maken.

Het uiteindelijke doel van het doctoraat is een volledige beschrijving geven van het verloop van het PHXTR-ongeval in de MYRRHA-reactor met behulp van geschikte en gevalideerde computercodes, rekening houdend met alle fasen en het voorspellen van de potentiële implicaties veroorzaakt door de gebeurtenis.

List of Figures

List of Tables

Glossary of Abbreviations

ADS	Accelerator Driven System
ALFRED	Advanced Lead Fast Reactor European Demonstrator
BLEVE	Boiling-Liquid Expanding-Vapor Explosion
BoL	Beginning of Life
BR2	Belgian Reactor 2
CCI	Coolant Coolant Interaction
CDT	Central Design Team
CFD	Computational Fluid Dynamic
CHF	Critical Heat Flux
CIRCE	CIRCulation Experiment
DBC	Design Basis Condition
DHR	Decay Heat Removal
DWO	Density Wave Oscillations
ELSY	European Lead SYstem
EoL	End of Life
ERAER	European Research Area of Experimental Reactors
ESFRI	European Strategic Forum on Research Infrastructures
ESNII	European Sustainable Nuclear Industrial Initiative
ETPP	European Technology Pilot Plant
FA	Fuel Assembly
FANC	Federaal Agentschap voor Nucleaire Controle
FASTEF	FAst Spectrum Transmutation Experimental Facility
FCI	Fuel Coolant Interaction
GIF	Generation IV International Forum
HEM	Homogeneous Equilibrium Model
HFM	Homogeneous Frozen Model
HLLW	High Level Long-lived radioactive Waste
HLM	Heavy Liquid Metal
HLW	High Level Waste
HTC	Heat Transfer Coefficient
HX/SGTR	Heat eXchanger/Steam Generator Tube Rupture
HXTR	Heat eXchanger Tube Rupture
ILW	Intermediate Level Waste
IPS	In-Pile Section
IVFHM	In-Vessel Fuel Handling Machine
IVFS	In Vessel Fuel Storage

JHR	Jules Horowitz Reactor
KIT	Karlsruhe Institute of Technology
KTH	Kungliga Tekniska Hogskolan
LBE	Lead Bismuth Eutectic
LFR	Lead Fast Reactor
LLFP	Long-Lived Fission Products
LLW	Low Level Waste
LOCA	Loss Of Coolant Accident
LOOP	Loss Of Offsite Power
LWR	Light Water Reactor
MA	Minor Actinides
MAXSIMA	Methodology, Analysis and eXperiments for the "Safety In MYRRHA Assessment"
MOX	Mixed OXide
MTR	Material Testing Reactor
MYRRHA	Multi-purpose hYbrid Research Reactor for High-tech Applications
PCG	Primary Cover Gas
PCT	Peak Clad Temperature
PHX	Primary Heat eXchanger
PRS	Pressure Relief System
PVS	Primary Ventilation System
RV	Reactor Vessel
RVACS	Reactor Vessel Auxiliary Cooling System
SCK•CEN	StudieCentrum voor Kernenergie – Centre d'étude Energie Nucleaire
SCS	Secondary Cooling System
SFR	Sodium Fast Reactor
SGTR	Steam Generator Tube Rupture
SNE-TP	Sustainable Nuclear Energy - Technological Platform
SRA	Strategic Research Agenda
STCS	Secondary and Tertiary Cooling System
STH	System Thermal-Hydraulics
TALL	Thermal-hydraulic ADS Lead-bismuth Loop
TCS	Tertiary Cooling System
TRU	TRans-Uranic

Introduction

Since its creation in 1952, the Belgian Nuclear Research Centre (SCK•CEN) at Mol has always been heavily involved in the conception, the design, the realisation and the operation of large nuclear infrastructures. The Centre has even played a pioneering role in such type of infrastructures in Europe and worldwide. SCK•CEN has successfully operated these facilities at all times thanks to the high degree of qualification and competence of its personnel and by inserting these facilities in European and international research networks, contributing hence to the development of crucial aspects of nuclear energy at international level.

One of the flagships of the nuclear infrastructure of SCK•CEN is the BR2 reactor [I.1], a flexible irradiation facility known as a multipurpose materials testing reactor (MTR). This reactor is in operation since 1962 and has proven to be an excellent research tool, which has produced remarkable results for the international nuclear energy community in various fields such as material research for fission and fusion reactors, fuel research, reactor safety, reactor technology and for the production of radioisotopes for medical and industrial applications such as Silicium doping, Molybdenum irradiation. BR2 has been refurbished twice, (consisting of the replacement of the beryllium matrix and considerable safety improvements), in the beginning of the eighties and in the mid-nineties. The BR2 reactor is now licensed for operating until 2016 and the necessary refurbishment studies are on-going to allow BR2 to operate for another 10 years until 2026. However, seen the age of BR2, replacement of this major research facility by another facility to guarantee the uniqueness and scientific excellence of SCK•CEN for the long term is seen as mandatory. Therefore, the Belgian Nuclear Research Centre at Mol is working since several years at the pre- and conceptual design of a multi-purpose flexible irradiation facility that can replace BR2 MTR and that is innovative to support future oriented research projects needed to sustain the future of the research centre.

To determine the characteristics of this multi-purpose flexible irradiation facility, an analysis of the present day needs of the international community has been conducted in particular in the European Union.

At international level, there is a clear need to obtain a sustainable solution for the high level long-lived radioactive waste (HLLW) consisting of minor actinides (MA) namely Np, Am, Cm and long-lived fission products (LLFPs). These MA and LLFP stocks need to be managed in an appropriate way. Reprocessing of used fuel followed by geological disposal or direct geological disposal are today the envisaged solutions depending on national fuel cycle options and waste management policies. The required time scale for geological disposal exceeds the time span of profound historical knowledge and this creates problems of public acceptance. The Partitioning and Transmutation (P&T) concept has been pointed out in numerous studies in the past [I.2], [I.3], [I.4], more recently in the frame of the GEN IV initiative as the strategy that can relax the constraints on the geological disposal and that can reduce the monitoring period to technological and manageable time scales (from ~300000 years to ~300 years).

The reduction of the volume, heat-load and half-life of HLLW (thereby relaxing the constraints of geological repositories) can be achieved conceptually in two generic types of scenarios:

- A fleet of fast critical reactors that will simultaneously produce electricity and transmute the actinides. Finally, the only input should be natural or depleted uranium and the outputs will be electricity and the High Level Waste (HLW) and Intermediate Level Waste (ILW) including the fission fragments, activation products and actinide reprocessing losses. The MA can be homogeneously diluted within the whole fuel or heterogeneously in dedicated targets.
- A "double strata" reactors fleet. The first stratum will be a set of reactors dedicated to electricity production using "clean fuel" containing only U and Pu. The reactors in this stratum can be either present or future LWR or fast reactors. The second stratum will be devoted to transuranic waste TRU or MA transmutation and will be based on dedicated fast spectrum systems, special fast critical reactors or more probably, subcritical fast systems, typically Accelerator Driven Systems (ADS) loaded with homogeneous fuels with high MA content.

Even when considering the phase out of nuclear energy, the combination of P&T and dedicated burner technologies such as ADS (although at European regional scale) is needed to relax the constraints on the geological disposal and reduce the monitoring period to technological and manageable time scales for existing waste. Hence, since ADS represents a possible major component in the P&T framework, the demonstration of the sub-critical dedicated burner concept is needed. The need for a demonstration of the ADS concept in Europe was indicated in the EU vision document on the Strategic Research Agenda (SRA) [I.5].

Since 2000, the Generation International Forum (GIF) [I.6] has selected 6 Generation IV (GEN IV) concepts of which 3 are based on the fast spectrum technologies namely: the sodium fast reactor (SFR), the lead cooled fast reactor (LFR) and the gas cooled fast reactor (GFR). The SNE-TP community has at present given a higher priority to the SFR technology but indicated also the need for the development of an alternative coolant technology being lead or gas. The technological development of the fuel and materials of these concepts requires the availability of a flexible fast spectrum irradiation facility. The vision document and the Strategic Research Agenda (SRA) of the SNE-TP has also stated that Europe should be in a front-runner position for Gen IV reactor development. Indeed after the closure of PHENIX in 2009, there is no longer a fast spectrum reactor in Europe.

Taking into account these national, European and even worldwide needs in terms of demonstration and irradiation capabilities, SCK•CEN is proposing MYRRHA as a flexible fast spectrum irradiation facility able to operate in sub-critical and critical mode.

MYRRHA, as pool-type reactor cooled by HLM, will not be limited to demonstrate the ADS concept, but will be also able to play a major role in the roadmap for the development of the Lead Fast Reactor as the European Technology Pilot Plant (ETPP) as identified in the European Sustainable Nuclear Industrial Initiative (ESNII) [I.7].

True to its tradition, SCK•CEN is positioning MYRRHA within the European Research Area of Experimental Reactors (ERAER, see Figure 1). As stated in the SRA of SNE-TP [I.5], Europe will hold its worldwide leading position in the field of research reactor technology and its future development only if this community fosters its efforts towards the realisation of a European Research Infrastructure. The flexible irradiation capacity should be based on three pillars:

- Jules Horowitz Reactor (JHR) at Cadarache in France, of which the construction has been started in March 2007 in the frame of a European collaboration. JHR will be

answering the needs for industrial applications for GEN II & III in terms of structural material and fuel performance improvement as well as some generic GEN IV researches. JHR will also be acting as backup irradiation facility for radioisotopes production

- MYRRHA at Mol in Belgium, a flexible fast spectrum irradiation facility, operating as a sub-critical (accelerator driven) or critical system for material and fuel developments for GEN IV and fusion reactors and in a back-up role for radioisotopes production. Operation as an accelerator driven system allows to responding to the need expressed in the international community for an ADS demo at reasonable power level, demonstrating the ADS concept and the efficient transmutation of high-level nuclear waste (Minor Actinides). MYRRHA will also be able to contribute to the objectives of developing an alternative to the sodium fast rector technology due to its heavy liquid metal based coolant technology.
- PALLAS at Petten in The Netherlands, presently under design for securing the radioisotopes production for medical applications for Europe and as a complementary facility in support of the industrial needs for technological development for present and future reactors.

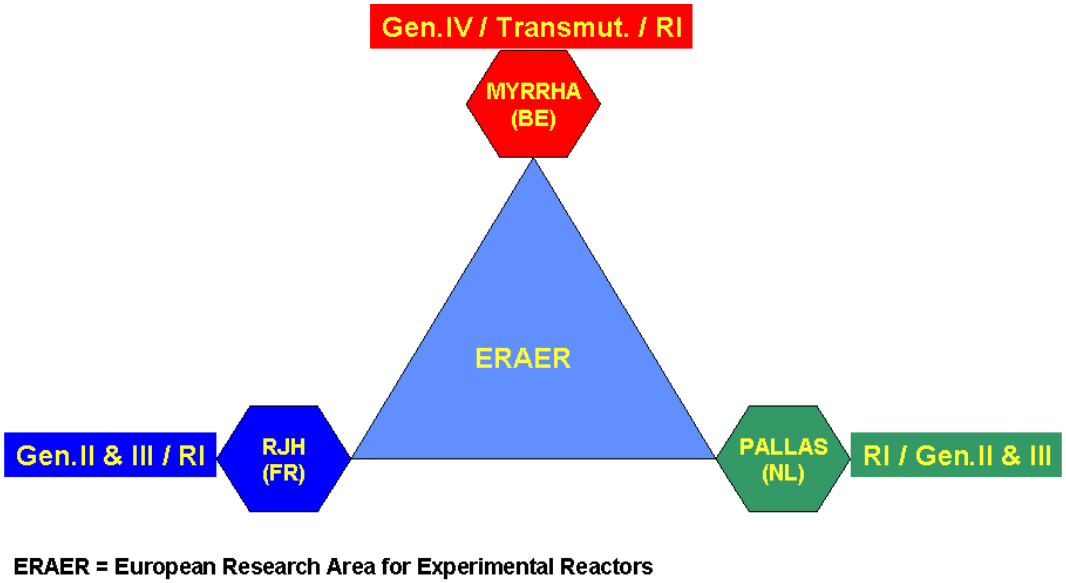

Figure I.1 - The position of MYRRHA in the ERAER

Based on the large innovative research opportunities offered by MYRRHA, it was recognised by the European community as a new large research infrastructure of major importance and top-ranked in the list of European Strategic Forum on Research Infrastructures (ESFRI) [I.8].

References

[I.1] "BR2 Reactor - Onderzoeksreactor met vele toepassingen," SCK•CEN, Mol, 2011.

[I.2] OECD/NEA, "Accelerator-driven Systems (ADS) and Fast Reactors (FR) in Advanced Nuclear Fuel Cycles, A Comparative Study," 2002.

[I.3] OECD/NEA, "Physics and Safety of Transmutation Systems, A Status Report," 2006.

[I.4] FP6-PATEROS, "Partitioning and Transmutation European Roadmap for Sustainable Nuclear Energy," [Online]. Available: http://www.sckcen.be/pateros/.

[I.5] EURATOM, "The Sustainable Nuclear Energy Technology Platform, a vision report," Directorate-General for Research, 2007.

[I.6] US-DOE, "A Technology Roadmap for Generation IV Nuclear Energy Systems," Nuclear Energy Research Advisory Committee, 2002.

[I.7] SNETP, "European Sustainable Nuclear Industrial Initiative (ESNII)," ESNII Task Force and SNETP Secretariat, October 2010.

[I.8] ESFRI, "European Strategic Forum on Research Infrastructure - Grant Agreement n° 654213," StR-ESFRI project, 2016.

Chapter 1: MYRRHA Overall Design Description

MYRRHA (Multi-purpose hYbrid Research Reactor for High-tech Applications) is a pool-type Material Testing Accelerator Driven System (ADS), cooled by Lead-Bismuth Eutectic (LBE) with the ability to operate also as a critical reactor.

MYRRHA plant main targets can be summarized as:

- Flexible fast-spectrum irradiation facility [1.1]
- Minor Actinides (MAs) transmutation demonstrator [1.2]
- ADS demonstrator [1.3]
- GEN-IV European Technology Pilot Plant (ETPP) in the roadmap for Lead Fast Reactor (LFR) [1.4]

The MYRRHA project has been recognized as a high priority infrastructure for nuclear research in Europe. Several European FP6 and FP7 projects had, as main target, to finalize a preliminary design of the MYRRHA reactor:

- FP6 IP-EUROTRANS [1.5], leading to the finalization of MYRRHA/XT-ADS version of MYRRHA in June 2008
- FP7 Central Design Team (CDT) [1.6], defining the MYRRHA/FASTEF version in March 2012
- FP7 MAXSIMA [1.7] (started in November 2012, ongoing), more focused on the MYRRHA safety analyses and component qualification

The outcome of these European FP projects has been partly used to define the latest version of the MYRRHA design, which has been finalized in June 2014 [1.8] and is currently in the verification phase. Though representing the current status, such version is not definitive: the MYRRHA design is still evolving taking into account results from the parallel R&D program.

SCK•CEN has actively participated in these FP6 and FP7 projects focusing on the safety analysis through use of system codes by performing code-to-code comparison of steady-state and transient calculations on the MYRRHA reactor operating in sub-critical and critical mode.

The LBE coolant presents the following advantages in comparison with other typical liquid metals used in nuclear applications:

- More operation flexibility (and limited problems towards primary coolant freezing) thanks to the low melting temperature of the eutectic (~125 °C), allowing:
    - operating a fast-spectrum irradiation facility with a relatively high core temperature difference without incurring in corrosion problems
    - Easier facility management for partial load operation or during long maintenance periods
- Low chemical interaction with water and air excluding the possibility for fire or explosions

A drawback connected with use of LBE as primary coolant is the accumulation of radioactive isotopes (mainly Po^{210}), which could pose difficulties during primary system maintenance or in case of accidental conditions in terms of radiological releases.

Further details on LBE properties are available in [1.9], [1.10].

The core and all the primary system internals are placed inside the Reactor Vessel filled with LBE until a free level interface with a cover gas layer. A general list of the main design features of the MYRRHA primary reactor system current design is provided in the [1.11].

Table 1.1 - MYRRHA main . The design status here presented is based on MYRRHA design revision 1.6 [1.8].

The MYRRHA plant is designed to operate in both sub-critical and critical operation modes to reach different purposes.

The MYRRHA plant is able to operate as an ADS sub-critical system as well as a critical reactor. In sub-critical mode (k_{eff} ~ 0.97) the chain reaction is sustained by a proton beam impinging, through a metallic window placed in the core center, into the LBE itself, thus generating neutrons through spallation reactions. Such feature is particularly interesting for the material irradiation and the Minor Actinides (MA) transmutation: the sub-critical mode is characterized by a particularly high neutron flux in the central core zone. Moreover, a $k_{eff} < 1$ provides additional control margin, especially useful in presence of MOX and/or MA fuel to avoid reactivity excursion transients.

Critical mode, on the other hand, is operated and controlled similarly to a “classical” power reactor.

No electrical power generation is foreseen: the power will be simply delivered to the external environment.

1.1 MYRRHA main design features

In [1.11].

Table 1.1 - MYRRHA main the most important MYRRHA design parameters are summarized together with some general dimensions [1.11].

Table 1.1 - MYRRHA main design parameters

General design parameters	Value
Maximum core power	100 MW_{th}
Reactor power	110 MW_{th}
Temperatures	
Shutdown state	200 °C
Maximum core inlet temperature	270 °C
Maximum average active core ΔT[1]	90 °C
Average core outlet temperature	360 °C
Maximum hot plenum temperature	325 °C
Maximum cladding temperature	466 °C
Fuel pin	
Fuel type	MOX, max. 30wt.% PuO_2
Fuel pin clad	15-15Ti
Fuel pin length	1400 mm
Fuel active height	65 cm
Fuel assembly	
Assembly type	Hexagonal fuel bundle with wrapper
Number of pins	127
Wrapper material	15-15Ti
Spacer type	Wire spacer in 15-15Ti
Assembly length	2536 mm
Assembly weight	58 kg
Maximum LBE bulk velocity	2 m/s
Core parameters	
Number of core positions	211
Core total mass flow rate	7710 kg/s
Core inlet temperature	270 °C
Core average outlet temperature	360 °C
Core peak outlet temperature	430 °C
Upper plenum temperature	325 °C
Core average temperature difference	90 °C
Core maximum temperature difference	187 °C
Plena temperature difference	55 °C
Core average linear power	112 W/cm
Core peak linear power	228 W/cm
Maximum core pressure drop	2.5 bar
Reactor vessel	
Internal diameter	10200 mm
Length	15960 mm
Thickness	110 mm
Weight	660 ton
Material	AISI 316L
Reactor diaphragm	
Material	AISI 316L

[1] Here only the active FAs are counted, excluding therefore the dummy FAs.

In-vessel fuel storage capacity	300 positions
Outer shell diameter	10000 mm
Height	11075 mm
Weight	320 ton
Primary heat exchangers	
Type	Tube-and-shell
Material	AISI 316L
Number of exchangers	4
Rated power	27.5 MW
Primary coolant fluid	Liquid LBE
Primary mass flow rate	3450 kg/s
Maximum primary fluid inlet temperature	325 °C
Maximum primary fluid outlet temperature	270 °C
Secondary coolant fluid	Saturated water/steam
Secondary mass flow rate	47 kg/s
Secondary coolant fluid pressure	16 bar
Secondary coolant fluid temperature	200 °C
External diameter	860 mm
Total Length	11720 mm
Weight	8.2 ton
Primary pumps	
Type	Axial flow pump
Material	AISI 316L
Number of pumps	2
Mass flow rate	6900 kg/s
Discharge head	3.0 m
External diameter	1400 mm
Length	12000 mm
Weight	45 ton
LBE inventory	~7600 ton

Figure 1.1 shows an overview of the reactor with its main components.

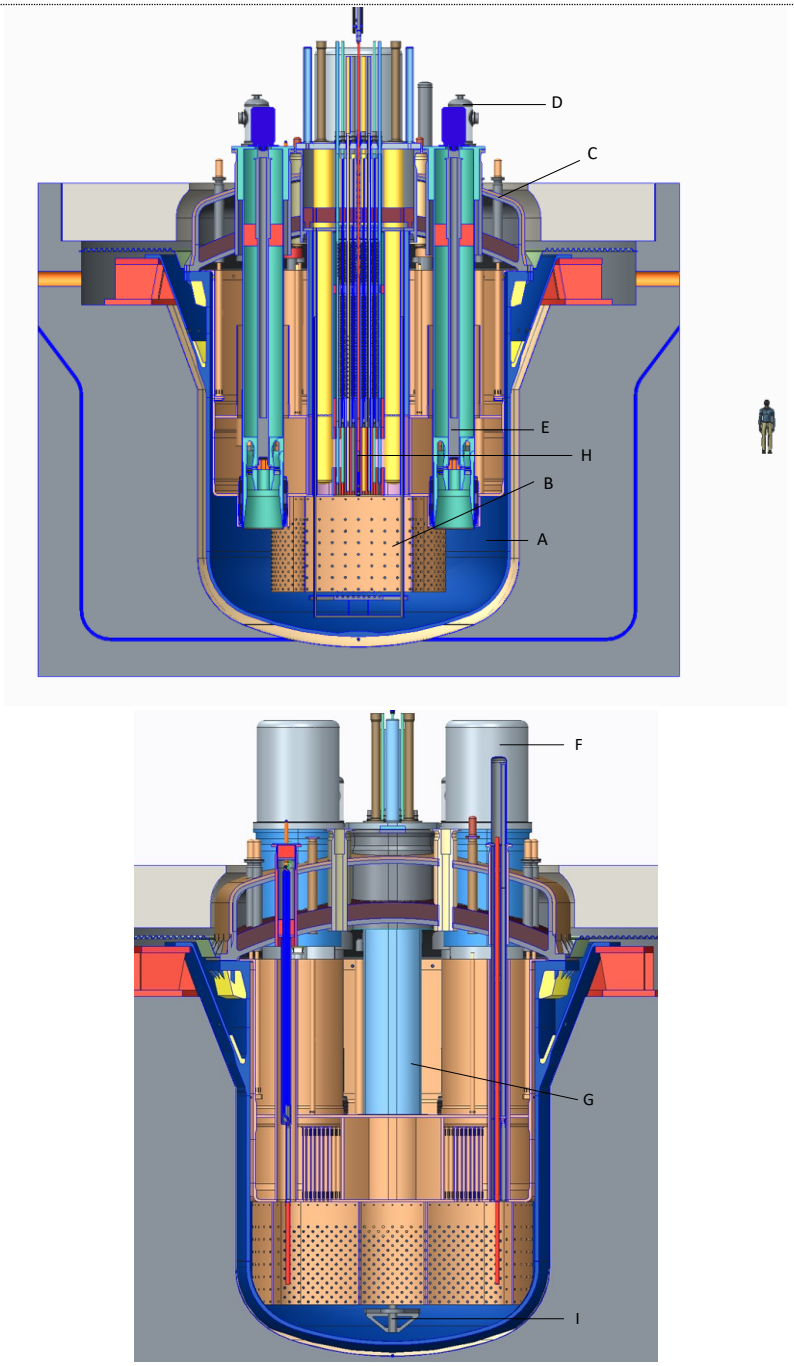

A. Reactor vessel
B. Diaphragm
C. Reactor Cover
D. Primary Heat Exchanger
E. Primary Pump
F. In-Vessel Fuel Handling Machine
G. Core Barrel
H. Reactor core
I. Core Restraint System

Figure 1.1 - Overview of the MYRRHA-FASTEF reactor

1.1.1 MYRRHA core configurations

To fulfill its purposes, the MYRRHA reactor is designed to operate in both critical and sub-critical mode. Two different reference core configurations have been defined, corresponding to the highest power ("maximum") core.

A section view of the MYRRHA core in critical mode is provided in Figure 1.2, while the sub-critical core is shown in Figure 1.3 [1.12].

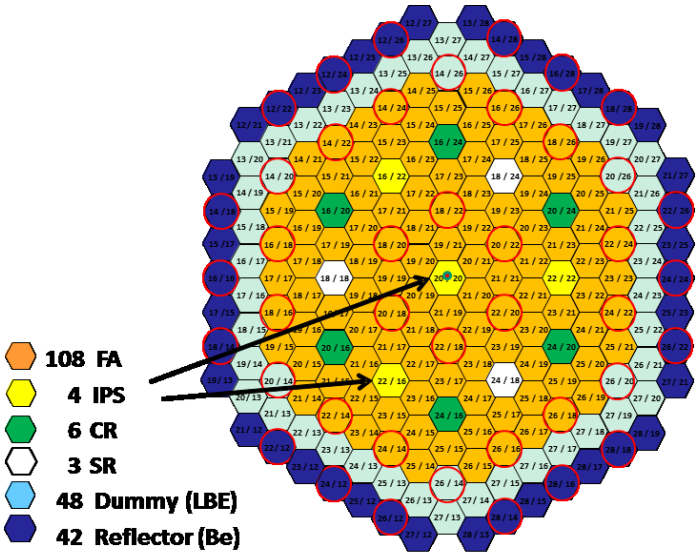

- 108 Fuel Assemblies (FA)
- 4 In Pile Sections (IPS)
- 6 Control Rods (CR) channels
- 3 Safety Rods (SR) channels
- 48 Inner Dummies (ID) channels
- 42 Outer Dummies (OD) channels

Figure 1.2 – Critical core section view

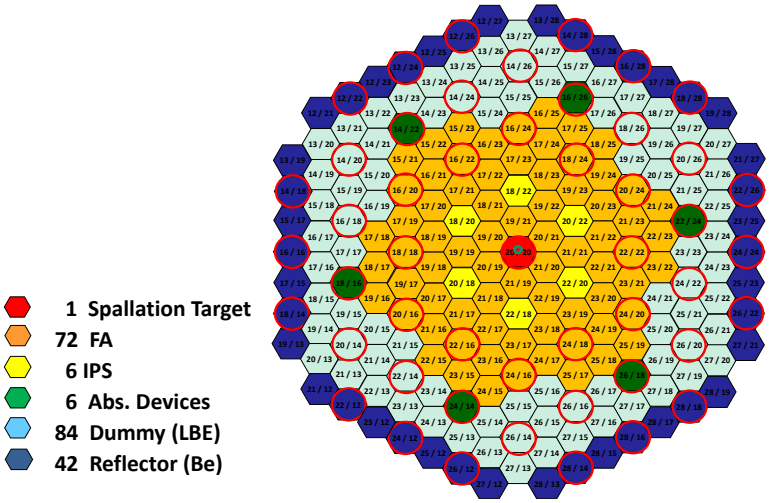

- 72 Fuel Assemblies (FA)
- 1 Spallation Target
- 6 In Pile Sections (IPS)
- 6 Control Rods (CR) channels
- 84 Inner Dummies (ID) channels
- 42 Outer Dummies (OD) channels

Figure 1.3 – Sub-critical core section view

The total number of core positions remains the same for both configurations (211), but the arrangement of core channels presents a series of differences (Table 1.2):

Table 1.2 – Main differences between operating modes

Parameter	Critical	Sub-critical
FA number	108	72
Spallation source	0	1
IPSs number	4	6
Control Rods number	6	6
Safety Rods number	3	0
Internal Dummy positions	48	84
External dummy position	42	42

The maximum power for the critical core is 100 MW_{th}, while the sub-critical core power is limited to 70 MW_{th}. This is justified by the need to maintain the Peak Clad Temperature (PCT) below a specific value (466 °C) to avoid corrosion issues on the pin clad: the clad temperature is function of the linear power, so the sub-critical mode, with less FAs, must reach a lower maximum power level to achieve approximately the same linear power value in both core configurations[2].

It is here important to remind how the power is not a direct requirement for the MYRRHA reactor, while the neutron flux is indeed important to fulfill the plant objectives. The two parameters are linked so that a higher power is reached through a higher flux, but the former is an integral measure, while the latter is defined in each core point. The important feature consists in achieving a high flux in specific core positions devoted to the material tests (In-Pile Sections), regardless of the total plant power.

The MYRRHA Fuel Assembly (FA) is shown in Figure 1.4. The FA is identical for both operating modes. It features 127 pins in hexagonal lattice. A wire spacer is adopted. An external hexagonal wrapper encloses the fuel pins and provides separation between the FAs to guarantee cooling and to provide rigidity to the core structure.

[2] Sub-critical configuration shows a slightly higher core power due to the lower LBE core inlet temperature. See Reactor Load Control for further details.

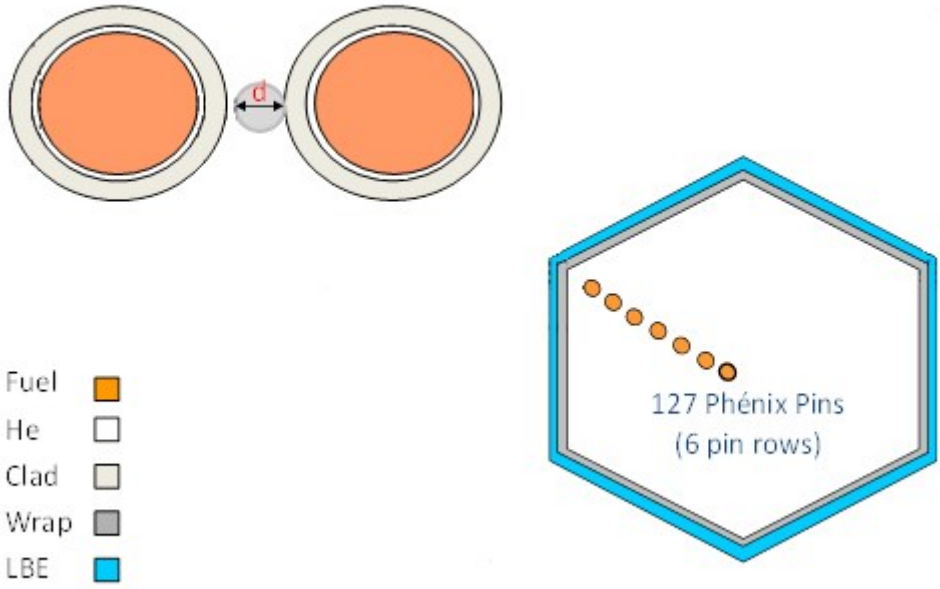

Figure 1.4 – MYRRHA Fuel Assembly overview [1.6]

A complete analysis of the flow distribution within the core channels has been conducted to finalize the Primary System thermal balance. Moreover, a deep study of the flow distribution within the single FA has been completed: the mass flow rate characterizing the different FA sub-channels (inner, edge, corner) [1.13] has been evaluated through specifically set analytical models. The complete set of results has then been confirmed with a RELAP5-3D code core model.

1.1.2 MYRRHA Primary System main components general description

An overview of the main MYRRHA Primary System components is provided as follows:

- The Reactor Vessel contains the primary coolant, LBE, and supports the Reactor Cover, which holds the internals. It guarantees the integrity of the Primary System as third confinement barrier. The Reactor Vessel is a welded structure without nozzles, made of a cylindrical shell with a torispherical bottom head. It is closed by the Reactor Cover. The Reactor Cover and Diaphragm are bolted with the Reactor Vessel. Due to the design pressure, a thickness of 110 mm has been chosen for the Reactor Vessel. Between the outer radius of the Diaphragm and the inner radius of the Reactor Vessel, a gap of 150 mm is foreseen.
- The Reactor Diaphragm separates the cold, high pressure LBE plenum from the hot, low pressure LBE plenum. The Diaphragm supports all the penetrations for the reactor internals (PHXs, Primary Pumps, IVFHMs) and hosts also the In-Vessel Fuel Storage (IVFS) guaranteeing for its cooling (safety-related function).
- The Core Barrel is a cylindrical tube of about 9 m long with 1.8 m diameter, located in the center of the reactor. It is secured with a flange inside the reactor cover and runs down vertically to the bottom of the diaphragm.

- Primary Pump (PP): two PPs are present in the primary vessel, each serving two PHXs, providing a nominal head of ~3 bar with a nominal mass flow rate of ~6900 kg/s.
- Primary Heat Exchanger (PHX): four PHX units are present in the primary vessel. Each PHX is coupled with a single Secondary Cooling System loop. The nominal primary LBE temperature difference in the PHX is 55 °C.
- IVFHM provides for the core and IVFSs loading and unloading. It operates by inserting the FAs from below and upwards, turning the LBE buoyancy force as an advantage.

The LBE inventory in the primary vessel has been estimated in ~740 m^3 (total weight: ~7600 ton). In detail, the "hot LBE" amounts to ~307 m^3, while the "cold LBE" total quantity is ~433 m^3.

In addition to the Primary System main components, two additional systems are relevant for the PHX Tube Rupture event evolution analysis:

- Primary Cover Gas System
- Pressure Relief System

1.1.2.1 Primary Cover Gas System

The reactor section above the LBE free level is filled with the inert gas nitrogen[3] (Volume ~240 m^3). This cover gas has to be conditioned and monitored for operational and safety reasons by a specially designed Primary Cover Gas conditioning (PCG) system in order to guarantee continuous and safe operation of the reactor. Besides the PCG system a Ventilation System (PVS) is required that minimizes spread of contamination in the reactor hall during opening of connections on the top of the reactor cover.

In order to meet the dynamic confinement requirements in normal operation and maintenance, the cover gas will be maintained at an underpressure with respect to the reactor hall (normally slightly below 1 bar). This minimizes reactor hall contamination by leakage of cover gas from the reactor to the reactor hall.

There are several operating modes for the reactor, which require two different confinement regimes [1.11] and, in turn, different PCG conditioning and behavior.

- The operating modes implying a "closed reactor" (refueling, shut down, start up and operation) have very high potential contamination levels within the reactor cover gas section. In these modes, the system is a completely sealed containment enclosure.
- In the operating modes with reactor cover open, the LBE temperature is much lower which results in less production and evaporation of contaminants. However, being the Primary System no more completely confined, the consequences of the PHX tube break can be more challenging in terms of radiological releases.

The cover gas can contain moisture originating from leakage of a PHX reactor cooler. Under normal operating conditions, the cover gas will be water free. For that reason, the moisture content of the cover gas from the reactor vessel is monitored as an indication of PHX leakage. It is expected the PCS to be the first system to provide a signal towards PHX tube

[3] The oxygen concentration during normal operation in the gas will be minimized to reduce LBE oxidation

rupture event. The signal itself could be generated by moisture detection in the nitrogen, or by pressurization of the cover gas.

The PCG will be installed for a major part in the primary containment (reactor hall or in dedicated compartments).

1.1.2.2 Pressure Relief System

A Pressure Relief System (PRS) is adopted to protect the Reactor Vessel from internal pressures above its design pressure caused by three (or less) simultaneous PHX tube ruptures.

In accidental conditions, the PRS shall:

- Dump the content of one SCS into suppression tanks in order to mitigate the effect of a DBC event
- Limit the Reactor Vessel pressure to its design pressure

The reactor cover is equipped with two specific nozzles connected to two rupture disks which are designed to burst when the reactor internal pressure reaches respectively 5 bar and 7 bar and to dump the steam following a Tube Rupture accident: this avoids an excessive reactor vessel pressurization, which could bring to mechanical failures.

The system relieves to an atmospheric suppression tanks collecting system. Following the burst of the 5 bar disk, the content of the failed SCS is dumped in the collection and suppression subsystem. The system is sized to condense 7.2 kg/s of superheated steam at 4 bar and 325 °C. These design data are based on preliminary and conservative estimations of water release rate and LBE-water heat transfer, which have been reviewed in this work.

When the reactor internal pressure reaches 7 bar, the second rupture disc bursts opening a free channel for the steam to flow into the reactor hall. Cover gas pressure is not supposed to rise beyond such value.

The PRS is composed by five different vessels in series where the moisture exiting the 5 bar rupture disk is dumped. The first vessel, defined “knock-out vessel”, serves the purpose of collecting the possible LBE droplets entrained in the steam flow. After this stage, the steam flows to the “suppression vessels”, a set of four (identical) vessels filled with water, which is heated up by the steam going through it while cooling down and condensate.

A bypass line between the SCS loops and the suppression vessels is foreseen to allow to dump the content of a loop directly to the suppression vessels without flowing through the reactor via the ruptured PHX tubes picking up radionuclides and contaminants. However, this bypass line is not considered in the following analyses, to estimate the most aggravating consequences of a PHX Tube Rupture event.

1.1.3 MYRRHA main process flow and thermal balance

The MYRRHA plant main process flow is here illustrated, together with the thermal balance at the maximum power (100 MW_{th}) in critical mode[4].

The cold LBE (270 °C) at high pressure flows from the reactor Lower Plenum through the Fuel Assemblies installed in the core unit. The fluid through the fuel assemblies (about 7710 kg/s) heats up to an average temperature of 360 °C. The remaining LBE (about 6090 kg/s) flows through the dummy channels and other core bypasses (CRs, SRs, IPSs, Inter-Wrapper Flow), removing much less power compared to the core flow, thus rising considerably less in temperature. The two streams, mixing in the Upper Plenum, will define the (average) Upper Plenum temperature[5]. This explains why the LBE temperature in the Upper Plenum (325 °C) is lower than the LBE temperature at the core outlet (360 °C). The pressure drop over the core amounts to ~ 2.5 bar.

An additional power input of 10 MW is considered due to heat sources such as the polonium decay, PP heat dissipation, IVFS heat production and the spallation power (for sub-critical mode only). This brings the plant design power at 110 MW. Such value is assumed as a reference for the design of the Primary Heat Exchanger and the Balance of Plant systems.

The temperature difference of 55 °C between the hot plenum and the cold plenum generates thermal stresses on the diaphragm, especially problematic for the flat plate; according to the construction code adopted [1.14], the stresses are below the maximum allowed.

After mixing in the Core Barrel and flowing through the Hot Plenum, the LBE enters the PHXs at 325 °C and exits at 270 °C, delivering the power to the Secondary Cooling System loops (27.5 MW per unit). The cold LBE flows then into the pump, which evacuates the LBE to the Lower Plenum, closing the loop. The pressure drop from the inlet of the heat exchanger to the inlet of the pump is estimated at 0.5 bar. Consequently, the PPs rated head is estimated as ~3 bar.

1.1.4 Balance of Plant

The functional requirement of the Balance of Plant systems consists in removing the power from the Primary System and deliver it to the external environment. Such function is accomplished through two different systems:

- Secondary Cooling System (SCS)
- Tertiary Cooling System (TCS)

Four identical and independent STCS loops are foreseen.

[4] Sub-critical mode thermal balance is qualitatively similar. Further specifications can be found in [11].

[5] This definition represents a simplification: in a large plenum of a pool-type reactor, especially when two streams are mixing, the identification of a single temperature value is not possible; it is indeed necessary to evaluate the correct temperature distribution. However, it has been shown through CFD simulations how, for the reactor thermal balance, this definition still holds a reasonable accuracy.

The Primary System is linked to the four SCSs through the four PHX units. Each SCS is divided in two sub-loops (Figure 1.5):

- First sub-loop connecting PHX with the Steam Separator
- Second sub-loop connecting the Steam Separator with the Aero-Condenser

The SCS first sub-loop is operated with a two-phase water mixture at 16 bar (~200 °C), in forced circulation: the water enters the PHX in almost saturated conditions and exits with a quality ~0.3[6]. The two-phase moisture is then separated in a Steam Separator, from where the vapor phase is directed towards an Aero-Condenser (second sub-loop, operated in natural circulation) while the liquid phase is recirculated to the PHX through the Feedwater Pump.

The value of 16 bar (and, consequently, 200 °C) represents a compromise between the need to maintain a reasonable margin towards the LBE freezing temperature (~125 °C) and to avoid unnecessary high pressure value, not required for the MYRRHA applications because no turbine expansion is foreseen. Moreover, a lower SCS pressure mitigates the consequences of the PHX Tube Rupture: the pressure wave released in the reactor primary vessel by the expansion of lower pressure steam are easier to withstand.

The power is then released to the external environment through the TCS Aero-Condenser, where the saturated steam is condensed and then recirculated into the Steam Separator. Each TCS includes six air fans (in parallel) whose rotational velocity is logically connected to the Steam Separator pressure for power removal balance (see Reactor Load Control).

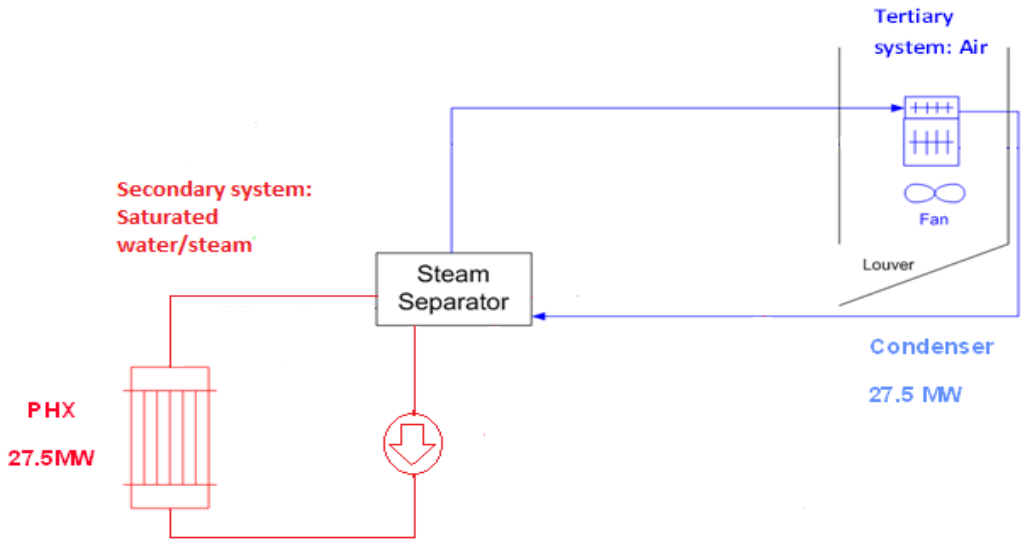

Figure 1.5 - Secondary Cooling System (single loop) schematic concept.

The Primary System is located in the reactor hall, acting as primary containment (Volume ~15000 m^3). The Steam Separator is located outside the reactor hall to avoid excessive pressurization in case of SCS line break. Isolation valves are placed on the lines passing through the containment walls (riser line bringing the water-steam mixture to Steam

[6] At full power conditions; partial loads result in lower steam quality.

Separator and recirculation line through the Feedwater Pump), similarly to PWR common practice.

The TCS Aero-Condensers chimneys are placed on the reactor building roof, conveniently separated to limit common cause failure.

1.2 Reactor Power Load Control: analysis and definition

The MYRRHA application catalogue, based on the reactor being a material testing and demonstration plant and emphasizing the correct functioning of the In-Pile Sections (IPSs), requires the primary system to be flexible with respect to the operation power and by this to be able to vary thermal-hydraulic conditions. The system must be able to operate at different power levels in compatibility with performances needed. To meet the irradiation performance needs, however, differently from power reactors, it is possible to vary the primary system thermal-hydraulic conditions without any major consequence on these performances.

Hence, the reactor control, no more bound to preserve fixed thermal-hydraulic conditions in the primary vessel, can be designed in order to achieve better operational and safety requirements.

The MYRRHA reactor power program adopted follows the following logic:

- Primary mass flow rate is kept constant in any condition
- Secondary mass flow rate is also kept constant in any condition
- SCS pressure and temperature are always kept constant, in any core power load conditions:
    - Water pressure: 16 bar in the PHX lowest point
    - Water temperature: ~200 °C (saturation temperature or slight subcooling degree)
- Primary system temperatures may vary, according to the core power, between 200 °C (shutdown temperature) and the nominal temperatures at maximum power
- Secondary water PHX outlet quality also varying in function of core power

Figure 1.6 shows the temperature variation in function of the core power at every power level.

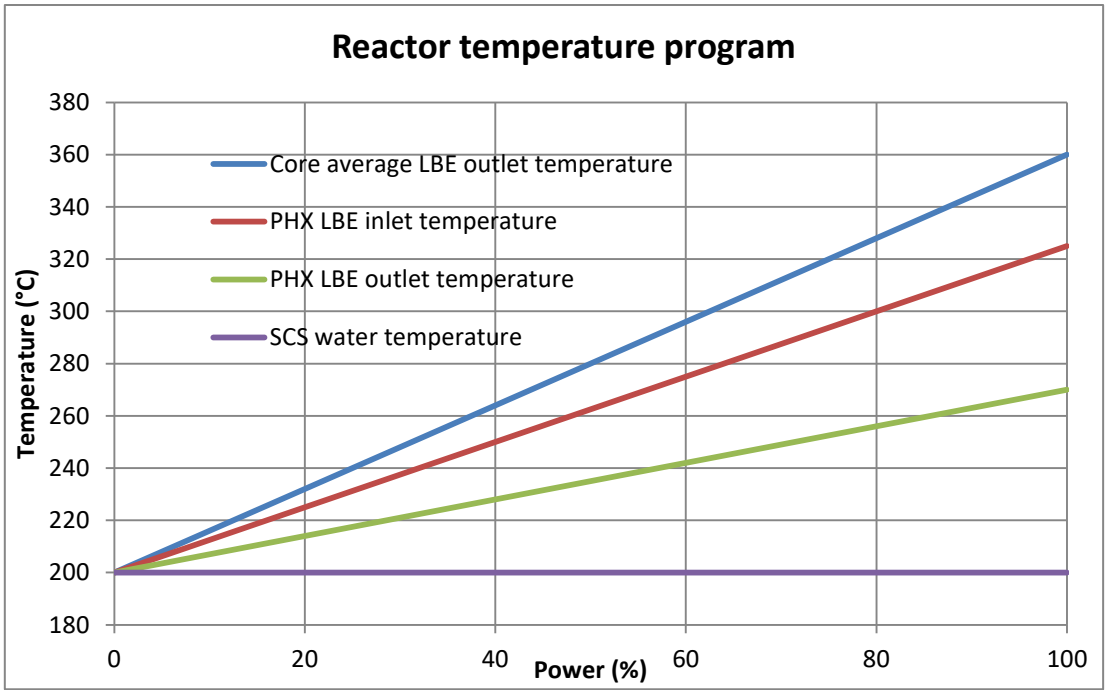

Figure 1.6 – MYRRHA reactor temperature program

During the reactor operations, the PHX performances are progressively degraded because of oxide layers build-up on both LBE and water sides of the stainless-steel tubes. It is assumed a maximum oxide layer of 40 μm on the external (LBE) and 10 μm on the internal (water) tube sides, respectively. The PHX maximum inlet temperature (i.e. max upper plenum temperature) is 325 °C, at core full power, while the outlet temperature is 270 °C.

Assuming a "clean" PHX, the maximum temperatures (at 100% power) are shifted down by 20 °C because of higher PHX efficiency, thus having a PHX inlet/outlet temperature of 305 °C/250 °C. The water temperature remains constant as foreseen by power program.

The importance of the PHX for the reactor power load is thus clear: the PHX efficiency is defining the maximum Primary System temperatures. A high heat transfer surface, as well as a high heat transfer, is thus desired to maintain lower temperatures. However, the PHX dimensions are a result of a compromise between required efficiency and available space in the reactor pool.

One key feature of the MYRRHA reactor power load lies in the constant pressure and temperature maintained in the SCS at every power load. The main reason of this choice consists in the fact that, being MYRRHA a MTR, a partial load operation is not uncommon. If the Primary System temperatures should be maintained constant, a very low power level (that is, low temperature difference between systems) would translate in very high water temperature and pressure. In order to avoid that, a constant SCS conditions program is preferred.

The constant SCS pressure is maintained through the TCS fan rotational velocity, which acts on the Aero-Condenser side HTC: the higher the velocity, the higher HTC. The power removed is thus changed while keeping the pressure to a constant level[7].

[7] The 16 bar are imposed in the PHX bottom head.

Each time the reactor is restarted to proceed with a new irradiation cycle, the operating temperatures in the Primary System will be, in general, different from the previous one in terms of operating temperatures. However, during the same cycle, thermal-hydraulic core conditions are not supposed to vary. Mechanical stresses induced by thermal loads variation during a single cycle are thus excluded.

1.3 Plant safety features

The MYRRHA plant, as any nuclear system, must guarantee the power removal in every conditions: this does not only include the normal operation, but also the abnormal and incidental conditions. In particular, it is important that, following any accidental event, the Decay Heat Removal (DHR) function is always guaranteed, thus maintaining the reactor core cooled towards a safe shutdown state.

For this purpose, all three reactor cooling systems are designed to operate in passive mode for the DHR function: the reactor design must guarantee that the Decay Heat can be removed without any active means of cooling, and that no active actions are required for at least 72 hours after the accidental event [1.15].

The STCS represents the first DHR system and, as such, must be able to accomplish the DHR function in passive mode. Each STCS loop has the capability to passively remove all DH power (conservatively estimated in 7% of total power[8]), thus having a redundancy of 4x100%. Such redundancy is required as the DHR function accomplished by STCS foresees the mitigation of accidental events of DBC2 class (assumed with a frequency of 10^{-2} events/year) [1.16].

A second system accomplishing the DHR function is the Reactor Vessel Auxiliary Cooling System (RVACS), which is called in operation for the mitigation of a specific class of DBC4 (or higher) accidents [1.11].

1.3.1 Licensing activities

The MYRRHA plant, in its current official version, entered the pre-licensing process, consisting in proving to the Belgian Nuclear Safety Authority (FANC: Federaal Agentschap voor Nucleaire Controle) that a consistent and coherent design has been finalized and all the safety-related aspects have been properly considered and evaluated, showing no major or unsolvable issue.

A series of Deliverables has been agreed and sent to FANC on different safety-related topics, all together providing a comprehensive file on the MYRRHA reactor safety case. Several Deliverables have been already accepted and finalized.

Among the others, several Deliverables report the evolution and the consequences of the typical accidents normally studied in a pool-type reactor [1.17]; in particular, the following events have been postulated[9]:

- Loss Of Forced Flow
- Diaphragm Rupture
- Reactivity Insertion[10]
- Reactor Vessel Break

[8] 7% is the DH percentage just after reactor shutdown: it drops to ~4% after one minute and to ~1% after 6 hours. Nevertheless, the STCS is required to remove 7% of the total power.

[9] These postulated events represent an envelope of a series of Initiating Events

[10] And its sub-critical counterpart, the Proton Beam Overpower.

- Primary Heat Exchanger Tube Rupture

The transient analysis has been performed through the means of RELAP5-3D STH code [1.18]. A specific model has been realized according to the latest official design specifications, with a complete documentation [1.19]. The model includes all reactor components and systems, all the control logics and the chance to use neutron kinetics; moreover, the different reactor operating modes (critical and sub-critical) are available.

A scheme of the RELAP5-3D model used for the MYRRHA safety analysis is reported in Figure 1.7.

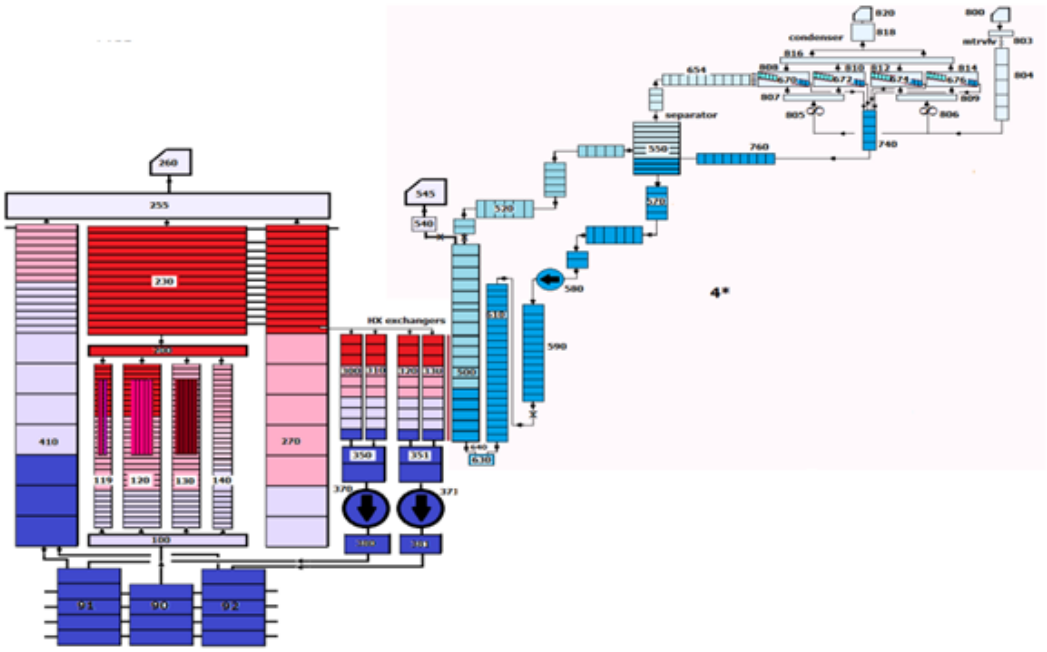

Figure 1.7 – MYRRHA RELAP5-3D model scheme

For some specific transients, a section of the model has been extracted and readapted by adding or modifying some feature. One interesting case is the PHX Tube Rupture transient, for which the RELAP5-3D code shows some limitations that must be overcome by suitable modeling assumptions and, mostly, by adopting different simulation approaches.

The transient analysis preliminary outcome and conclusions has been very positive: the Deliverable sent to the Safety Authority have proven the respect of the safety limits and the reactor design resistance to the events considered. Nevertheless, a series of questions and comments have been formulated by FANC. SCK•CEN is now performing the required additional analyses to provide the reply.

1.3.2 Primary Heat Exchanger Tube Rupture accident

The Primary Heat Exchanger Tube Rupture (PHXTR) is, in the current design, considered as DBC2 event, with a return period > 10^{-2}/year. This statement can be translated in the fact that one (or more) PHXTR are indeed expected during the reactor lifetime.

The PHXTR event will jeopardize the functionality of one SCS, because of the involved depressurization and water inventory loss. It is then important to promptly detect such event and proceed with the reactor shutdown. The SCS redundancy is enough to guarantee the safety function (system coolability).

For a complete assessment of the PHXTR accidental consequences, it is necessary not to limit to the normal operation, but to extend the safety analysis to all the possible reactor statuses [1.11] during which the accident can be initiated. Despite the power generation, it is not obvious that the direst consequences can happen during reactor operation. Indeed, the maintenance period with "reactor open" has been identified as the most problematic scenario because of the Polonium compounds releases in the reactor hall.

The first signal identifying a PHXTR event is expected to come from the PCG system, by water moisture detection in the nitrogen atmosphere. Being the cover gas constantly monitored in all reactor states, it is reasonable to assume such signal can be indeed the quickest.

A subsequent signal should come from the PCG pressure detection: the progressive pressurization of the cover gas will be detected before reaching the rupture disks threshold.

Other signals will be generated by the SCS (depressurization, SS level decreasing…); due to the system dynamics and the time constants involved, it is reasonable to assume the SCS detection signals will be slower compared to the PCG.

From an accident management point of view, it has been decided [1.15] that any signal (with the usual necessary redundancy to avoid spurious) will be treated according to the following sequence:

- Reactor shutdown
- Complete release of the SCS water inventory through the PHX tube break (it is assumed the SCS isolation valves to fail[11])
- Reactor cover rupture disk open
- Release of water inventory in the Pressure Relief System

The phenomenology related to the water inventory release in the Primary Vessel and the physical and chemical interactions with LBE will be described in detail in the following chapters.

[11] Such valves are "fail open" to guarantee the SCS cooling function.

References

[1.1] H. A. Abderrahim, "Multi-purpose hYbrid Research Reactor for High-tech Applications a multipurpose fast spectrum research reactor," *International Journal of Energy Research,* vol. Vol. 36, pp. pages 1331-1337, October 2011.

[1.2] N. Cerullo and G. Lomonaco, "Generation IV reactor designs, operation and fuel cycle," *Nuclear Fuel Cycle Science and Engineering,* pp. pages 333-395, 2012.

[1.3] G. Lomonaco, O. Frasciello, M. Osipenko, G. Ricco and M. Ripani, "An intrinsically safe facility for forefront research and training on nuclear technologies – Burnup and transmutation," *European Physical Journal – Plus,* vol. Vol. 129, p. 10 pp., 2014.

[1.4] "SNETP - Strategic Research and Innovation Agenda," February 2013.

[1.5] D. D. Bruyn, S. Larmignat, A. W. Hune, L. Mansani, G. Rimpault and C. Artioli, "Accelerator Driven Systems for Transmutation: Main Design Achievements for the XT-ADS and EFIT Systems within the FP6 IP-EUROTRANS Integrated Project," in *ICAPP '10 conference*, San Diego, June 2010.

[1.6] M. Sarotto, D. Castelliti, R. Fernandez, D. Lamberts, E. Malambu, A. Stankovskiy, W. Jaeger, M. Ottolini, F. Martin-Fuertes, L. Sabathé, L. Mansani and P. Baeten, "The MYRRHA-FASTEF cores design for critical and sub-critical operational modes (EU FP7 Central Design Team project)," *Nuclear Engineering and Design,* vol. Vol. 265, pp. pages 184-200, December 2013.

[1.7] D. Castelliti, M. Sarotto, A. Rineiski, A. Ferrari, S. Mueller, G. Bandini and M. Polidori, "FP7-MAXSIMA Work Package 2 "Safety Analysis in Support of MYRRHA" Main Outcome and Conclusions," in *NURETH-17*, Xi'An, September 2017.

[1.8] D. D. Bruyn, R. Fernandez and J. Engelen, "Recent Developments in the Design of the Belgian MYRRHA ADS Facility," in *ICAPP-16*, San Francisco, April 2016.

[1.9] Nuclear Science Committee; Working Party on Scientific Issues of the Fuel Cycle; Working Group on Lead-Bismuth Eutectic, "Handbook on Lead-Bismuth Eutectic Alloy and Lead Properties, Materials Compatibility, Thermal-Hydraulics and Technologies," Nuclear Energy Agency, 2015.

[1.10] K. Tuček, J. Carlsson and H. Wider, "Comparison of sodium and lead-cooled fast reactors regarding reactor physics aspects, severe safety and economical issues," *Nuclear Engineering and Design,* vol. Volume 236, p. pp. 1589–1598, August 2006.

[1.11] R. Fernandez, "Mechanical design of the primary system," SCK•CEN Internal Report, Mol, September 2015.

[1.12] E. Malambu and A. Stankovskiy, "Revised Core Design for MYRRHA-Rev1.6," SCK•CEN Internal Report, Mol, October 2014.

[1.13] N. Todreas and M. Kazimi, Nuclear Systems Volume 1 - Second Edition, CRC Press Taylor & Francis Group, 2012.

[1.14] AFCEN, RCC-MRx - Design and Construction Rules for Mechanical Components of Nuclear Installations, Paris, 2012.

[1.15] G. Scheveneels and on behalf of the MYRRHA Team, "Design Options and Provisions File," SCK•CEN Internal Report, Mol, 2017.

[1.16] D. Castelliti, "Preliminary Design Description of the Secondary Cooling System (SCS) and Tertiary Cooling System (TCS)," SCK•CEN, Mol, 14 December 2016.

[1.17] G. Scheveneels, "Internal initiating events (MYRRHA v1.6)," SCK•CEN Internal Report, Mol, February 2017.

[1.18] RELAP5-3D Code Manual, Idaho Falls: INEEL-EXT-98-00834, Idaho National Laboratory, 2014.

[1.19] D. Castelliti, "RELAP5-3D MYRRHA ver. 1.6 Model Description," SCK•CEN Internal Report, Mol, April 2016.

Chapter 2: Primary Heat Exchanger functional and technical description

The main thermal connection between the Primary System and the Secondary Cooling System is provided by the Primary Heat Exchanger (PHX).

The PHX main function is to deliver the power generated in the reactor core to the Secondary Cooling System. Four identical PHX units are located in the Reactor Vessel. Each unit receives hot LBE from the upper plenum, transferring the power to the SCS and thus cooling the primary fluid. The cold LBE is then directed towards the Primary Pump box.

The PHX design, as part of the complete MYRRHA Design Version 1.6 concept [2.1], is based on a countercurrent shell and tube concept with primary LBE flowing downward in the shell side and secondary two-phase water mixture flowing upward in the tubes.

This choice proves to be very efficient for several reasons:

- Dimension compactness allowed by high overall Heat Transfer Coefficient values
- Low performance sensitivity to relatively small thermal-hydraulic perturbations (mass flow rates, local power, etc…)
- Limited water inventory in the Primary Vessel

The PHX must be able to remove the maximum power from the Primary System. Therefore, each PHX unit is designed to remove 27.5 MW in normal operation. However, the SCS safety function reflects on the PHX as well, imposing a series of additional requirements.

2.1 Primary Heat Exchanger functional requirements

According to the design specifications [2.2], the PHX must fulfill three main functional requirements:

- Normal operation mode: during normal operation, the PHX must be able to remove the power generated by the reactor core and by all the other heat sources (pumps, polonium decay, In Vessel Fuel Storages, beam window…) in the Primary System. In this condition, the PHX operates in forced circulation regime on both sides (LBE and water).
- During shutdown periods: once the decay heat power is low enough to be compensated by the thermal heat losses through the reactor Primary System boundaries, it is necessary to provide power to the LBE in order to prevent freezing. This function is primarily accomplished by the LBE Conditioning System or, as back-up choice, by an external power source located in the SCS, from where the power is then transferred to the primary LBE through the PHX operating in a 'reverse' mode. This is not a safety function. The safety option to prevent freezing on the long term will consist of electric heaters in the primary system.
- In abnormal or accidental conditions, the PHX must be able to remove in passive mode (natural circulation on both sides) the decay heat of all power sources in the Primary System in order to guarantee the DHR function.

During shutdown periods, once the decay heat power is low enough to be compensated by the thermal heat losses through the reactor primary vessel, it is necessary to provide power to the primary LBE in order to prevent freezing.

Two systems are devoted to this task[1], one of which being the SCS itself, by heating the secondary water with an external power source and then transferring power to the primary LBE through the PHX operating in a "reverse" mode.

[1] One system being the LBE Conditioning System [1].

2.2 Primary Heat Exchanger design characteristics

2.2.1 PHX design concept

The PHX design (see Figure 2.1) chosen for MYRRHA is a counter-current shell-and-tube concept. The main features can be summarized as follows:

- 684 stainless steel (AISI 316L) tubes
- 2 tube plates
- A double-walled central feedwater pipe connected to the SCS feedwater line
- A double-walled bottom head, collecting feedwater and connected to the tube bundle
- A top head providing connection with the SCS Riser line
- An external shroud separating the PHX internals from the upper plenum, driving the flow through the tube bundle towards the Primary Pump

All metallic surfaces separating primary LBE by secondary water, with the exception of tube bundle, are equipped with a double-walled structure: this is motivated by the need to avoid the risk of interaction of LBE and water in case of failure. Consequently, the bottom head and the feedwater pipe are double walled, while the external shroud and the top head maintain a single wall structure.

As mentioned, the tubes structure is not double-walled: this is done to preserve a high heat transfer through the tube wall, resulting in a reduced heat transfer surface, that is a more compact PHX. The compactness is a very important requirement for every component of the MYRRHA design, whose vessel external diameter should be limited as much as possible, so it has been chosen to adopt a single-wall structure for the tube bundle.

While such choice is favorable from the efficiency point of view, it introduces some shortcomings for the reactor safety. In particular, while the failure of a double-walled structure is excluded "by design", a single-walled structure failure must be considered in the reactor safety case.

The compromise adopted in the MYRRHA design includes a double-wall only for the structures where the complete SCS water inventory is flowing. A failure of such structure would release a notable quantity of water, in a short time frame, in the reactor Primary Vessel, with probable undesirable consequences on reactor internals. On the other hand, a single PHX tube failure would cause a slower water release with less problematic issues.

However, the single PHX tube rupture, as DBC2 event [2.3], presents a reasonable probability of happening during the reactor lifelime (return time > 10^{-2} events/year). As such, it must be thoroughly studied to guarantee that the reactor safety functions are not jeopardized by the event itself and that the safety limits are respected.

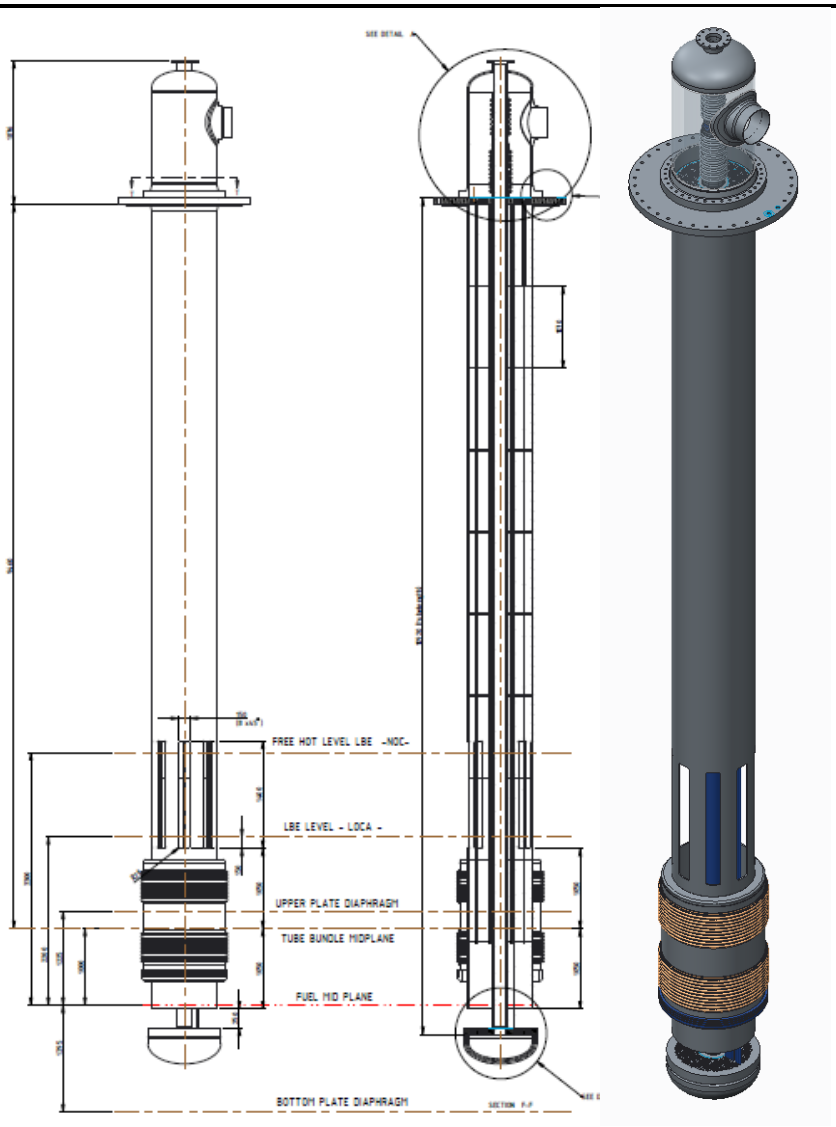

Figure 2.1 - Primary Heat Exchanger

2.2.2 PHX main design choices

The LBE from the upper plenum (~325 °C in nominal operating conditions) enters the PHX from the inlet openings in the external shroud. The flow is then directed downwards, through the tube bundle, where the actual heat exchange takes place. Outlet openings, directing the LBE flow towards the Primary Pump box, provides the exit path for the cold (~270 °C) LBE.

On the secondary side, water at 16 bar and in nearly saturated conditions (~200 °C)[2] flows down the central downcomer pipe into the PHX bottom head and then upwards through the tubes where it is heated by the counter-current flowing LBE, thus producing a water steam mixture with an outlet quality of ~0.3.

A summary of the main geometrical and thermal-hydraulic PHX parameters is shown in Tables 2.1 and 2.2.

[2] Saturation temperature at 16 bar is 201.4 °C.

Table 2.1 - MYRRHA PHX main geometrical parameters

Parameter	Unit	Value
Power in one PHX	MW	27.5
Shroud external diameter	mm	850
Shroud internal diameter	mm	820
Feed water pipe external diameter	mm	200
Water tubes number	-	684
Water tubes pitch	mm	26
Water tubes external diameter	mm	16
Water tubes internal diameter	mm	14
Thickness of water tubes	mm	1
Total length of water tubes	mm	10920
Active length of water tubes	mm	2100

Table 2.2 - MYRRHA PHX main thermal-hydraulic parameters

Parameter	Unit	Value
PHX LBE inlet temperature	°C	325
PHX LBE outlet temperature	°C	270
LBE safe shutdown temperature	°C	200
PHX LBE mass flow rate	kg/s	3450
PHX water inlet temperature	°C	200
PHX water outlet temperature	°C	201.4
PHX water mass flow rate	kg/s	47
PHX water pressure	bar	16
PHX water outlet quality	-	0.3
PHX water outlet void fraction	-	0.9
LBE velocity	m/s	0.93
Primary side pressure drop[3]	bar	0.04
Water outlet velocity	m/s	3.3
Steam outlet velocity	m/s	18.63
Water side pressure drop	bar	0.95

As shown in Figure 2.1, the tube bundle is extended from the bottom tube plate to the top tube plate, as standard for shell-and-tube HXs. However, the LBE inlet is placed at ~ 2.35 m from the bottom plate, instead of being located at top of the component (~11 m). This configuration defines an "active length" for the tube bundle of ~2.1 m where the LBE flow and the vast majority of the heat transfer actually takes place.

The hot LBE free surface level, located ~1.6 m above the active length, is in contact with the tube bundle. Above free surface, the nitrogen cover gas fills the space between shroud and feedwater pipe[4].

[3] Not including entrance and exit contribution

The "active" length is defined as the part of tube bundle actually taking part in the counter-current flow heat transfer. It is conventionally defined as the tube bundle fraction extending below the inlet window.

The "non-active" length, extending from the inlet windows up to the first tube plate, is present with the purpose of carrying the water-steam mixture outside the PHX towards the SCS riser line.

Despite representing a relevant fraction of the total tube bundle length, the amount of heat transfer involving the non-active length is considered negligible compared to the power transferred in the active portion.

The PHX inlet windows extend ~1.4 m in axial length. The inlet windows are almost completely submerged, in normal operation, below free surface. This gives several advantages:

- Adopt a wide inlet for LBE, counting on more heat transfer surface than what provided by active length only, thus making the design estimations conservative in terms of LBE temperatures[5].
- Guarantees a minimum flow area for the natural circulation path in case of LBE level decrease caused by a Primary Vessel break event (primary LOCA).

Several other objectives can be achieved by adopting the proposed configuration:

- The high aspect ratio between the PHX shroud and tube bundle length on the primary side contributes to develop a better counter-current flow through the bundle.
- The two-phase water flow is well developed inside the PHX tubes from the bottom inlet up to the top of the component, with no phase separation to be expected within the tubes.
- Only one (out of two) tube plate (and hence one set of welding's) located under LBE. The upper tube plate is positioned above the hot free surface in order to avoid thermal stresses caused by the temperature difference between water and hot LBE in the thick plate structure.
- Direct access to tube bundle outlet from the reactor hall, simplifying the inspection and repair processes

There are, on the other hand, several possible disadvantages coming from this design configuration:

- High two-phase pressure drop in the tube bundle, with potential increase of dynamic instabilities and consequent need to design a suitable orifice to generate enough pressure drop in the monophasic (inlet) zone
- The notable tube length could lead to important mechanical stresses in the tube plates (weight and thermal induced) and in the tube bundle itself (bundle vibration), even with the implementation of tube plates

[4] Heat exchange through cover gas and tube bundle is neglected.
[5] The additional heat transfer surface is not considered in the PHX thermal analysis.

- The tube bundle is in contact with the free surface zone leading to possible problems due to differential thermal expansion and level fluctuations resulting in thermal fatigue

It is important to mention how adopting a two-phase regime as normal operation condition could have a negative impact on the SCS loop stability[6]. This topic is currently under analysis.

2.2.2.1 PHX lower head design

The PHX lower head (see Figure 2.2) has been dimensioned according to the thermal-hydraulic and mechanical evaluations performed on the tube bundle.

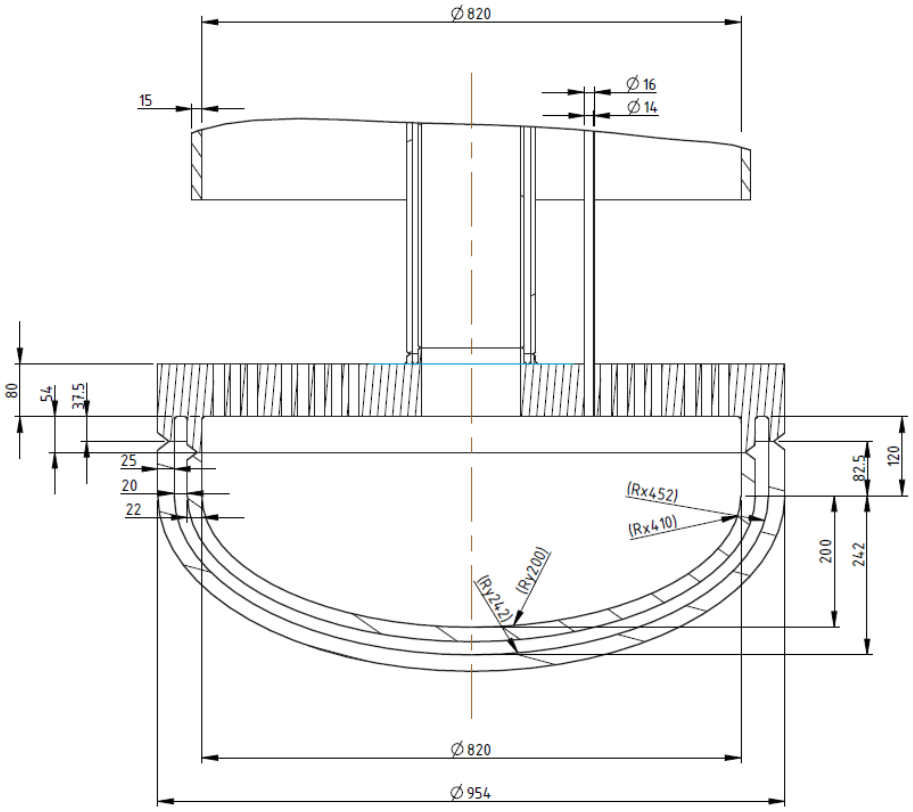

Figure 2.2 - Proposed PHX lower head layout

2.2.2.2 PHX upper head design

A detailed analysis of the PHX upper head has been conducted: several solutions have been considered in order to optimize the connection with the SCS on both inlet (PHX feedwater pipe connection with SCS feedwater line) and outlet side (PHX steam chamber connection with SCS riser line).

The selected solution consists in a bolted flange with feedwater pipe inserted.

The solution (see Figure 2.3) presents the following significant advantages:

[6] At least in some specific operation windows.

- The upper head is removable in order to grant total access to the tubes bundle without restriction.
- A certain degree of axial dilatation for the feedwater pipe is possible, thus decreasing the stress issues in the tube plates.
- All the different parts to remove for inspection and plugging are located outside the PHX main body (interesting solution also considering the remote handling compatibility needed).
- Vertical seals are proven technology already used in other research reactors[7].
- Limited problem in case of leakage through the seal connecting the feedwater pipe to the PHX head because of water being part of the same loop (but potential difficulties in detection could arise).

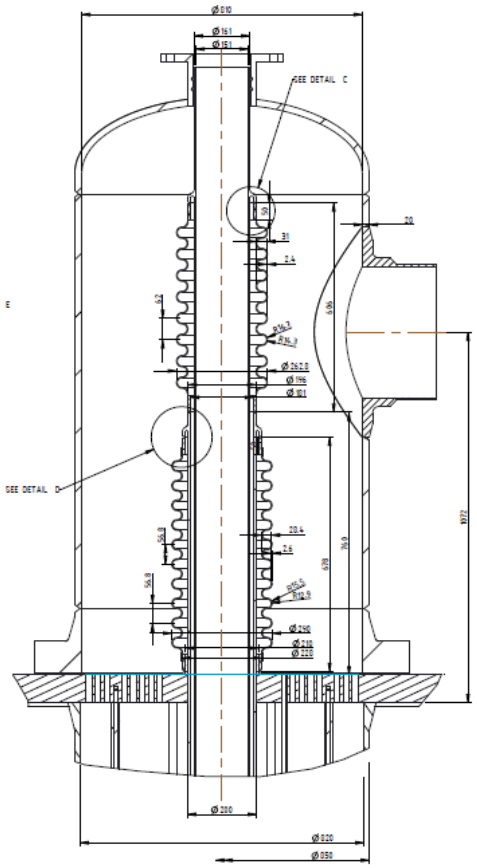

Figure 2.3 - Proposed PHX upper cover layout

2.2.3 Preliminary tube inspection and plugging solution proposal[8]

2.2.3.1 Inspection procedure for the tube bundles

As a complete remote handling compatibility is a requirement for all procedures to be conducted inside the reactor hall, the inspection procedure will be accomplished by remote

[7] In the Belgian Reactor 2 it is possible to retrieve the use of such devices.

[8] A complete comparative analysis of the different inspection and plugging potential solutions considered can be found in [1]

handling machine (with the possibility to share functions with other remote handling devices already present in the reactor hall, e.g. the machine removing the upper head).

The functional system concept is currently foreseeing the use of a rigid cable with a suitable probe at one end. This system is based on the Eddy current testing method. Such option has been selected because a Non-Destructive technique is needed to inspect potential defects at LBE side placed near tube sheet, and thanks to the possibility of using a probe able to fit into tube diameter (14 mm).

Being the inspection procedure still not analyzed in all its aspects, certainly not for an innovative nuclear reactor application, further R&D effort is required for this inspection technique to be proven.

2.2.3.2 Plugging procedure for the failed tubes

The plugging procedure for the failed tubes to be applied to the PHX is particular, because the cracked tubes have to be plugged on both ends, with only one end accessible.

While the upper head (located outside the reactor cover) can be opened and accessed from the top, it is not possible to directly reach the lower head (welded and located into the reactor vessel below the LBE hot free level) without extracting the whole component. In order to avoid the PHX extraction, several options have been examined.

The investigations proved the mechanical expansion plug technique is the most suitable solution for in-situ tube plugging, because of the compactness of the machinery required, operation easiness and rapidity and a certain degree of testing already performed.

Such solution consists in pulling a wider mandrel through a sealing ring against the tube inner diameter, thus assuring the sealing through deformation of the sealing ring material.

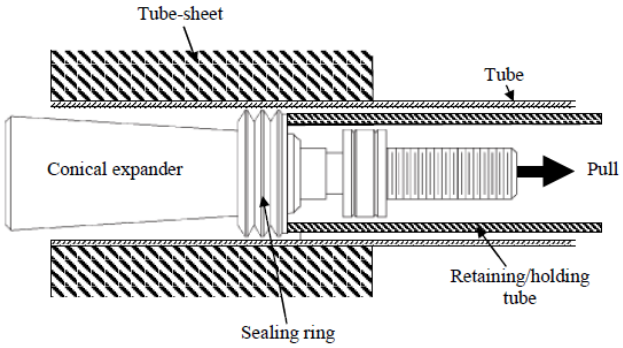

Figure 2.4 - PHX tube plugging

Hydraulic expansion is assumed as potential back-up solution.

2.3 Primary Heat Exchanger analysis

2.3.1 Thermal-hydraulic assessment main results and conclusions

A MATLAB [2.4] model has been programmed in order to evaluate the PHX active length and the steady-state axial distribution of the main thermal-hydraulic parameters under different plant power levels. The balance equations (Mass, 1-D momentum and energy conservation), coupled with the required closure relations and thermo-physical properties, are solved over an axial mono-dimensional domain discretized in 1000 axial volumes[9].
The boundary conditions for primary and secondary side are taken from the plant specifications. A summary is provided as follows:

- Inlet LBE temperature: 325 °C
- Outlet LBE temperature: 270 °C
- Inlet water temperature: 200 °C
- Inlet water pressure: 16 bar

All the other parameters are evaluated starting by these boundary conditions, making use of the physical models encoded in the program.

The LBE thermo-physical properties implemented in the model have been taken by the OECD-NEA LBE Handbook [2.5], collecting the state of the art correlations available. The two-phase water properties, well known, have been derived from the X-Steam database [2.6].

Next to the balance equations and the thermo-physical properties, a suitable set of closure relations has been applied. In particular, two numerical models to simulate the Heat Transfer Coefficients (HTC) on both LBE and two-phase water have been introduced:

- LBE side: Ushakov correlation [2.7]:

  $$Nu_{LBE} = \left(7.55 * \frac{P}{D}\right) - \frac{20}{\left(\frac{P}{D}\right)^{20}} + \frac{0.041}{\left(\frac{P}{D}\right)^{2}} * Pé^{0.56+0.19*\frac{P}{D}} \qquad (2.1)^{10}$$

  $$1.3 < \frac{P}{D} < 2.0, \quad 1 < Pé < 4 * 10^{3}$$

  This correlation is advised for rod bundles with an imposed heat flux distribution (typically, nuclear fuel rod) cooled by liquid metal. However, due to the scarcity of data on configurations more similar to the MYRRHA PHX (tube bundles with an imposed temperature distribution), it has been decided to use this correlation[11].

[9] The axial discretization allows taking into account the non-linearities not included in a lumped evaluation.
[10] Nu_{LBE} = Nusselt number, LBE side; P = Tube bundle pitch; D = Tube external diameter; Pé = Péclet number.
[11] Preliminary studies based on CFD evaluations [11] have shown that Ushakov correlation could actually overestimate by a factor ~1.25 the real value.

- Two-phase water side: a series of models has been selected, allowing to account for the difference in velocities between liquid and vapor phase in a two-phase flowing mixture, and its impact on pressure drops and heat transfer. Specific models to evaluate the void fraction distribution, the two-phase pressure drops and the heat transfer associated to the various flow regime have been encoded. A comprehensive database of such models can be found in [2.8].

The estimated active length value required to remove the nominal power (27.5 MW) in the most penalizing[12] conditions results to be 2.1 m.

All the results have been verified and confirmed through a dedicated RELAP5-3D [2.9] model, which has been extracted by the main MYRRHA model used for the reactor safety analysis [2.10] by replacing the primary and secondary loops with the same boundary conditions applied to the MATLAB model.

The main thermal-hydraulic parameter distribution along the active length are shown in the Figures from 2.5 to 2.9 below:

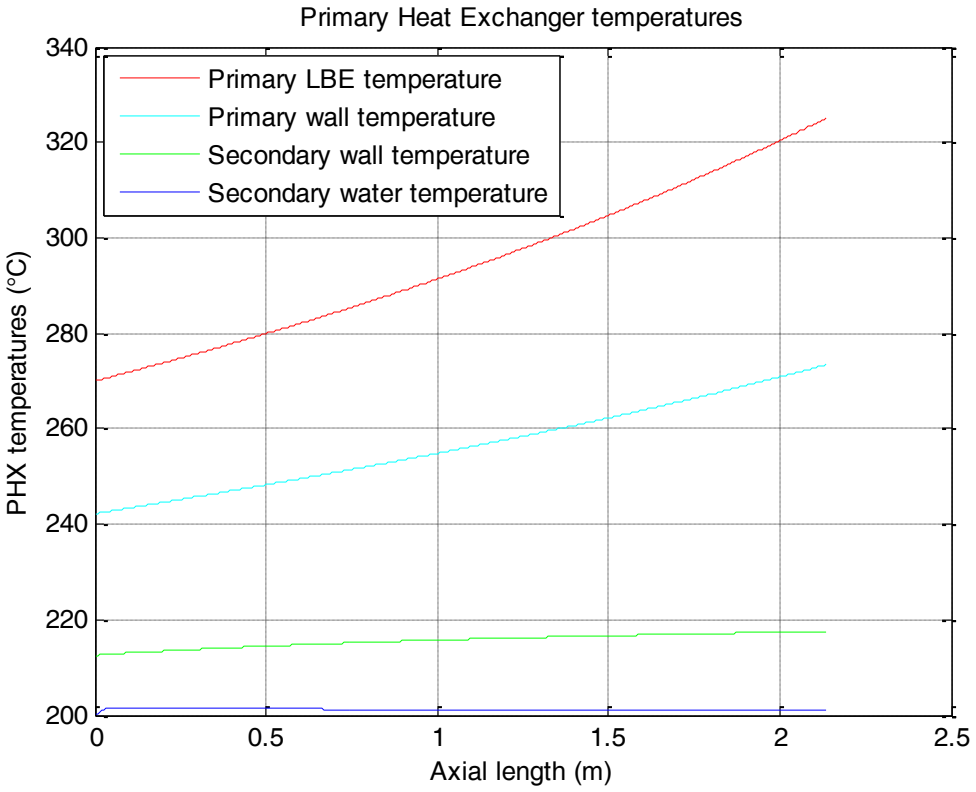

Figure 2.5 – PHX axial temperatures distribution

[12]Accounting for 40 μm oxide layer on total active length of the tubes primary side and 10 μm oxide layer on secondary side.

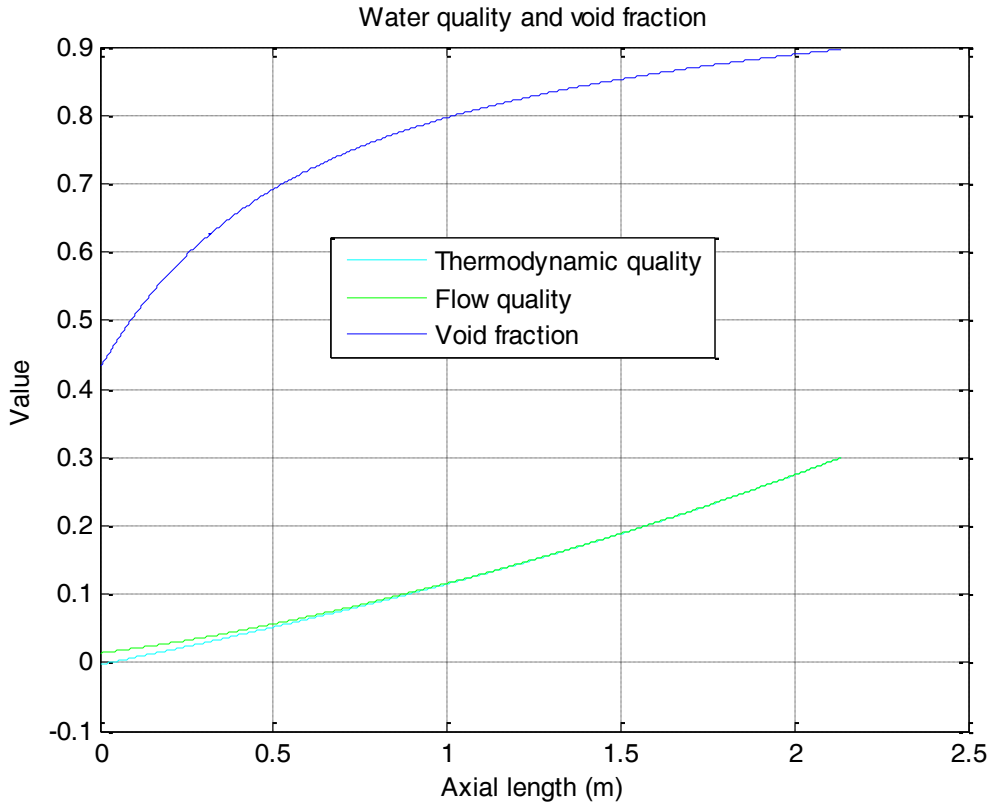

Figure 2.6 – Quality and void fraction distribution

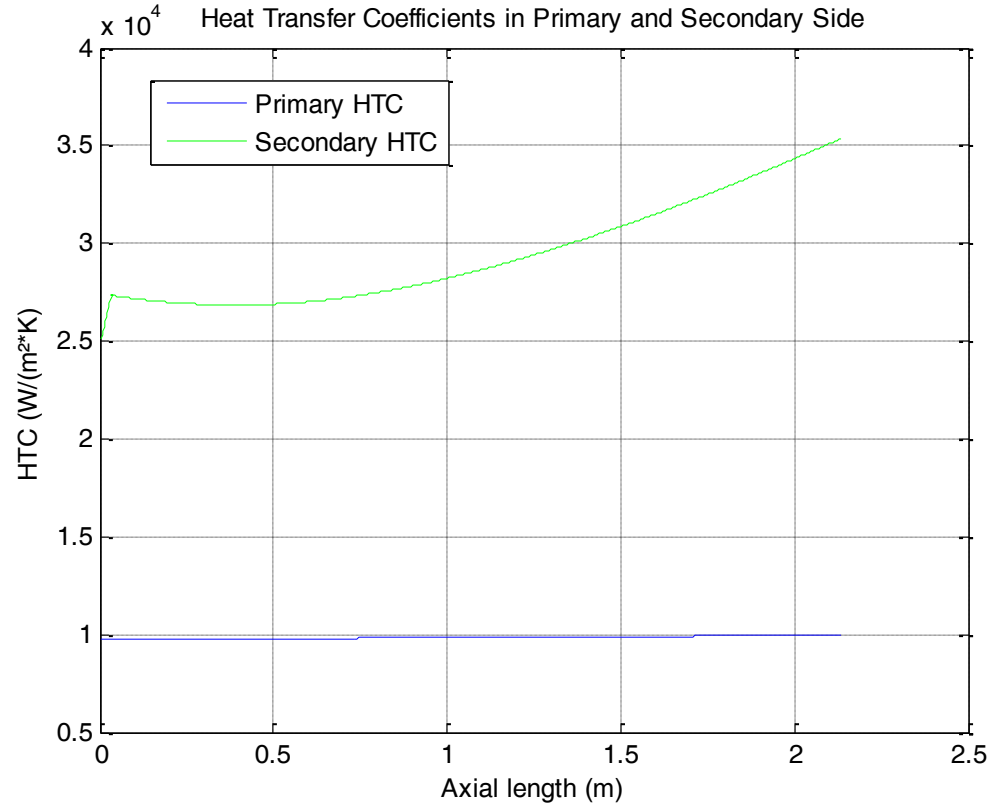

Figure 2.7 – Heat Transfer Coefficients evolution

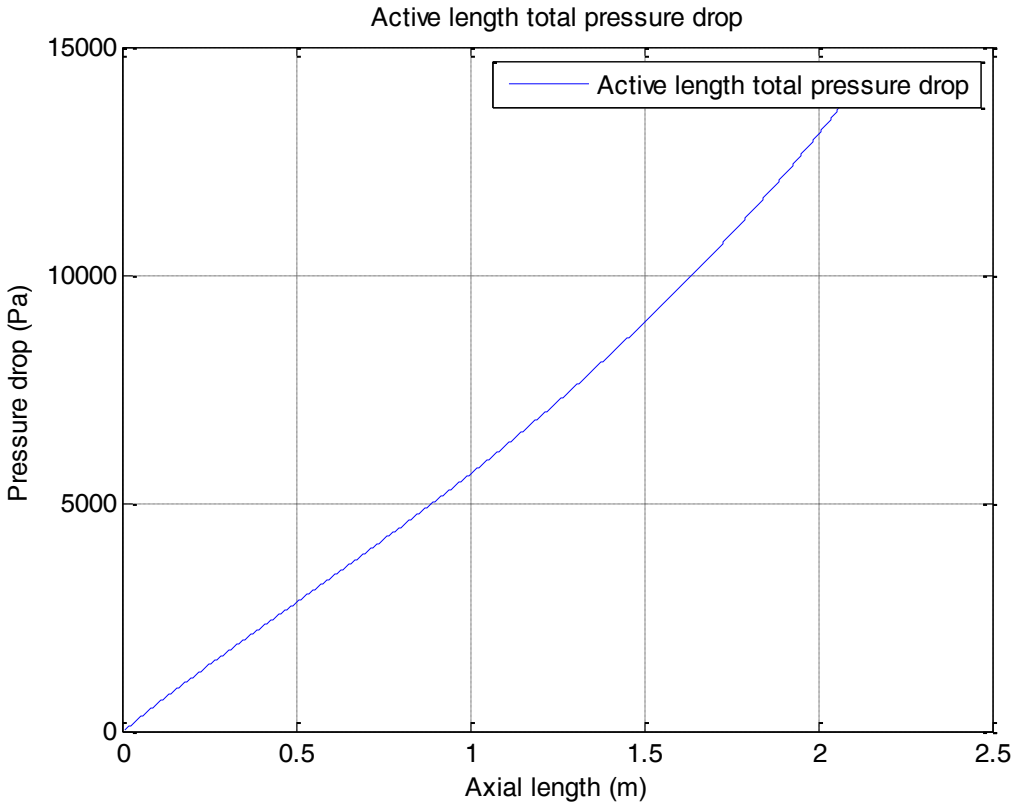

Figure 2.8 – Total active length pressure drop (tubes only)

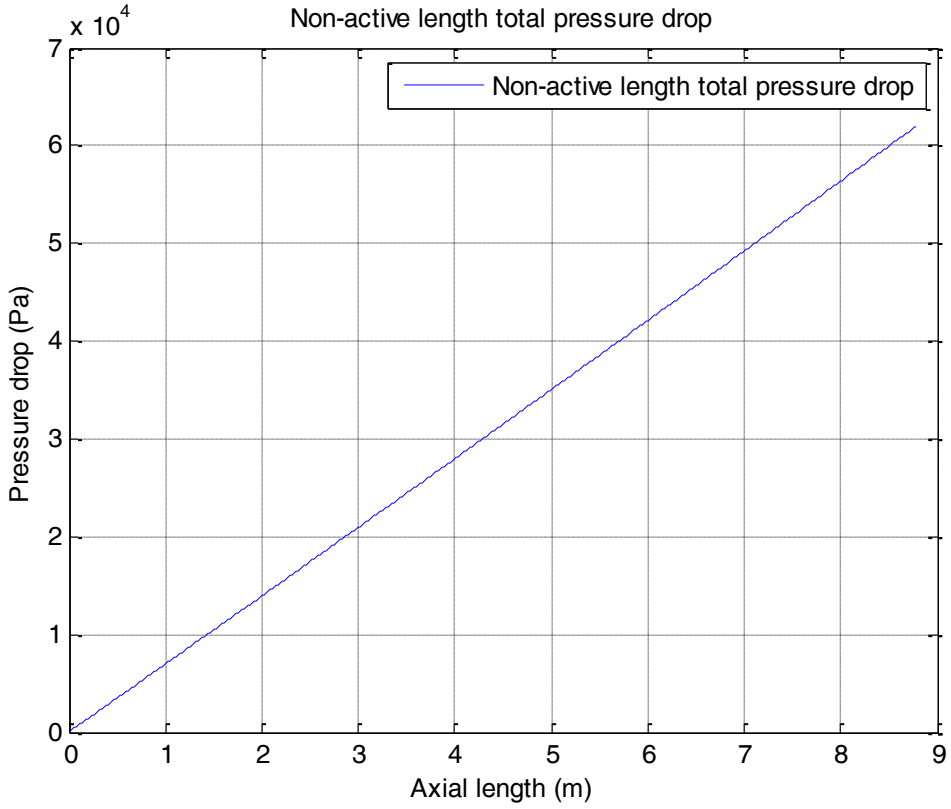

Figure 2.9 – Total non-active length pressure drop (tubes only)

The tube wall temperatures on the primary side varies from 240 °C to 275 °C, while on the secondary side the variation range is restricted to 215 °C – 220 °C (Figure 2.5). The water temperature, reaching almost immediately the saturation conditions, maintains on the saturation value (slowly decreasing because of pressure drops). The HTC evolutions (Figure 2.7) provide a qualitative explanation to these temperature distributions.

Since the water enters the tubes with a very small subcooling (~1 °C), the water inlet wall temperature exceeds the saturation temperature, thus the water is in Subcooled Nucleate Boiling (SNB) state as soon as it enters the PHX tubes[13]. Therefore, (Figure 2.6) the inlet void fraction is not 0 but shows a value of ~ 0.45.

The outlet steam quality is 0.3, while the outlet void fraction is 0.9. The evaluations make use of non-equilibrium correlations for the two-phase closure relations.

The complete assessment of the PHX is not limited to the active length, but also includes the non-heated tube sections and the central feedwater pipe. In particular, this is required for the evaluation of the pressure drops in the PHX, especially referring to the water side: for this purpose, all the local pressure drops, including the orifice at the tube inlets in order to stabilize the flow in case of pressure or flow perturbations, have been included.

Pressure drops are normally divided in four different types:

- Friction pressure drops: the loss of pressure occurring due to the effect of the fluid's viscosity near the surface.
    - Local pressure drops: specific kind of friction losses occurring in case of geometrical discontinuities
- Gravitational pressure drops: the pressure difference (not necessarily negative) occurring due to the change in elevation of a fluid
- Acceleration pressure drops: the pressure difference due to the fluid velocity change

In Figure 2.8 and Figure 2.9 the pressure drops in the active and non-active length are shown. A value of ~ 0.15 bar has been estimated for the former, while a value of ~ 0.62 bar has been found for the latter.

In the Table 2.3 below the various contributions to the total PHX water side pressure variations (from feed-water inlet flange to riser outlet flange) are indicated in detail.

Table 2.3 – PHX secondary side total pressure variations (with and without orifice)

Section	K-factor	Pressure drop (Pa)	Note
Feed-water pipe inlet	0.0602	236.6349	
Feed-water pipe	-	-1.048E+05	
Feed-water pipe outlet	0.9333	3.6698E+03	

[13] SNB is a specific two-phase flow regime characterizing the flow boiling incipience: the bulk temperature is still below saturation temperature, while the tube wall temperature is above saturation. This causes the bubbles generated on the tube wall to collapse in the middle.
The SNB state explains the difference (Figure 2.6) between the flow quality and the thermodynamic quality.
Further details on flow regimes can be found in [8].

Tube bundle inlet	1.8	1.39E+04	
Active tube bundle	-	1.44E+04	Two-phase
Non-active tube bundle	-	6.1958E+04	Two-phase
Tube bundle outlet	0.994	4.0637E+03	Two-phase
PHX outlet flange	0.5	5.4586E+02	Two-phase
Total tube bundle	-	9.43E+04	
Total PHX	-	-6.062E+03	

It is interesting to note how in the feedwater pipe the total pressure variation is negative in the flow direction: this is due to the gravitational head, which surpasses, in absolute value, the friction component. All the other contributions provide positive pressure variations in the flow direction, but the total pressure variation through the PHX is still negative: the contribution of the feedwater gravitational component is enough to compensate all the other pressure variations in the PHX.

2.3.2 PHX primary side pressure drop evaluation

The pressure drops on primary side, limitedly to the active section of the tube bundle, can be quantified through the well-known monophasic friction factor definition. A value of 0.05 bar can be assumed, if only referring to the active bundle friction pressure drop with no geometrical discontinuities.

A more accurate estimation, requiring the consideration of the complex 3-D cross-flow through the inlet and outlet windows and of the actual angular distribution of LBE across the tube bundle, has been performed [2.11]. The pressure drops induced by the spacer grids to stabilize the tube bundle has also been evaluated. Such evaluations have been performed through ANSYS-CFX CFD code [2.12].

Figure 2.10 and 2.11 show the pressure drop K-factor associated to the PHX inlet and outlet windows and the K-factor associated to a single spacer grid.

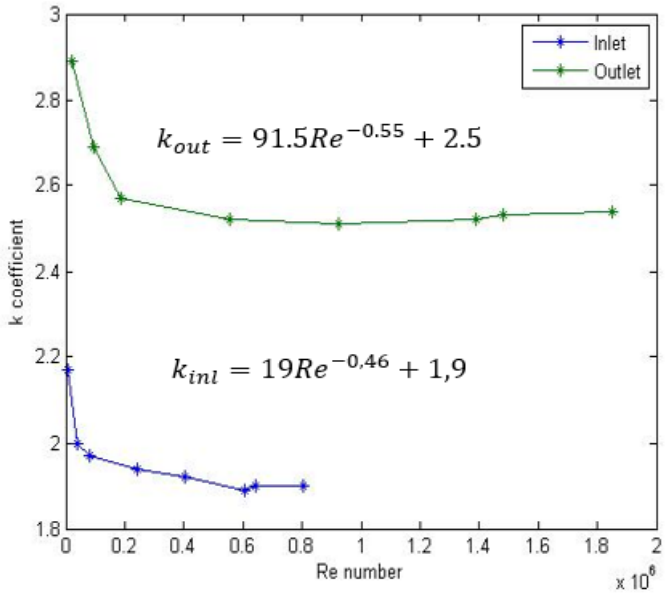

Figure 2.10 – Pressure drop factor associated to PHX inlet and outlet

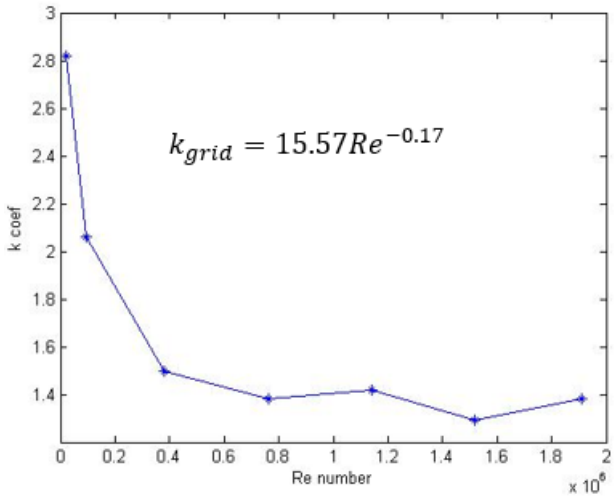

Figure 2.11 – Pressure drop factor associated to a single PHX spacer grid

The total pressure drops in the active length, accounting for the contribution of the "bare" tube bundle, the inlet and the outlet windows and two spacer grids, reaches a value of ~1 bar. This must be considered when reviewing the Primary Pump total head.

2.3.3 Tube bundle stability analysis results and conclusions

A solid PHX design requires a complete assessment of two-phase flow instabilities and the potential implementation of a suitable stabilizing device (orifice) to reduce the impact of the perturbations along the channel. The stability assessment should take in consideration all the possible reactor operational power levels in order to prove the stable behavior under all operational conditions.

The two-phase flow instability problem has been extensively studied for several cases and applications, one of them being the BWR boiling channels [2.8].

Being MYRRHA PHX featuring two-phase water in the tubes, it becomes important to well understand the potential unstable behavior of the component, properly mapping the flow regimes and conditions where the instabilities are more likely to incur.

It is important to note that the PHX, differently from a BWR core, is not a system with an imposed heat flux but with imposed wall temperature. The way the boundary conditions are imposed to the system provides a proper simulation of this feature.

Generally speaking, a number of different two-phase instabilities can be found in a boiling channel [2.13]:

- Ledinegg instability belongs to static type instability and involves a sudden change in the flow rate to a new, stable operating condition. It can occur when the slope of the channel pressure-drop - flow-rate curve becomes in some portion negative.
- Flow pattern transition instabilities belong to static type instability. These instabilities have been postulated as occurring when the flow conditions are close to the point of transition with slug flow. A temporary increase in bubble population in bubbly-slug flow (arising from a temporary reduction in flow rate) may change the flow pattern to annular flow with its characteristically lower pressure drop, which will speed up the flow rate. This, in turn, causes the vapor generated to become insufficient to maintain the annular flow, and the flow pattern then reverts to bubbly - slug flow.
- Density wave oscillations (DWO) instability belong to dynamic type instability. The mechanism involves the propagation of disturbances. A temporary reduction of inlet flow in a heated channel increases the rate of enthalpy rise, thereby reducing the average density. This disturbance affects the pressure drop as well as the heat transfer behavior. For certain combinations of geometrical arrangement, operating conditions, and boundary conditions, the perturbations can acquire a 180° out-of-phase pressure fluctuation at the exit, immediately transmitted to the inlet flow rate and become self-sustained.

In addition to this, by introducing in the system a perturbation, perturbing the flow in one channel through, for instance, a mass flow rate disturbance or a power spike, it is possible to induce flow oscillations that can dump or amplify in time depending if the system is in the stable region or over the instability threshold (in the unstable region).

The main scope of the PHX instability analysis can be divided into two different steps:

- To carry out a complete assessment of the tube bundle behavior in its original configuration, in order to understand the reaction of the system against the various types of instabilities.
- To design an adequate stabilizing device to extend as much as possible the stability range to include in it all the PHX operating conditions.

The tube bundle stability assessment has been carried out by following a similar procedure used for BWR fuel channels [2.14], through a specific RELAP5-3D model representing the PHX and able to evaluate the propagation of a density wave in the tube length.

A series of suitable boundary conditions, on both primary and secondary side, and perturbation triggers have been foreseen into the model, so to discover all kind of unstable behavior.

The PHX stability analysis is initially performed on the "original" tube bundle without the adoption of any stabilizing devices, in order to check the "natural" behavior of the system. The possible adoption and design of an orifice will be then conducted based on this preliminary study.

More details on the two-phase flow instabilities in MYRRHA PHX, together with a detailed description of the applied methodology and the results, can be found in [2.15].

2.3.3.1 RELAP5-3D model for instability analysis

The MYRRHA plant has been modeled in its integrity (primary, secondary, tertiary system) through a RELAP5-3D model. The PHX is a relevant section of the model, connecting primary LBE system with the four SCSs.

Looking forward to the stability analysis, the PHX model has been extracted from a general plant nodalization, making it self-standing through the application of six boundary conditions, as shown in Figure 2.12:

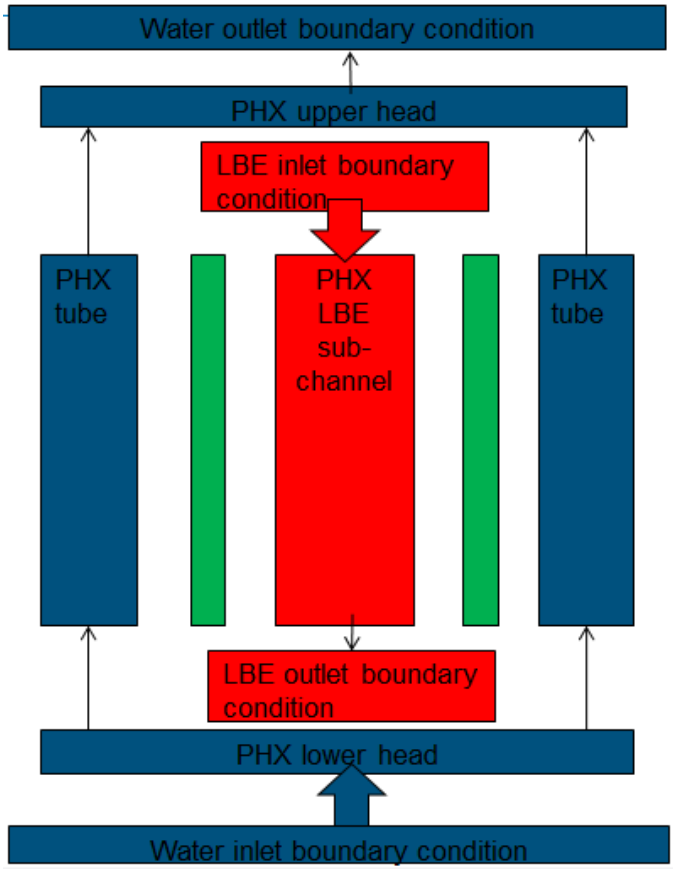

Figure 2.12 - PHX simplified RELAP5-3D model scheme

The PHX tube bundle has been simulated with three Pipe components and two Heat Structures. One pipe, in the primary side, represents two primary channels[14]. Other two pipes, in the secondary side, represent two secondary tubes. The two heat structures, simulating the AISI 316L tube material, connect the primary pipe with each of the secondary pipes.

The number of nodes used in the simulation is ~300 (50 for the primary channels, ~250 for the secondary channels), with a volume length always maintained in the range between 0.04 m and 0.09 m. Adjacent volume length variation is always kept within a factor 2.

LBE flow rate is kept always constant[15], while the inlet and outlet temperatures are varied according to the reactor control strategy to simulate different power levels.

The secondary water inlet conditions, in terms of mass flow rate and temperature, are varied as sensitivity parameters.

A series of features have been introduced in the RELAP5-3D PHX model to achieve a higher accuracy in the instability region definition:

- The physical properties adopted for the heat structures, thermal conductivity and volumetric heat capacity in the stainless steel tubes, have been modified on purpose to try and eliminate any transient effect due to the thermal inertia of such solid structures. In particular, the thermal conductivity assumed a very high value, while the volumetric heat capacity has been lowered to negligible importance.
- The inlet and outlet water collector volumes at the bottom and the top of the PHX tubes have been greatly reduced in size in order to reduce any lag in density wave propagation.

All the local pressure drops coefficients have been derived from [2.16] and applied in the RELAP5-3D model.

A series of Control Variables [2.17] has been programmed in order to evaluate the parameters of relevant interest for the problem and to allow an accurate definition of the stability curve.

2.3.3.2 Two-phase instability typologies found in PHX analysis

Ledinegg instability

The PHX behavior against Ledinegg instability has been studied through a simplified version of the RELAP5-3D PHX model, only featuring one water tube heated by one LBE channel.

[14] The LBE pipe element has been modeled according to inner elementary cell geometry, thus neglecting edge tubes effect. This has an impact on flow area, hydraulic diameter and, as a consequence, on mass flow rate.

[15] The mass flow rate has been evaluated as twice the mass flow rate of a single PHX unit divided by the total number of secondary tubes.

In order to investigate Ledinegg instability, the water channel pressure difference in function of the water mass flow rate must be evaluated. Thus, assuming constant primary power (i.e., constant LBE temperatures), the water mass flow rate has been progressively reduced.

The evaluation has been performed at power levels of 100% and 7%, respectively representing full power conditions and decay heat removal conditions.

The conclusions are shown in Figure 2.13.

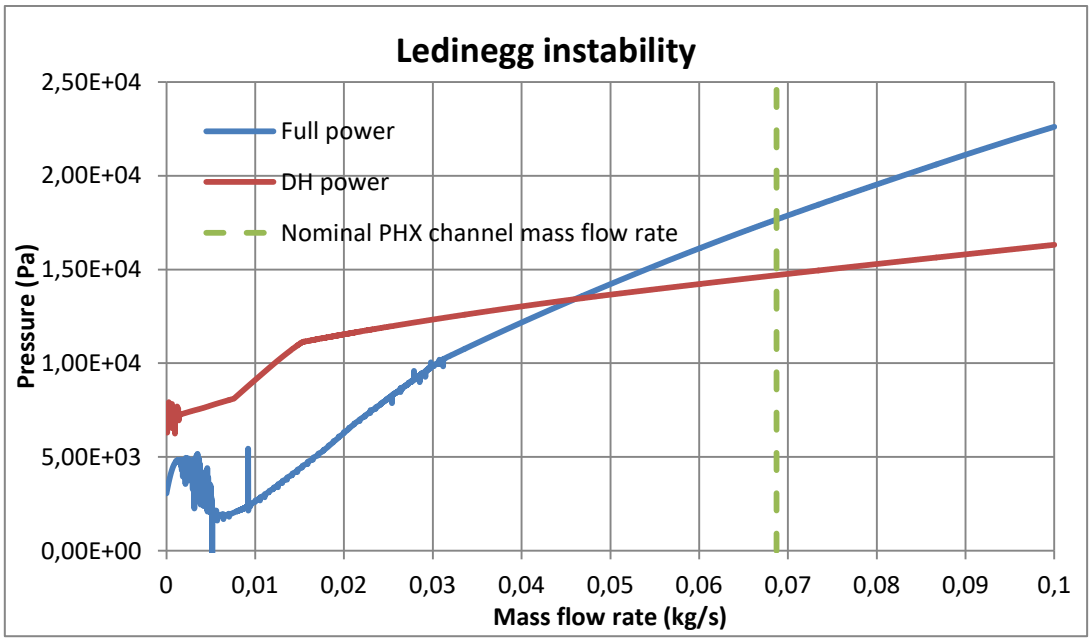

Figure 2.13 - PHX Ledinegg instability chart

From the evaluation, it appears that the system undergoes Ledinegg instabilities only at very low mass flow rates ranges (~15% of nominal value), which are not considered during normal operation. The stability margin is assured by the low nominal exit quality (~30%) which prevents the system to operate in proximity of unstable regimes

In case of DHR, the instability threshold shifts to ~3% of the nominal mass flow rate value, which is well above the natural circulation value [2.18].

In conclusion, Ledinegg instability does not represent an issue for the MYRRHA PHX.

However, this type of instability will be better assessed when the MYRRHA SCS detailed design is available. It has to be noticed that the adoption of a properly designed pump in the SCS, for normal operation, could result in a stabilizing mean for this type of instability.

Flow pattern transition instabilities

The PHX tube could also be affected by a series of instabilities induced by some specific two-phase flow regimes. In particular, in case PHX active length majority is filled with two-phase water in slug flow or churn flow regime (that is, within certain specific intervals of P/m[16] and

[16] P/m = power over water flow rate ratio.

at certain inlet subcooling levels), the channel flow becomes unstable. Being this instability linked to the channel prevalent flow regime, it cannot be solved through orificing [2.13]. It is important to limit as much as possible the unstable P/m ranges in all the operational conditions by shifting the channel into annular flow.

This kind of instability could represent an issue especially during the reactor operational transients (start-up) or, in general, during operations at low power regimes.

In this case, a power ramp has been simulated through the LBE primary boundary conditions changing linearly from 0% to 100%. Thus, all the relevant flow regimes are encountered and it is possible to see an unstable behavior of the PHX tubes. The water has been considered flowing at full flow and entering the PHX at 200 °C.

From the RELAP5-3D analyses, it appears that, in the considered water conditions, the PHX tube active section is mainly lying in the slug flow regime with primary power between 10% and 20% (Figure 2.14).

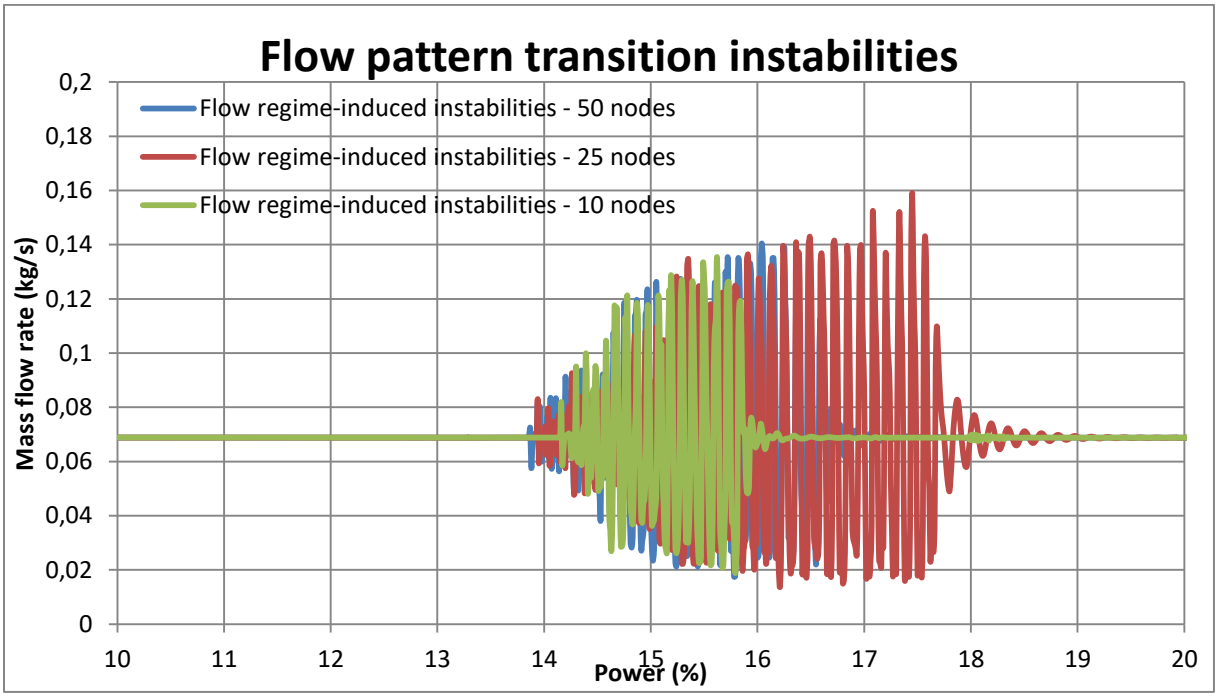

Figure 2.14 - PHX slug flow pattern transition instabilities (100% water mass flow rate)

At lower inlet temperatures (higher subcooling), the flow pattern transition instability is "incorporated" into the DWO instability range extending on a range of 10÷100% power. Thus, it is not possible to distinguish between the different kinds of instabilities: the pattern transition induced instabilities are studied only when clearly separated from other effects.

In Figure 2.14 it is also shown the effect of different nodalization refinements on flow pattern transition instabilities: it can be noted that all models can predict the insurgency of such instabilities in the same range, with some variability in the highest end of the range.

Density wave oscillation instabilities

In order to study the PHX response to DWO instabilities, a series of tests have been run by varying several parameters in the PHX RELAP5-3D model and performing different runs.

The following three parameters variations have been included in the DWO study:

- The primary system temperatures (providing the primary system conditions representing the different power input).
- The subcooling temperature[17].
- The secondary mass flow rate.

A number of different input decks have been run, each one with a different combination of the three mentioned parameters. A series of Control Variables inserted in the input deck has allowed judging the stability of the selected configuration.

In general, the following effects of different parameters on system stability have been noted:

- Primary power increase shows a destabilizing effect.
- Water mass flow rate decrease shows a destabilizing effect.
- Inlet subcooling temperature increase has a stabilizing effect when near saturation but a destabilizing effect at higher subcooling levels.

An increase in outlet quality seems to shift the system towards a less stable condition, while the effect of inlet subcooling temperature is not always affecting the system in the same way.

These results are in agreement with the approach described in [2.19] and with the general DWO stability theory. In particular, it is possible to draw a single 2-D stability map making use of two non-dimensional numbers including, in their formulation, all the effects described above[18]:

- Phase change number

$$N_{pch} = \frac{q}{m*h_{lv}} * \frac{v_{lv}}{v_l} \qquad (2.2)$$

- Subcooling number

$$N_{sub} = \frac{h-h_f}{h_{lv}} * \frac{v_{lv}}{v_l} \qquad (2.3)$$

From the formulation of the two non-dimensional numbers, it appears clear how two parameters' combinations are enough to understand the DWO instability: the (q/m) ratio identifies the quality evolution in the water tube, while the ($h - h_f$) difference provides a measurement for the subcooling.

These two factors are weighted on the water pressure through the density and the vaporization enthalpy: it appears that the pressure has, in general, a slightly positive effect on

[17] With "subcooling temperature", the temperature difference between the saturation temperature and the actual tube inlet temperature is assumed.

[18] q = primary power; m = water mass flow rate; h_{lv} = water vaporization enthalpy; v_{lv} = water specific volume phasic difference; v_l = saturated liquid specific volume; h = water inlet enthalpy; h_f = saturated liquid enthalpy

the system stability but the outcome is not always obvious and the variation magnitude is smaller compared to the two previously mentioned factors.

By reshaping all the input parameters' combinations (LBE temperature, water subcooling temperature, water mass flow rate) into the two non-dimensional numbers above mentioned, the following stability map (Figure 2.15) is obtained.

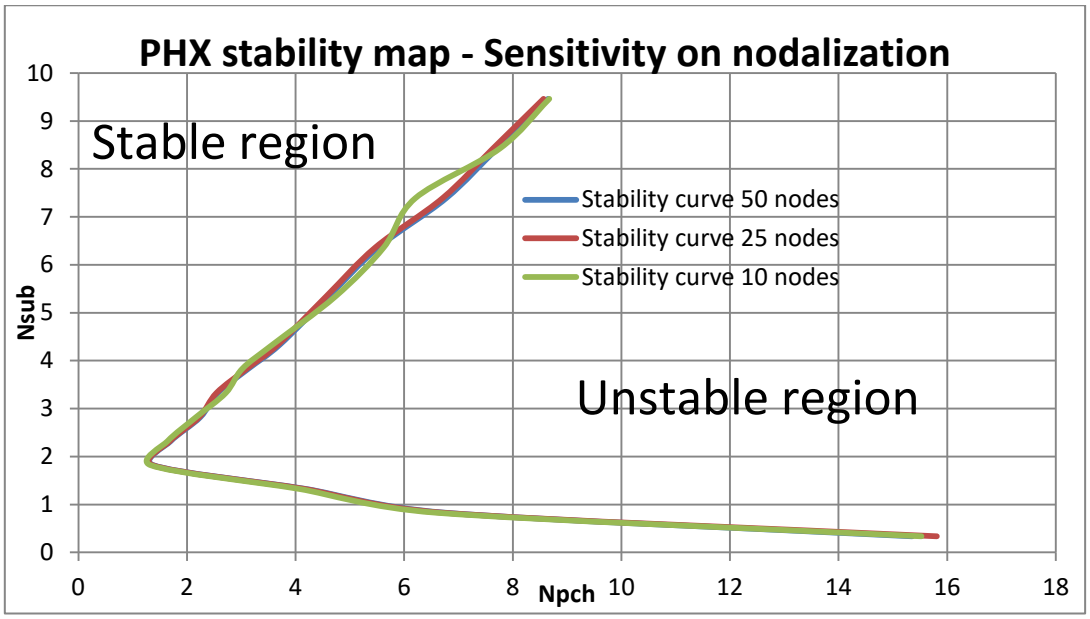

Figure 2.15 - PHX non-dimensional stability map

A sensitivity study on the number of spatial nodes used to simulate the PHX tube bundle active length has also been performed: three different sets of simulations (respectively with 50, 25 and 10 nodes) have been run to draw the PHX stability map.

The main conclusions can be summarized as follows:

- At nominal mass flow rate and subcooling conditions, it is possible to run the reactor at ~ 30% of maximum power before incurring in DWO instabilities.
- In case of increased subcooling (up to ~8 °C less than saturation temperature), the maximum achievable power could be reduced < 5% nominal power. By furtherly increasing the subcooling, the stability range increases (N_{sub} > 2).
- The three different nodalizations are nearly equivalent at low N_{sub} values (tube inlet temperature close to saturation), while some minor differences can be noted while increasing N_{sub}. The overall qualitative trend is, however, the same.

In conclusion, the PHX does not seem to offer a satisfying response against DWO instabilities. The adoption of corrective measures is thus strongly recommended and actuated through the insertion of an additional pressure drop throttling device (orifice) in the monophasic region.

2.3.3.3 Orifice dimensioning

In order to limit unstable channel behavior and to extend the reactor operational ranges, especially looking at DWO instabilities, it is possible to place an inlet throttling device (orifice) at the inlet of the tubes in the bundle, so to increase the local pressure drop in the single phase region, thus compensating the two-phase pressure drops and increasing the stability region in the map.

The further analysis has been conducted by relying on the more refined model.

By assuming a local pressure drop factor K = 1.8, an orifice with the following dimensions has been identified [2.15]:

- Diameter: ~3.1 mm (about 22% of the tube internal diameter, corresponding to ~5% of the flow section)
- Length: 80 mm (same length of the lower tube plate)

The overall effect can be noted on the DWO stability map, where the stability line is shifted towards right, thus increasing the operating parameters ranges.

It could be possible to further increase the local pressure drop factor by decreasing the orifice diameter, but the influence on the stability region extension would be limited and potential problems with local water velocity could arise.

The orifice has been represented in the RELAP5-3D model through the adoption of correct section, pressure drop factor and hydraulic diameter in the junction connecting the PHX lower plenum with the two PHX tubes.

The stability map of the orificed tube bundle can be seen in Figure 2.16.

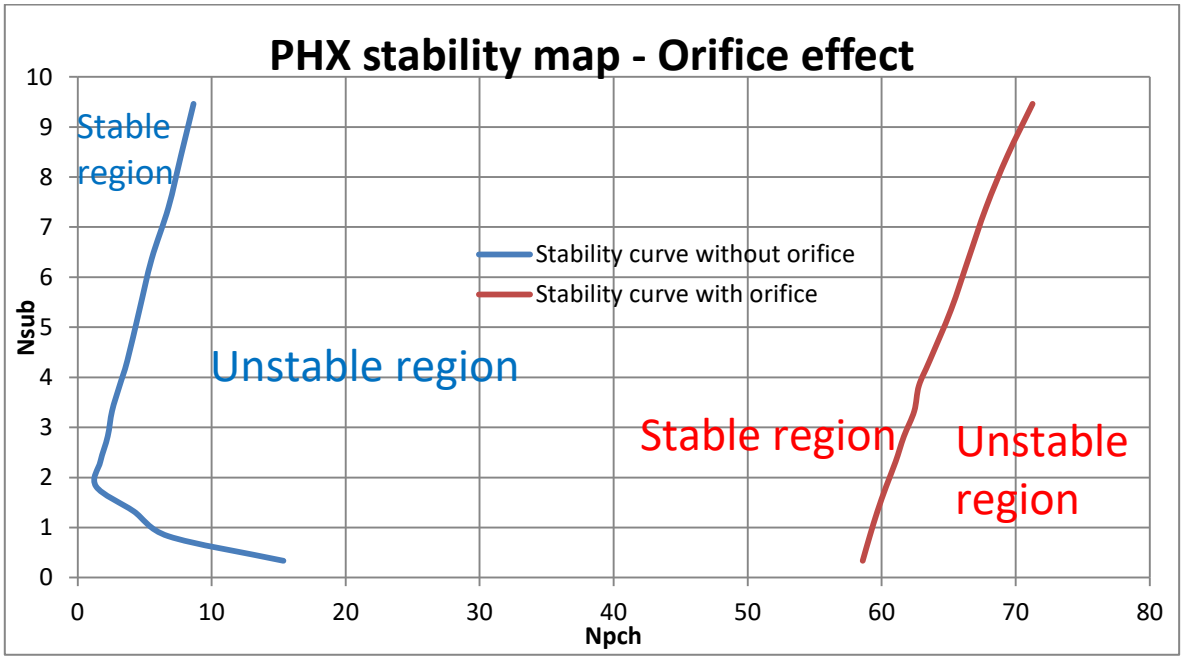

Figure 2.16 - PHX tube bundle stability map (with orifice)

From the new stability map it is possible to note how the stability range has been greatly increased towards high values of N_{pch}, which means that high P/m ratios can be achieved without incurring into DWO instabilities. In particular, the nominal operation condition for the PHX is now stable, with stability range extending also with increased ΔT_{sub}. In general, all conditions within the nominal P/m ratio are stable against DWO, with a limit occurring at ~110 % power when N_{sub} ~0.3.

2.3.3.4 Perturbation induced instability

The adoption of an orifice allows extending the stable region considerably. However, resolving or mitigating the different instabilities in a boiling channel configuration proves to be not enough to guarantee the stability of the continuous PHX operation. An additional requirement concerns the stability to induced perturbations through local mass flow rate disturbances or local power spikes. Such "induced instability" usually appears at power levels found to be stable for DWO but relatively close to the instability threshold.

An induced flow perturbation has been simulated in the RELAP5-3D PHX model through a sinusoidal closure valve semi-cycle with duration of 0.2 seconds applied to a servo-valve component placed at the inlet of one of the two tubes. Second tube flow is maintained unperturbed.

When the plant is operating in normal operation conditions, including the previously dimensioned orifice, the behavior of the system subject to the mass flow rate perturbation can be represented as follows (Figure 2.17).

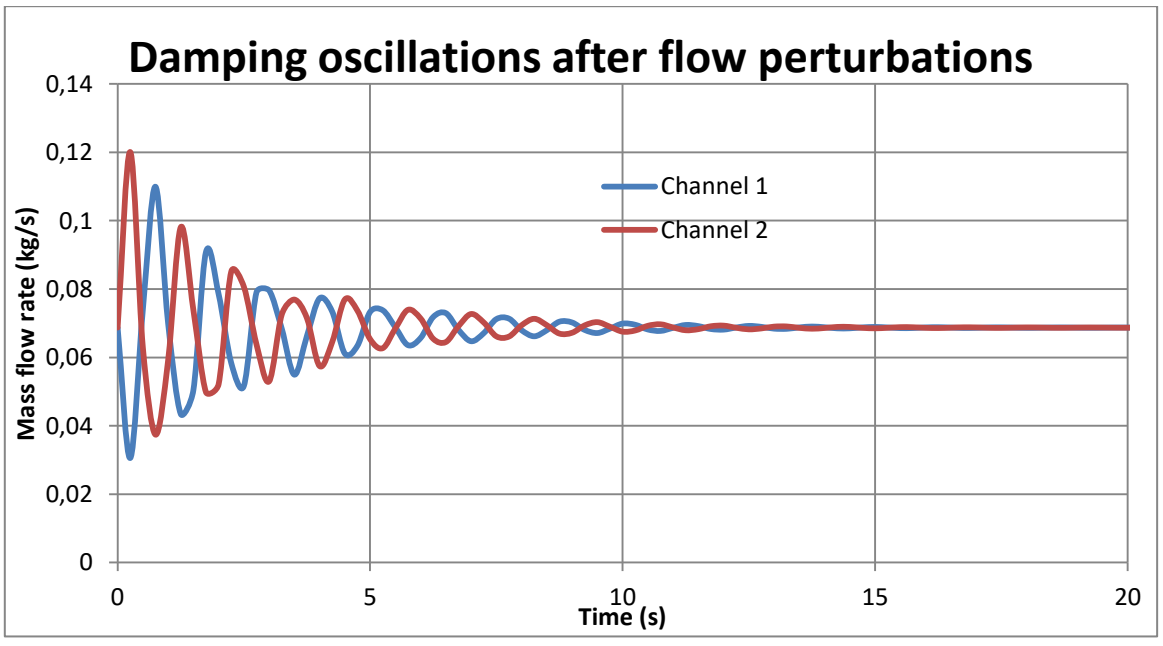

Figure 2.17 - Damping oscillations following a mass flow rate perturbation

In this specific case (not representative of all possible configurations), the mass flow rate perturbation has been imposed during a simulation of normal operating conditions, which resulted to be stable to DWO instabilities after the adoption of the orifice.

A series of oscillations is triggered in the two channels after the perturbation. The induced oscillations can be considered completely extinguished after ~20 seconds from the mass flow rate perturbation. This system behavior is considered qualitatively acceptable since no amplitude increase is noted in oscillations. However, a stability criterion has to be chosen in order to maintain in any operating conditions an adequate margin from the instability threshold and this has to be established in conjunction with the control system requirements.

Without the orifice placed at the tube bundle inlet, the system in normal operating conditions would have been in the unstable region for DWO instabilities, while the adoption of the orifice shifts the system in the stable zone, also reaching a satisfying behavior against flow perturbations.

In general, an induced perturbation is damped more quickly at lower power, while it tends to oscillate slightly more in case of higher subcooling.

While approaching the DWOs instability limits (see Figure 2.15 and Figure 2.16), a slower oscillation damping or even the insurgency of amplifying oscillations following a single channel perturbation can be noted. This phenomenon imposes a more stringent constrain to the PHX design against instability, which can be quantified according to the chosen stability criterion.

2.3.4 Mechanical assessment main results and conclusions

Once the PHX thermal-hydraulic design has been completed, proving that all functional requirements are satisfied, a mechanical assessment is required.

A preliminary mechanical analysis revealed the existence of a number of potential issues, generated by the differential thermal expansion of the feedwater tube, the tube bundle and the external shroud. A series of features has been introduced to limit the impact of such mechanical issues on the correct and safe operation.

The mechanical analysis of the PHX has been performed according to the RCC-MRx v2010 [2.20] construction code rules.

The Level A loading conditions (normal operation[19]) are applied during the normal operation mode and the maintenance mode. Specifically, the design pressure assumed for all the pressurized components is 30 bar, while for the parts not subject to pressure a value of 5 bar has been considered. The thermal loads are based on the normal operation temperatures.

A complete seismic assessment will be required as a part of the mechanical design.

[19] Design Basis Condition 1 (DBC1).

2.3.4.1 Load analysis

Level A loadings include primary loads (type P) and secondary loads (type S). The former are more penalizing during maintenance mode, while the latter are generally higher in normal operation mode. The PHX Level A mechanical analysis has taken into account the highest loads for conservativeness.

The damage prevention analysis from Level A type P and S loadings has been conducted through analytical design formulas from RCC-MRx construction code and by the use of ANSYS 14.0 finite element code [2.12].

The analytical verification has been applied for the following components:

- Tube bundle
- Feed-water pipe
- External shroud
- Bellows in the upper head

Two bellows (see Figure 2.18) have been inserted in the design to relieve stresses caused by differential thermal expansions:

- Internal and external feedwater pipe walls (relative displacement: 21.5 mm)
- Upper tube sheet and external feedwater pipe (relative displacement: 19.4 mm)

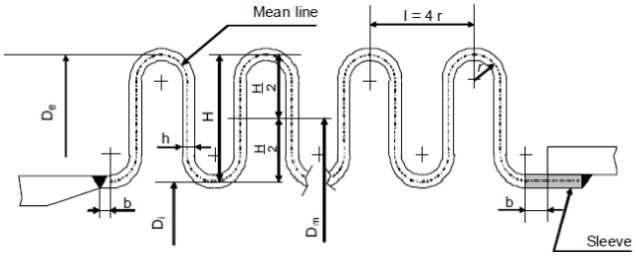

Figure 2.18 – Bellow design

The insertion of the bellows caused a decrease of the space available for the tubes. Therefore, the PHX outer diameter has been increased (with respect to the first thermal-hydraulic evaluation) to preserve the thermal efficiency.

The FEM analysis has been applied for the overall mechanical verification and the local verification of the upper and lower tube sheets. Moreover, a specific model has been built to preliminary assess the restraints foreseen against vibrations (spacer grids). In total, four different FEM models have been realized, with different degrees of details:

- Complete PHX
- Single tube
- Tube sheet
- Tube beam model (for vibration analysis)

Table 2.4 shows the overall mechanical verification results for prevention of type P and type S loading conditions[20]:

Table 2.4 – PHX mechanical verification results

	P_m (MPa)	S_m (MPa)	P_m+P_b (MPa)	1.5 S_m (MPa)	P_m+P_b+Q (MPa)	3 S_m (MPa)
Lower tube sheet	33.14	110.8	75.18	166.2	165.42	332.4
Upper tube sheet	35.98	117.6	68.18	176.4	67.94	352.8
Lower head internal wall connection to lower tube sheet	34.51	117.6	133.77	176.4	57.74	352.8
Lower head external wall connection to lower tube sheet	13.95	110.8	45.71	166.2	248.26	332.4
Shroud connection to upper tube sheet	26.19	110.8	58.39	166.2	238.18	332.4
FWP external wall connection to lower tube sheet	53.49	110.8	89.71	166.2	197.73	332.4
FWP internal wall connection to lower tube sheet	74.01	117.6	85.08	176.4	76.68	352.8
Flange	43.69	117.6	74.65	176.4	147.63	352.8

All the combination of mechanical loads foreseen by the RCC-MRx code (membrane, membrane + bending, membrane + bending + secondary loads) are below the foreseen maximum value: the PHX design is thus considered as proven.

2.3.4.2 Vibrational analysis

The PHX is characterized by a long tube bundle, which will require adequate supports to prevent mechanical fatigue failure due to excessive vibrations.

A preliminary vibrational analysis determined two additional features to strengthen the tube bundle:

- The replacement of 8 tubes with 8 tie-rods.
- The positioning of 7 support plates (spacer grids), spaced 1070 mm each other.

[20] A complete description of mechanical analysis can be found in [22].

The spacer grids have been already considered in the determination of the primary side pressure drops.

2.4 Primary Heat Exchanger design implications towards DHR functionalities

The thermal connection between the primary and the secondary system is provided by the PHX. Among its functional requirements, the PHX must be able to operate in DHR conditions, transmitting the decay power from the primary LBE to the SCS.

2.4.1 Heat Transfer Coefficient variations in function of mass flow rates

The MYRRHA SCS, operating with two-phase water pressurized at 16 bar, assumes, in abnormal or accidental condition, the function of DHR-1 system. As such, it is required to be able to remove the decay heat power only relying on natural circulation, driving the system parameters towards a safe shut-down condition. This is a very important functional requirement because it is directly connected to the system safety and the respect of the failure limits.

The PHX design is favorable to the onset of natural circulation in both primary and secondary loops:

- The geometrical center of the PHX active tube bundle length is positioned 1 m above the geometrical center of the active core[21, 22]: this component arrangement supports the natural circulation onset in the primary system.
- The large water feedwater tube located in the PHX center is thermally insulated by the primary system thanks to the double-wall structure, while tube bundle is not insulated: this feature supports the water natural circulation onset in the correct direction thanks to the density decrease in tube bundle (flowing upwards), avoiding reverse flow.

The small variability of overall HTC has a very positive impact on the DHR function as well. In case of Loss Of Offsite Power (LOOP) accident, the reactor is shut down and all the systems are supposed to work in natural circulation. It has been noticed how the primary LBE natural circulation mass flow rate stabilizes to a value of ~15% of the nominal rate, while the secondary water flow is reduced to ~50% of its nominal value [2.21].

These variations are not enough to determine a severe drop in overall HTC coefficient across PHX tubes, thus the global decay heat removal capability remains very efficient. As a direct consequence, the primary system temperatures evolve toward a safe shutdown conditions and the clad failure limit is respected with wide margin.

On the other hand, this feature could lead to issues related to SCS overpressure and, in the longer term, to LBE freezing. Such scenarios should be evaluated and suitable actions taken for prevention and mitigation.

[21] This is a design requirement.

[22] In natural circulation, the distance between the thermal centers is higher than the geometrical centers, thus providing additional driving force for the fluid [2].

2.4.2 Importance of the extended inlet windows

The PHX inlet windows extend ~1.4 m in axial length. The possibility to adopt a wide inlet for LBE allows the implementation of an extended inlet flow area in nominal conditions and a guaranteed minimum flow area for DHR conditions in case of primary vessel break. It is thus possible to use a greater length (compared to the active length defined) of the tube bundle in normal operation, while guaranteeing the natural circulation path in case of LBE level decrease caused by a vessel break.

References

[2.1] R. Fernandez, "Mechanical design of the primary system," SCK•CEN Internal Report, Mol, September 2015.

[2.2] D. Castelliti, "Preliminary Design Description of Primary Heat Exchanger," SCK•CEN, Internal Report, 1172152, Mol, 22 August 2016.

[2.3] G. Scheveneels, "Internal initiating events (MYRRHA v1.6)," SCK•CEN Internal Report, Mol, February 2017.

[2.4] "http://www.mathworks.com," [Online].

[2.5] OECD/NEA, "Physics and Safety of Transmutation Systems, A Status Report," 2006.

[2.6] X-Steam function of Matlab R2010a for water and steam thermodynamic properties, IAPWS IF97 standard.

[2.7] P. Ushakov, A. Zhukov and N. Matyukhin, "Heat transfer to liquid metals in regular arrays of fuel elements," High Temperature, 1977.

[2.8] N. Todreas and M. Kazimi, Nuclear Systems Volume 1 - Second Edition, CRC Press Taylor & Francis Group, 2012.

[2.9] RELAP5-3D Code Manual, Idaho Falls: INEEL-EXT-98-00834, Idaho National Laboratory, 2014.

[2.10] D. Castelliti, "RELAP5-3D MYRRHA ver. 1.6 Model Description," SCK•CEN Internal Report, Mol, April 2016.

[2.11] A. Nalbandyan, "Hydraulic Assessment of the MYRRHA Primary Heat Exchanger," FH Aachen University of Applied Sciences, Jülich, September 2017.

[2.12] "ANSYS CFX Reference Guide," 2012.

[2.13] J. A. Boure, A. E. Bergles and L. S. Tong, "Review of Two-Phase Flow Instability," *Nuclear Engineering and Design,* vol. Volume 25, pp. pp. 165-192, July 1973.

[2.14] L. Mansani, "Flow stability studies for the CIRENE reactor," in *JUICE Meeting*, Toronto, 14-15 August 1978.

[2.15] D. Castelliti and G. Lomonaco, "A preliminary stability analysis of MYRRHA Primary Heat Exchanger two-phase tube bundle," *Nuclear Engineering and Design,* vol. 305, pp. pp. 179 - 190, 2016.

[2.16] I. E. Idelchik, Handbook of Hydraulic Resistances, 4th Edition Revised and Augmented ed., Begell: Hemisphere Publishing Corporation, 2008.

[2.17] RELAP5-3D Code Manual Volume II: User's Guide and Input Requirements", Idaho National Laboratory: INEEL-EXT-98-00834, Rev. 4.2, 2014.

[2.18] D. Castelliti, G. V. D. Eynde, K. V. Tichelen and B. Arien, "Safety Analysis of the MYRRHA Reactor," in *NURETH-16 conference*, Chicago, August-September 2015.

[2.19] M. Colombo, A. Cammi, D. Papini and M. E. Ricotti, "RELAP5/MOD3.3 study on density wave instabilities in single channel and two parallel channels," *Progress in Nuclear Energy,* 2012.

[2.20] AFCEN, RCC-MRx - Design and Construction Rules for Mechanical Components of Nuclear Installations, Paris, 2012.

[2.21] D. Castelliti, "FP7-MAXSIMA Work Package 2 "Safety Analysis in support of MYRRHA" Main Outcome and Conclusions," in *NURETH-17*, Xi'An, September 2017.

[2.22] A. Van Ende, "MYRRHA - Mechanical design of the Primary Heat Exchanger," Tractebel Engineering, Internal Report, Brussels, 2012.

Chapter 3: Primary Heat Exchanger Tube Rupture Accident

In a liquid metal cooled reactor (critical or ADS), the Heat Exchanger/Steam Generator tube rupture (HX/SGTR) represents an important accidental event, whose consequences have to be deeply analyzed especially in case of pressurized water as secondary cooling fluid, as it is the case for heavy liquid metal (HLM) reactor designs and for MYRRHA.

Some of the HLM plants currently in design phase (in particular the facilities having electricity generation as main purpose) operates the secondary water/steam system at high pressures (~180 bar) and temperatures (~450 °C), by producing overheated steam. In the case of MYRRHA, the power exchange between LBE and water does not lead to steam generation (water temperature maintained in nearly saturated conditions at ~16 bar/200 °C).

Because of this, in the MYRRHA case, such event is referred as "Primary Heat Exchanger Tube Rupture" (PHXTR).

3.1 Heat Exchanger/Steam Generator Tube Rupture (HX/SGTR) accidental event analysis: state of the art

PHXTR accident evolution in the MYRRHA reactor can be divided into 4 main phases determining an accidental sequence potentially leading to multiple scenarios:

1. Water release in the Primary Vessel (critical mass flow rate)
2. Pressure wave induced by rupture and liquid displacement and sloshing consequences on surrounding internals
3. Potential Coolant-Coolant Interaction and steam explosions risk
4. Multiphase transport

In comparison with the analysis reported in [3.1], including only the last three phases, the first one has been added at the beginning of the event. A correct and appropriate estimation of the mass flow rate leaking from the PHX is required in order to estimate the most correct "source term" to be used as a boundary condition for the following phases, hence the need to study the two-phase critical mass flow rate expected in the early stages of the transient evolution.

This accidental sequence can have several consequences [3.1]:

- A pressure shock wave generated by a sudden high pressure discharge into the HLM cooled primary system: this could lead to the damage of other neighbour tubes inside the PHX due to the mechanical loads generated by the pressure wave, thus initiating a very dangerous "domino effect" that could potentially bring to a fast release of a considerable fraction of the water inventory present in a secondary loop.
- A pressure peak in the reactor vessel due to the sudden energy release into the primary vessel (2-phase water flashing) that could have serious consequences on the vessel integrity.
- A sloshing phenomenon, consisting in the formation and expansion of a "mixed zone" volume (HLM-superheated steam) and causing the displacement of the primary coolant, with potential damage for the core, core above structures, pump, or PHX itself.
- A potential steam explosion, that could happen in case a colder pressurized liquid interacts thermodynamically with an hot liquid metal ($T > T_{sat}$) and flashes into steam.
- A gradual pressurization of the vessel, expected as a consequence of the steam phase build-up into the primary vessel.
- A relatively low quantity of steam bubbles could be carried by the HLM flow through the pumps and into the core, with possible positive reactivity insertion.
- An entrainment phenomenon could happen in case some HLM droplets are carried upwards by the steam flow through the safety valve, with the risk to limit or block the valve functionalities and to entrain Polonium molecules dissolved in LBE.

3.2 Previous studies for each accident evolution phase

Several detailed studies have been approached in order to analyze each phase of a typical HX/SGTR event. A review of the state of the art for each phase is provided.

3.2.1 Two-phase critical mass flow evaluation

First step for the PHXTR event analysis in the MYRRHA reactor consists in evaluating the most correct amount of water release in the Primary Vessel. A correct estimation can be provided by two-phase critical mass flow rate through the break, in function of the break size, shape and position in the PHX tube.

The evaluation must be done accordingly to the real PHX geometry [3.2] and taking into account the actual SCS layout and water content [3.3].

Several two-phase critical flow models have been developed, assuming different hypotheses, in order to achieve a better simulation of the phenomenon. An adequate two-phase critical flow model must be selected in order to evaluate the initial mass flow rate through the break, which is independent from the primary LBE conditions in terms of pressure and temperature.

An extensive review of all the possible approaches is provided in [3.4], where the two-phase critical flow models available are classified according to their assumptions and hypotheses.

Several models classifications are possible [3.4]:

- Equilibrium models: models which assume thermodynamic equilibrium throughout the expansion
    - Homogeneous models: equal vapor and liquid velocities (HEM)
    - Non-homogeneous models: different velocities for the two phases
- Non-equilibrium models: models which assume no thermodynamic equilibrium, no mechanical equilibrium and no chemical equilibrium persists between the two phases
    - "Frozen"[1] models
    - Full non-homogeneous models

The most promising two-phase critical flow models appear to be [3.5] the Henry-Fauske model [3.6] and the Ransom-Trapp model [3.7] both used in the latest release of RELAP5-3D code [3.8]: both of them belong to the non-equilibrium and non-homogeneous category but, in their simplest form, it is possible to reduce them to frozen models.

[1] "Frozen" is intended in the sense that the quality at the pipe inlet is preserved to the outlet, or, that no mass or energy transfer is supposed to happen between the two phases.

3.2.2 Pressure waves and dynamic interactions between the discharged jet flow and the molten LBE

Once the water mass flow source term has been defined through two-phase critical flow analysis, the second stage is characterized by the two-phase mixture flashing and quick expansion.

The result of this first two-phase water interaction with LBE is a pressure shockwave caused by sudden steam expansion, whose force generated on neighboring tubes has to be properly assessed in order to understand the risk of a "domino effect" due to successive tube breaks. This analysis is especially important to avoid the risk of a "catastrophic break" of the PHX with sudden release of a considerable fraction of the complete water inventory into the primary pool; in case of tube break, it is not unlikely for the neighboring tubes to be structurally weakened (for very same reason causing the break), thus emphasizing the importance of an accurate mechanical load estimation.

A simple model for shock-wave predictions in HLM environment has been evaluated in [3.9], by using one-dimensional balance equations and Homogeneous Equilibrium Model (HEM) for two-phase water.

A more accurate estimation of the shockwave generation in a liquid metal and its propagation to the other structures has been provided through methods used for accidental release of liquefied gases (Boiling-Liquid Expanding-Vapor Explosion, BLEVE) [3.10] [3.11], which provided results with good agreement with experiments.

However, it could be envisaged to explore the shockwave propagation and its "translation" into mechanical loads through the application of finite elements code especially suitable to evaluate impacts and explosions simulations. The determination of the induced stresses to other reactor structures is important to determine the consequences of a PHXTR accident in a real pool-type nuclear installation: it is thus foreseen to evaluate this scenario in the MYRRHA reactor conditions.

3.2.3 LBE displacement and pool sloshing

During the third phase of a typical HX/SGTR accident, the two-phase mixing zone will experience an expansion, following the shockwave release. The expansion will be driven by the potential instability of the discharged jet of boiling liquid and subsequent dispersal of the volatile coolant into LBE. The multi-phase mixing zone is experiencing an expansion during this phase and, as a consequence, the structures in the vessel will be interested by the sloshing caused by this motion with potentially dangerous consequences.

A simple, first approximation approach attempted by Dihn [3.1] for the mixture expansion could consist in assuming that no mixing occurs between the water (liquid and steam) phase and the LBE phase. The steam phase is thus collected into one single bubble which will expand (steam cavity); volume and internal thermal-dynamic conditions can be estimated through mass and energy balance equations. The expansion can be notable because of the

monotonic trend due to the fact that no condensation occurs, being the water-steam released into a low pressure, high temperature environment which will superheat the mixture.

A more complex approach, as shown by Beznosov [3.12], would imply to consider and evaluate the water-steam fragmentation and dispersion into the HLM in a complex multiphase scenario; despite being probably a less conservative approach for what concerns the pressure peak, a better estimation of the number and the size of the water and steam bubbles suspended in the LBE stream will lead to a more accurate prediction of the heat transfer phenomena involved, the energy releases and the kinetics of the interactions.

For what concerns the evaluation of the consequences of the HLM sloshing effects onto the reactor internals, an estimation of the mechanical loads on the structures could be done through similar computational tools used for the pressure wave loads.

3.2.4 Coolant-Coolant Interaction (CCI) and steam explosion

The fourth phase is of most relevance for the plant safety assessment for what concerns the steam explosion risk. The steam explosion risk is directly connected to the Coolant-Coolant Interaction (CCI) and the energetic balances linked to this phenomenon.

While a wide literature is available for the Fuel-Coolant Interaction problem (connected to the severe accident scenarios in LWRs), very little is present for the CCI. Nevertheless, it is possible to adapt some of these methods and derive certain approaches that could be used for CCI analysis as well.

In principle, the energy available in CCI is lower, considering the analogy with FCI phenomenon. It can be easily proven by comparing the energy available in a molten fuel drop (T ~3000 °C plus the latent fusion heat) with the energy carried by secondary system water (T ~200 °C, p ~16 bar). Moreover, the limited water-steam mass flow rate into the primary vessel will have a slowing effect on the bubble formation and interactions. Nevertheless, the potential consequences on reactor internals deriving from a steam explosion cannot be neglected, and a possible multiple chain-rupture effect should be assessed in order for the design to be modified accordingly. Also, even the relatively low-energetic CCI reactions could have an influence on the multi-phase transport phase, conditioning the bubble motion into the LBE.

A series of experiments [3.13] [3.14] [3.15] [3.16] of water jets released on a LBE pool have been performed, proving how no steam explosion should occur if the contact temperature is kept lower than the homogeneous nucleation temperature ($T < T_{hn}$).

However, as already mentioned, a HX/SGTR usually experiences (at least in its earlier phases) a two-phase critical discharge flow, which bears sonic or nearly-sonic velocities. As a consequence [3.1], it is physically reasonable to expect a low likelihood for large liquid drops to form in the mixing zone in the early time period. The triggering mechanism due to the collapse of a large steam bubble is, thus, not of major relevance, unless the conditions for large steam bubbles coalescence should verify.

A stability criterion for FCI steam explosion trigger (based on balance equations and closure state relations) has been developed in [3.17]: the overheated vapor layer is not only described

in its state properties but an evaluation of its growth and stability over time is also provided; a similar approach can be followed for the CCI basing not only on the total energy quantity available but also on the steam bubble expansion rate and eventual instability leading to an explosion.

The instability-induced fragmentation, as explored in [3.18], is one of the possible consequences of steam bubble instability, eventually leading to a steam explosion. The internally generated instability generates a shock-wave which (besides further sloshing effects in LBE) can perturb the equilibrium of other steam bubbles, thus "fragmenting" them in multiple explosions.

3.2.5 Multiphase mixture transport

The last phase of a HX/SGTR accident involves the interaction of the three phases (liquid water, vapor water and LBE) according to the multiphase balance equations. The multiphase mixture transport has been already analyzed in several studies performed with CFD and coarse-mesh codes (e.g. SIMMER III) aiming at qualifying the behavior of the liquid/vapor phase in the LBE stream.

The possible multiple scenarios can be a function of several parameters representing the initial and boundary conditions of the problem [3.19]:

- Bubble dimension
- LBE flow path and characteristics
- System geometry

All these parameters can be estimated through reasonable guesses, following the approach currently adopted, or be calculated using analytical and numerical models representing the accident evolution during the previous phases, as mentioned before.

The majority of these studies have been based on code simulations such as SIMMER-III [3.20], STAR-CCM [3.21], ANSYS CFX [3.22] and OpenFOAM [3.23], or on a number of preliminary experimental campaigns conducted in the framework of several European projects, e.g. FP6-ELSY [3.24], CDT [3.25], DEMOCRITOS [3.26], by means of different single effect testing HLM facilities at various research centers like ENEA (LIFUS5 [3.27] [3.28] and CIRCE [3.29] [3.30]), KIT (KALLA [3.31]), KTH (TALL [3.32]) and JAEA (TEF) [3.33].

Thus, the results provide a detailed overview of the potential multiphase transport scenarios following a HT/SGTR event, without, though, being able to adopt a coherent set of boundary and initial conditions, thus making the results varying within broad ranges which are not directly applicable to the MYRRHA design. Besides, the experimental campaigns have been mostly conducted by adopting sets of parameters not representing the foreseen MYRRHA design conditions, but more suited for other HLM reactors designs (e.g. ELSY, ALFRED)[2], thus making the results not directly useful for MYRRHA purposes.

[2] These facilities, designed to be power reactors, adopt pure Pb as primary coolant (→ high temperatures) and foresee very high pressures (~180 bar) in the secondary water system.

Moreover, these code analyses are only considering the multi-phase transport of water-steam into HLM. In order to complete the HXTR analysis in MYRRHA reactor, thus "closing" the problem, it is important to assess the potential LBE release into cover gas by steam entrainment effects. An approach has been attempted in [3.34], by describing the LBE entrainment, the transport in pipes and the possible droplet removal systems. It will be necessary to complete the analysis by implementing the whole MYRRHA configuration (i.e. including also the safety release valves and the steam dump system).

The code-based studies represent, nevertheless, a major effort towards an understanding of the multiphase transport phenomena of water-steam bubbles into a flowing HLM acting as primary coolant for a fast nuclear reactor.

The research studies mentioned, focused on the analysis of the phenomenology implied within the first phases of the SG/HXTR accident evolution, were not aimed at investigating the evolution and the consequences in a nuclear reactor environment but more concerned on a smaller scale behavior which does not take into account the complex environment of a pool-type reactor, while, on the other hand, for the multiphase transport phase several reactor simulations are available, with a number of them also investigating the possibility of reactivity insertion due to void transport into the core.

3.3 Recent studies

Though the problem has been preliminary studied by many different laboratories, the biggest efforts toward the comprehension, the classification, the mitigation and the prevention of this accidental event have been done in EU-funded projects focused on HLM-cooled reactors, where the majority of the efforts has been channeled in.

A description of the main findings and conclusions on the HX/SGTR accident from the different projects is exposed hereafter. As previously mentioned, with the exception of the analysis performed by KTH in the framework of ELSY project, the studies conducted through coarse and fine mesh codes mostly focus on the multiphase transport of bubbles.

3.3.1 FP6 ELSY project

Several analyses, simulations and experiments have been conducted in the framework of the European ELSY project. Though notable differences separate ELSY and MYRRHA reactor design (PHX design, operating temperatures and pressures), it is possible to draw some interesting conclusions from ELSY studies as well.

3.3.1.1 ENEA [3.35]

An experimental test has been conducted on LIFUS 5 facility at the ENEA Brasimone research center to simulate a Steam Generator Tube Rupture accident under the operating conditions foreseen in the ELSY reactor. Pre-test and post-test numerical calculation campaigns have been carried out at the University of Pisa to support the experimental activity. The tests have shown that a maximum pressurization level of about 3.2 MPa is reached in the reactor vessel after approximately 0.7 ms from the water injection time, being the pressure water injection equal to 18.5 MPa. A slightly lower value but of the same order or magnitude (2.9 MPa) is achieved in the cover gas. Moreover, two sharp pressure peaks (up to 3.5 MPa) not associated with energy accumulation in the vessel are found in the beginning stage of the transient. Although these peaks seem to be related to shock loads transmitted to the vessel walls, their nature needs to be deeper investigated. However, an important point to highlight here is that while on a full reactor scale it will be reasonably possible to avoid the pressurization peak by designing adequate relief systems (which could not be implemented in the experiment due to the LIFUS 5 facility design limitations), the first sharp peaks not related to energy accumulation might not be avoidable and could impact the surrounding structures and reactor internals. Besides, an experimental facility could not be completely representative (also at a qualitative level) of the full-scale plant.

As for the codes validation, the post-test calculations have shown that SIMMER-III is able to produce results that can be considered, as a whole, acceptable within the limits of the models employed; however, further code validation is needed to verify the SIMMER-III code against most challenging accidental scenarios.

3.3.1.2 KTH [3.36]

Following the approach suggested by [3.1], a more organic and complete approach has been attempted at KTH towards the HT/SGTR accident analysis. No code calculation has been performed, but a series of analytical and semi-empirical models have been applied in order to evaluate the event evolution.

Big uncertainties are present both in probability and consequences of HX/SGTR, which prevent reliable and transparent risk analysis potentially acceptable for a regulatory body. Therefore HX/SGTR may become a bottleneck in licensing of a pool type design of lead cooled systems.

The goal of HX/SGTR research should be the development of design and regulation measures which will reduce probability PHX tube degradation and limit consequences of HX/SGTR by defense-in-depth approach.

Reduction of uncertainty in probability and consequences are prerequisite for risk assessment of HX/SGTR in a lead cooled system. Therefore it is necessary to provide:

1. Deterministic study of tube degradation in HLM cooled systems (to assess the probabilities of tube leakage and rupture).
2. Deterministic study and assessment of severity of consequences of HX/SGTR.
3. Development of appropriate preventive and mitigatory measures in design and regulation (condition of exploitation, frequency of inspections, etc.) to reduce probability and consequences.

The first two steps are part of an iterative process at the end of which it is possible to proceed with the last point. Similar "iterative" design processes are quite common in nuclear technology (LWR steam generators design follows similar principles).

Combined probabilistic treatment and deterministic analysis of PHX tube degradation issues is necessary to give guidance on the “benefits” where further research could give more pay off in term of risk quantification. It is possible to identify now research areas which will give the highest return in terms of uncertainty reduction at the present state of knowledge about HX/SGTR in lead system.

3.3.1.3 JRC-IE [3.37]

A sensitivity study on gas bubble dimension, the velocity and the path taken in the liquid metal pool after the release from the break has been performed.

At first a validation of ANSYS-CFX12 has been made, by comparing calculations with experimental data regarding terminal rise velocities of bubbles in stagnant lead. The results show that the terminal lift velocity is underestimated by about 20%. The bubble model of CFX only allows incompressible bubbles counters to some extent the effect from underestimated lift velocity. As bubbles move deeper, the lift and drag forces are not reduced as they normally would due to increased pressure. The steam generator tube leakage calculations on the ELSY design were made for bubble sizes of 0.1÷10 mm diameter. The studies indicate

that, for leakages below 2 m depth with respect to the HLM free surface, all investigated bubble sizes can reach the core during normal operation. Larger bubbles of 10 mm diameter are least likely to reach the active core and most of them rise to the free surface level. Bubbles of about 1 mm diameter are the most likely to be dragged down to the core region. A bubble passing through the core is not a problem from a reactivity point of view. However, if bubbles collect below the core and at a certain moment pass through it together, not negligible reactivity insertion could arise.

Another issue that concerns steam generator tube leakages is that water/steam released into Pb disturbs the conditioning system of the primary loop, which could react to the sudden oxygen concentration increase before the reactor shutdown. However, the time constants involved in lead oxide formation and precipitation are considerably larger than typical HX/SGTR event time scales, so it is reasonable to assume a limited importance of conditioning system issues.

3.3.1.4 University of Pisa [3.38]

The studies have been focused on a preliminary approach to the HX/SGTR accident analysis (conservative analysis) with the main purpose to verify the suitability of the codes used (SIMMER-III, Marc/Dytran [3.39]) for this task, and to check the difficulties encountered in setting up the model used to represent the structures in the relevant accident conditions in order to rise preliminary attention to possible weak points of the PHX internal structure requiring possible updating improvements.

In the preliminary analyses for the ELSY reactor, the effects of a HX/SGTR accident, which is a design basis event, coupled to the possible arisen fluid-structure interactions, have been studied, highlighting the importance of the effect due to the sudden release of energy and the following increase of pressure, consequences of the water-lead interaction. The pressure peaks are mainly generated by the relative large water discharge and by the following vaporization as well as by the fluid structure interaction due to the fluid motion.

Preliminary numerical evaluations of the Von Mises equivalent stress showed that its maximum values seem to be located at the bottom of the PHX structure. Moreover, the obtained preliminary results highlighted that the PHX and the RV structures walls are locally undergoing high Von Mises stress values.

The fluid movement (sloshing) seems also to be caused by the pressure wave propagation, however with no significant structural consequences in term of stress intensity.

3.3.2 FP7 Central Design Team project

In the framework of Central Design Team (CDT), some code simulations have been performed for preliminary HX/SGTR analysis:

- SCK•CEN simulation (in collaboration with JAEA) [3.40]
- ENEA simulation
- CRS4 simulation

3.3.2.1 SCK•CEN results

The analysis performed at SCK•CEN for the PHX tube rupture in MYRRHA/FASTEF[3] was performed by the SIMMER-III code. The analyses for the single and multiple (seven tubes) tube ruptures were carried out as the reference accidents with some assumptions and approximations.

The results showed that the times when the cover gas pressure reached the limit value of 0.6 MPa (set-up pressure for the opening of the rupture disk) were 120 sec and 25 sec (the net times were 115 sec and 20 sec because the rupture occurred at 5 sec) for the single and multiple tube ruptures, respectively.

For the single tube rupture, the cover gas pressure increased linearly until 0.6 MPa.

The LBE pressures at the PHX and the bottom of the FA also increased linearly and converged on constant values after the safety valve opened although the peaks were observed when the rupture occurred.

For the multiple tube rupture, the results were similar to those in the single tube rupture case although the duration of the transient between the beginning and the opening of the safety valve was shorter than that in the single rupture one (which is coherent).

For the relation of the flow rates between the water from the PHX and the vapour through the rupture disk, the values were poorly-matched. The leakage flow rates from the PHX after the rupture disk opened were about 1.6 kg/s and 6.0 kg/s for the single and multiple cases, respectively (maximum flow rates value before disk rupture: 2.5 kg/s and 20 kg/s, respectively). On the other hand, the average[4] flow rates of the vapour, which were estimated from the integrated mass, were about 1.0 kg/s and 4.6 kg/s for the single and multiple cases, respectively. It was supposed that the cause of these discrepancies was the instability of the vapour flow at the safety valve. This cause was guessed as a numerical problem and it would become better if longer calculation (>150 sec) would be performed. So, it is considered the flow rates of water from the PHX and vapour at the safety valve will have the same values, finally. Further verifications are, nevertheless, required.

These analyses employed some assumptions and approximations due to the restrictions of the SIMMER-III code, but the results conclude that the single and multiple (seven tubes) tube ruptures were not severe and these could be managed by the safety valve. From the viewpoint of the structural analysis, it should be noted that the peak values of the LBE pressure at the PHX break level and at the bottom of the core level would be 1.3 MPa (1.6 MPa for multiple) and 1.0 MPa (1.0 MPa for multiple[5]), respectively. Once the valve is opened, the pressures are the same, regardless of the case evaluated.

[3] MYRRHA/FASTEF is the name of the MYRRHA reactor version that has been adopted in the Central Design Team (CDT) project.

[4] SIMMER III calculations showed a quite unstable solution, thus the reference value for the vapour discharge through the safety valve has been estimated through an average.

[5] Same value is found because of a pressure spike at the PHX break level.

3.3.2.2 ENEA results

ENEA experimental activity focused mainly on high-pressure (> 40 bar) water injection in the small pool of LIFUS 5 facility [3.27]. No tests have been conducted in MYRRHA conditions (a complete matrix is planned within MAXSIMA project), but a series of SIMMER-III calculations have been performed to simulate HX/SGTR event.

Main conclusions and findings:

- For guillotine single tube break, the pressure peak (1.2 MPa) remains within allowable limits for vessel and the void fraction entering the core does not exceed 0.2%.
- In case of "catastrophic" break (lower head collapse) with complete and sudden water inventory release, the pressure peak experienced by primary vessel is beyond design pressure (~3 MPa and the void fraction inserted into the core could reach values above 2%); this event has thus to be avoided "by design" by having double-walled surfaces where the water and the LBE are separated in the PHX (tube bundle excluded), in particular feed-water pipe and lower head.

3.3.2.3 CRS4 results

CRS4 has simulated [3.41] the HX/SGTR accident by means of CFD models (STAR-CCM+).

The approach followed has neglected the dynamic behavior involving the water flashing into LBE and the first seconds of the break, focusing the analysis on the path followed by steam bubbles coming out a break with a constant 2-phase water mass flow rate.

A CFD model has been built consistent with the design and nominal operation updated at July 2011 configuration. The model includes (partially) the influence of the PHX tube bundle geometry on the flow. A stable stationary LBE side flow (2352 kg/s) is obtained (within 1% difference of design value). The scenario consists in injecting 50 dm^3/s (~0.03 kg/s) of steam at the bottom of the PHX tube positioned closest to the pump. It is shown that it is impossible to avoid a large part of the steam entering the casing. Thanks to the flow diverter around the pump pipe, the steam is not entrained directly to the pump propeller, but rather settles and accumulates in the upper part of the casing, which acts as a buffer. It is important therefore that the upper part of the casing is hydraulically largely connected to the cover gas. The current design results to be very resistant to incidental steam entrainment into the cold plenum through the primary pump.

3.4 Evolutions to current state of the art

As shown before, the research on the evolution of the phenomena involved in a HX/SGTR event is advanced under several aspects covering all the accident evolution phases.

However, an extensive and detailed investigation considering the complete accidental sequence evolution taking into account all the phases and all the potential implications has never been attempted or performed.

Several remarks could be moved to the previous studies performed on the HLM HX/SGTR accident scenarios:

- Most emphasis has been placed in code simulations, which struggle in simulating the correct critical flow water input, bubble formation and evolution; this results in just assuming a steam bubble distribution, neglecting the real multiphase characteristics (steam quality, correct bubble diameter distribution, different phase velocities, etc.). The focus is on the last phase (multiphase transport) simply following the steam bubbles and neglecting the events taking place in the previous phases.
- It is assumed the liquid bubbles completely and immediately evaporate once in contact with hot liquid metals. This represents a strong approximation, especially considering how the time constants involved (complete bubble evaporation and bubble transport to the surface) are quite different. The potential damage on the reactor internals depends not only on the amount of water/steam mixture discharged into the primary vessel, but on the actual evaporation rate that dictates the expansive motion of HLM. No CCI can be noted if the liquid phase is neglected.
- Primary and secondary system models:
    - Most experiments and simulations performed so far have focused on the interaction between two-phase cold fluid and hot liquid metal, but with no real concern with regard to the actual system layout: a great number of models neglect the vessel real dimensions and the internals layout, and experimental facilities often cannot provide a correct simulation of a reactor primary pool.
    - The actual water content and the layout of the secondary systems are often not well represented, so the depressurization propagating upstream results to be incorrectly simulated: this could lead to a wrong estimation of the void fraction and, thus, of the break flow.
- The majority of the experimental campaigns performed so far have been focused on HLM reactor designs with different thermal-hydraulic characteristics compared to MYRRHA.

The multiphase flow regimes following the tube rupture are important for the potential consequences of Tube Rupture scenarios. Starting from the current state-of-the-art, several improvements could be envisaged in order to better understand the dynamics of a HX/SGTR and the consequences for a liquid metal pool-type reactor.

Considering the MYRRHA plant, a dedicated study of the HX/SGTR accidental event will prove to be extremely useful for the design and the safety analysis of the reactor.

In particular, it is important to conduct an analysis that could take into account the typical MYRRHA plant design and working conditions.

The HX/SGTR analysis could be developed into three main topics:

- A theoretical analysis investigating a new approach to predict the general evolution of a pressurized two-phase fluid (water) flashing into a hot ($T > T_{sat}$) heavy liquid metal pool, considering all the phenomena taking place in the five phases mentioned before, thus following the complete evolution of the multiphase mixture in the MYRRHA reactor environment, aiming at assessing all the potential consequences for the reactor itself.
- A series of computational simulations to analyze current codes capabilities to simulate a HX/SGTR accident and to properly predict its evolution and consequences.
- An extended experimental program to be conducted in MYRRHA-like conditions in different experimental facilities, in order to prove the validity of the theoretical models and to validate the codes used for the simulation of the event.

3.4.1 Theoretical model

A complete theoretical model should cover all the accident evolution phases previously detailed. A first step towards a "complete" model should require the analysis of the two-phase critical flow at the tube break in function of the break size and shape taking also into account the SCS structure which could play a non-negligible role in determining the most correct flow boundary condition for the problem.

Next step should consider the bubble formation dynamics during the water flashing (sudden evaporation with rapid volume increase) and the possibility of a pressure wave formation and propagation in function of the initial conditions of the water-steam inlet flow and the LBE in the primary system without neglecting all the possible interactions with the vessel internals (from neighboring PHX tubes to other structures). This effect is potentially very dangerous and must be avoided taking appropriate measures in design phase in order to prevent the "domino effect" (multiple tube damage leading to the failure of the entire tube bundle)[6].

Pressure wave propagation will also cause liquid displacement and sloshing phenomena, which will once again interest all the neighboring structures: a correct assessment of the LBE induced velocity is thus required to refine the analysis of the potential damages triggered by the HX/SGTR accident in MYRRHA reactor.

Several studies have been performed in the past over the FCI in the frame of LWR severe accidents analysis, and a number of theoretical semi-empirical models have been developed. But, for what concerns a fast reactor with HLM as primary coolant and pressurized water as secondary fluid, a complete different series of phenomena takes place, including but certainly not limited to the CCI. It is a conceptually different problem (pressurized two-phase water flashing in a pool of HLM at $T > T_{sat}$) that requires to be adequately analyzed in order to derive a set of closure correlation and constitutive laws allowing a prediction of this

[6] From Phénix experience, the major cause of plant non-programmed shutdowns has been the IHX failures. Being able to inspect and repair without extracting the component would lead to a decrease of unexpected shutdown periods due do HXTR.

phenomenon. While some models can be adapted, CCI still represents quite an unexplored field.

A number of models simulating gas bubble drag in HLM are already available [3.42]. The application of such models would help understanding bubble behavior during a PHXTR, assessing the possible bubble suction through the Primary Pump with consequent void insertion into the core.

Lastly, a proper LBE entrainment model is of relevance. Once steam bubbles have reached the hot free surface, cover gas pressure will keep raising until the rupture disk limit pressures have been reached (4 and 6 bar for the two disks). After rupture disk break, the moisture (steam, cover gas and entrained LBE) will be driven through the Pressure Relief System [3.43]. The entrained LBE could, though, suddenly freeze after being introduced in the cold environment (upper cover surface is supposed to be maintained at ~60 °C), leading to PRS tube blockage.

3.4.2 HX/SGTR computational simulations

The HX/SGTR is an event involving, by definition, several different phenomena: dynamic interaction of two different fluids (pressurized water flashing to steam into hot LBE), steam bubbles drag, potential void insertion into the core, entrainment of LBE from hot free surface to rupture disk.

Classical System Thermal Hydraulics codes (e.g.: RELAP5 [3.8], TRACE [3.44]) are unable to properly simulate all phenomena characterizing the HX/SGTR event: no more than one working fluid can be simulated, thus limiting the analysis potentialities to non-condensable gas-LBE interaction, which is clearly inadequate to simulate the tri-phase phenomena involved. Moreover, though able to simulate the overall behavior of complete plants, STH codes lack the detailed definition that would be required to properly simulate a similar event.

Nevertheless, STH codes could provide very good results for some selected phases: the critical flow release and the gas plenum pressurization can be proficiently simulated.

CFD codes (e.g.: ANSYS-CFX [3.22]) allow the presence of more than one fluid (and have been used for preliminary HX/SGTR analyses in CDT project) with the possibility to employ quite fine meshes and to represent the problem domain in its fullest definition; however, fast-occurring multiphase transient dynamic interactions modeling with CFD tools would present notable numerical and computational difficulties. Moreover, successful CFD applications to HX/SGTR problem have been limited to multiphase transport of water/steam into HLM flow, without considering the energy transfer between the phases and assuming the water/steam distribution as an initial condition (no water flashing simulated).

The best results have been thus achieved with "coarse-mesh codes" such as SIMMER-III and SIMMER-IV. This code series allows representing with reasonable simulation times the pressurized water flashing into the LBE pool and the further evolution of the steam bubbles, also considering potential core reactivity insertion consequences. In particular, SIMMER-III version, which has been used by JAEA and KIT for pool-type fast reactor analyses, is limited to a 2-D geometry, which is not always applicable to the real geometry, while SIMMER-IV allows 3-D geometry models but with extended simulation times.

Some results for what concerns the dynamic behavior of the reactor structures have been reached by means of FEM codes (e.g. Marc, Dytran), assuming the load input coming from water-LBE interaction to be derived from other sources.

However, the HX/SGTR event includes a great number of various multiphase interactions involving different disciplines: a "complete" code predicting all the possible implications (thermal-hydraulical, mechanical, neutronic, chemical) is beyond current possibilities.

In conclusion, there are still several uncertainties about the capabilities of such codes to represent all multi-phase phenomena involved in a HX/SGTR event, from the water/steam inlet and the potential shockwave generation and propagation to the entrainment of differently sized steam bubbles into LBE stream.

Moreover, code validation for the HX/SGTR event against experimental data is still mainly missing, especially in conditions representing MYRRHA facility.

A notable improvement would be to simulate MYRRHA environment, even if not representing all details, in order to provide a frame for the complete accidental evolution, from tube break to complete evacuation of fluid through the rupture disk (with the possibility of a fraction passing through the core).

A proper numerical simulation, supported by an experimental program (developed explicitly for MYRRHA) assuming the most suitable scaling approach, would allow having an extensive calculation tool validation against HX/SGTR accident, which is still missing.

3.4.3 HT/SGTR experimental program

Several experiments have been set up and realized in order to simulate pressurized liquid water being injected into heavy liquid metal pools.

Until now, though, most experiments have been performed in pressure and temperature conditions that are relatively far from MYRRHA working conditions (e.g. LIFUS5, TALL) [3.27] [3.45] [3.46] . In particular, majority of experiments have been realized for Pb-cooled reactors, whose conditions usually involve higher temperatures (up to 500 °C in normal conditions) and water pressure (up to 200 bar).

Though a relatively great number of information can be deduced from those experiments, the setup of a MYRRHA-suited experimental program is highly suggested in support of design and safety activities.

In the framework of the EU FP7-MAXSIMA project [3.47] the complete Work Package 4 ("Steam generator and cooling safety") is devoted to PHXTR in MYRRHA reactor. The experiments foreseen within this project can represent a very interesting support for theoretical models, and simulations realized through computer codes can be validated against these experiments.

The experimental program, realized at ENEA and KTH experimental facilities, includes the following three tests:

- A test involving the investigation of the effects of a full scale HXTR experiment performed in the CIRCE pool facility at ENEA. The HXTR event is characterized in a configuration relevant for MYRRHA. First objective is the assessment of the propagation of the tube rupture in a PHX bundle. Secondly, the propagation of the pressure wave in the PHX bundle (domino effect) and the mitigation effect of the PHX shell and the safety guard devices will be evaluated. Next, the potential steam trapping in the main LBE flow path and dragging towards the core inlet region is evaluated. Finally, an investigation of the formation of solid impurities after the HXTR event and a quantitative qualification of filtering performance in the pool will be done.
- The second experiment focuses on bubble size characterization and release rate for typical cracks in a steam generator tube in the LIFUS5 facility at ENEA. The leak rate is measured from pre-characterized cracks while the bubble formation frequency is measured by acoustic means. The outcome will serve as input for numerical simulations of the migration of steam in the vessel after a steam generator tube leak or rupture and will also be used for code validations of coarse-mesh codes (SIMMER series). In addition, an early detection system for leaking steam generator tubes, which could lower the probability of a HXTR event based on the "leak before break" principle, is tested.
- Third experiment has been performed at the TALL-3D facility at KTH. Its goal is to experimentally determine the drag coefficient of gas bubbles moving in LBE in various flow conditions. The outcome of this experiment will provide an insight on the behavior of the steam bubbles once released from the PHX break (after flashing) and will also serve as input for numerical simulations of steam migration in the MYRRHA reactor. The high pressure difference as a function of the vertical position of the bubble and the expected expansion occurring with rise may have a significant effect on the estimated drag coefficients.

References

[3.1] T.-N. Dinh, "Multiphase Flow Phenomena of Steam Generator Tube Rupture in a Lead-Cooled Reactor System: A Scoping Analysis," in *ICAPP 2007* , Nice, 2007.

[3.2] D. Castelliti, "Preliminary Design Description of Primary Heat Exchanger," SCK•CEN Internal Report 1172152, Mol, 22 August 2016.

[3.3] D. Castelliti, "Preliminary Design Description of the Secondary Cooling System (SCS) and Tertiary Cooling System (TCS)," SCK•CEN Internal Report, Mol, 14 December 2016.

[3.4] F. D'Auria and P. Vigni, Two-Phase Critical Flow Models, OECD-NEA Technical Addendum, 1980.

[3.5] A. Calvo, Assessment of two-phase critical flow models performance in RELAP5 and TRACE against Marviken Critical Flow Tests, 2012.

[3.6] R. E. Henry and H. K. Fauske, "The Two-Phase Critical Flow of One-Component Mixtures in Nozzles, Orifices, and Short Tubes," *Journal of Heat Transfer,* 1971.

[3.7] J. A. Trapp and V. H. Ransom, "A choked-flow calculation criterion for non-homogeneous, non-equilibrium, two-phase flows," *International Journal of Multiphase Flow,* vol. 8, no. 6, pp. pp. 669 - 681, 1982.

[3.8] RELAP5-3D Code Manual, Idaho Falls: INEEL-EXT-98-00834, Idaho National Laboratory, 2014.

[3.9] H. Hulin and N. Kolev, "Shock waves in multiphase flow of fuel-coolant interaction," *International Journal of Thermal Sciences,* vol. 39, no. 3, pp. pp. 354 - 359, 2000.

[3.10] G. Makhviladze and S. Yakush, "Modeling of Formation and Combustion of Accidentally Released Fuel Clouds," *Institutions of Chemocal Engineers,* vol. 83, no. B2, pp. pp. 171 - 177, 2005.

[3.11] R. Prugh, "Quantitative evaluation of "BLEVE" hazards," *Journal of Fire Protection Engineering,* vol. 3, no. 1, pp. pp. 9 - 24, 1991.

[3.12] A. V. Beznosov, S. S. Pinaev, D. V. Davydov, A. A. Molodtsov, T. A. Bokova, P. N. Martynov and V. I. Rachkov, "Experimental studies of the characteristics of contact heat exchange between lead coolant and the working body," *Atomic Energy,* vol. 98, no. 3, 2005.

[3.13] Y. Sibamoto, Y. Kukita and H. Nakamura, "Visualization and measurement of subcooled water jet injection into high-temperature melt by using high-frame neutron radiography," *Nucleat Technology,* vol. 139, 2002.

[3.14] Y. Sibamoto, Y. Kukita and H. Nakamura, "Simultaneous measurement of fluid temperature and phase during water jet injection into high temperature melt," in

NURETH-11, Avignon, 2005.

[3.15] Y. Sibamoto, Y. Kukita and H. Nakamura, "Small-scale Experiment on Subcooled Water Jet Injection into MoltenAlloy by Using Fluid Temperature-Phase Coupled Measurement and Visualization," *Journal of NUCLEAR SCIENCE and TECHNOLOGY,* vol. 44, no. 8, pp. pp. 1059 - 1069, 2007.

[3.16] Y. Perets, R. Harari and E. Sher, "Vapor Explosion of Coolant Jet When Penetrating a Hot Molten Metal," *Nuclear science and engineering,* vol. 150, 2004.

[3.17] M. Furuya, K. Matsumura and I. Kinoshita, "A Linear Stability Analysis of a Vapor Film in Terms of the Triggering of Vapor Explosions," *Journal of Nuclear Science and Technology,* vol. 39, no. 10, pp. pp. 1026 - 1032, October 2002.

[3.18] J. Liu, S. Koshizuka and Y. Oka, "Relationship between the structure of vapor explosion and fragmentation mechanisms," *Nuclear Engineering and Design,* vol. 216, no. 1 - 3, pp. PP. 121 - 137, 2002.

[3.19] S. Buckingham and L. Koloszar, "DEMOCRITOS PHASE 3 Final Report," VKI, Brussels, July 2014.

[3.20] "Models and Methods of SIMMER-III," JAEA.

[3.21] "CCM User Guide - Star-CD version 4.02," CD-adapco, 2006.

[3.22] "ANSYS CFX Reference Guide," 2012.

[3.23] "OpenFOAM - The Open Source CFD Toolbox - User Guide - Version 2.2.0," 2013.

[3.24] "ELSY Website," [Online].

[3.25] "FP7 Central Design Team (CDT) for a Fast-spectrum Transmutation Experimental Facility - Grant Agreement," 2009.

[3.26] "DEMOCRITOS project grant agreement".

[3.27] A. Ciampichetti, D. Pellini, P. Agostini, G. Benamati, N. Forgione and F. Oriolo, "Experimental and computational investigation of LBE-water interaction in LIFUS5 facility," *Nuclear Engineering and Design,* vol. 239, pp. pp. 2468-2478, November 2009.

[3.28] A. Ciampichetti, D. Bernardi and N. Forgione, "Analysis of the LBE-Water Interaction in the LIFUS 5 Facility to support the investigation of an STGR Event in LFRs," SIET, Piacenza, 2010.

[3.29] L. Barucca, G. Gherardi and L. Mansani, "The CIRCE Test Facility for Verification and Validation of the LBE-cooled XADS Concept Design Choices".

[3.30] P. Turroni and L. Cinotti, "The CIRCE Test Facility," ANS Winter Meeting, 2001.

[3.31] "KArlsruhe Liquid metal LAboratory (KALLA)," [Online]. Available: http://www.iket.kit.edu/334.php.

[3.32] "VELLA Deliverable 51," 2009.

[3.33] "Accelerator-Driven Transmutation Experimental Facility," [Online].

[3.34] J. Buongiorno, N. E. Todreas and M. Kazimi, "Heavy-metal aerosol transport in a lead-bismuth-cooled fast reactor with in-vessel direct-contact steam generation," vol. 138, 2002.

[3.35] A. Ciampichetti and D. Bernardi, "Report on test campaign of Pb/water interaction," ENEA, 2010.

[3.36] P. Kudinov, "Evaluation approach and case set-up for simulation of consequences of the SGTR event," KTH, 2010.

[3.37] J. Carlsson and D. Castelliti, "ELSY project - D30: Safety analysis of plant accident representative for design basis conditions," 2010.

[3.38] R. Lo Frano and G. Forasassi, "Preliminary evaluation of steam generator tube rupture (SGTR) accident in lead cooled reactor," Pisa, 2009.

[3.39] "MSC/DYTRAN User's Manual version 4.0," 1997.

[3.40] T. Sugawara and D. Castelliti, "Analysis for heat exchanger tube rupture in FASTEF by SIMMER-III," SCK•CEN Internal Report, Mol, 2011.

[3.41] V. Moreau, "CRS4 contribution to CDT project".

[3.42] M. Jeltsov, "Application of CFD to Safety and Thermal-Hydraulic Analysis of Lead-Cooled Systems," Royal Institute of Technology (KTH), Stockholm, June 2011.

[3.43] R. Fernandez, "Mechanical design of the primary system," SCK•CEN Internal Report, Mol, September 2015.

[3.44] "TRACE V5.0 Theory Manual," U.S. Nuclear Regularoty .

[3.45] S. Wang, "Evaluation of a Steam Generator Tube Rupture Accident in an Accelerator Driven System with Lead Cooling," *Progress in Nuclear Energy,* vol. 50, no. 2 - 6, pp. pp. 363 - 369, 2008.

[3.46] M. Flad, S. Wang and W. Maschek, "Simulation of a steam generator tube rupture in a lead-cooled accelerator driven system," in *18th International Conference on Nuclear Engineering*, Xi'an, May 2010.

[3.47] "Grant Agreement for FP7 MAXSIMA Collaborative Project Annex 1: Description of Work," 2012.

Chapter 4: Two-phase critical mass flow rate estimation

The PHXTR event evolution in the MYRRHA reactor can be divided into 5 main phases [4.1].

1. Water release in the Primary Vessel (critical mass flow rate)
2. Pressure wave induced by rupture
3. Liquid displacement and sloshing consequences on surrounding internals
4. Potential steam explosions risk
5. Multiphase transport

The first phase will be analyzed in detail in this chapter.

Due to the pressure difference between the Primary and the Secondary Cooling System (SCS), the water/steam mixture leaking from the break is in critical flow conditions.

The first step of the PHXTR analysis implies the evaluation of the correct two-phase critical mass flow rate through the break, in function of the break size, shape and position in the PHX tube.

The evaluation must be done accordingly to the real PHX geometry and taking into consideration the actual SCS layout and water inventory [4.2]. In particular, it is important to evaluate the smallest flow section in the SCS circuit and to compare it with the break section: as long as the break presents a larger section, the break flow will be limited by the SCS geometry. Smaller breaks will, instead, characterize the transient evolution.

By considering the SCS layout [4.2], the smallest flow section can be found in the PHX itself. In particular, the single tube orifice, located at the bottom of each tube to stabilize the flow (see Chapter 2), represents the smallest flow section.

A PHXTR scenario will thus be limited, accounting for the two flow sections, as follows:

- Bottom section: by the orifice in case of tube break larger than orifice section
- Top section: by the crack size (tube section being the upper limit)

The sum of the mass flow rates from these sections defines the water input in the MYRRHA Primary System pool.

4.1 Two-phase critical mass flow models

In single phase, the critical (also defined as choked) flow occurs when the speed of flow equals the speed of sound. The fundamental reason that choking occurs is that pressure (acoustic) signal can no longer propagate upstream: the speed of sound is the maximum speed of the compressible fluid when it flows from the region of higher pressure to region of lower pressure, since the information about the downstream conditions cannot travel upstream anymore.

The well-known phenomenon of critical flow can be visualized in the following Figure 4.1. A typical problem of a fluid discharging from a tank is presented: the p_o and p_R are the pressures inside the tank and at the end of the pipe, respectively [4.3].

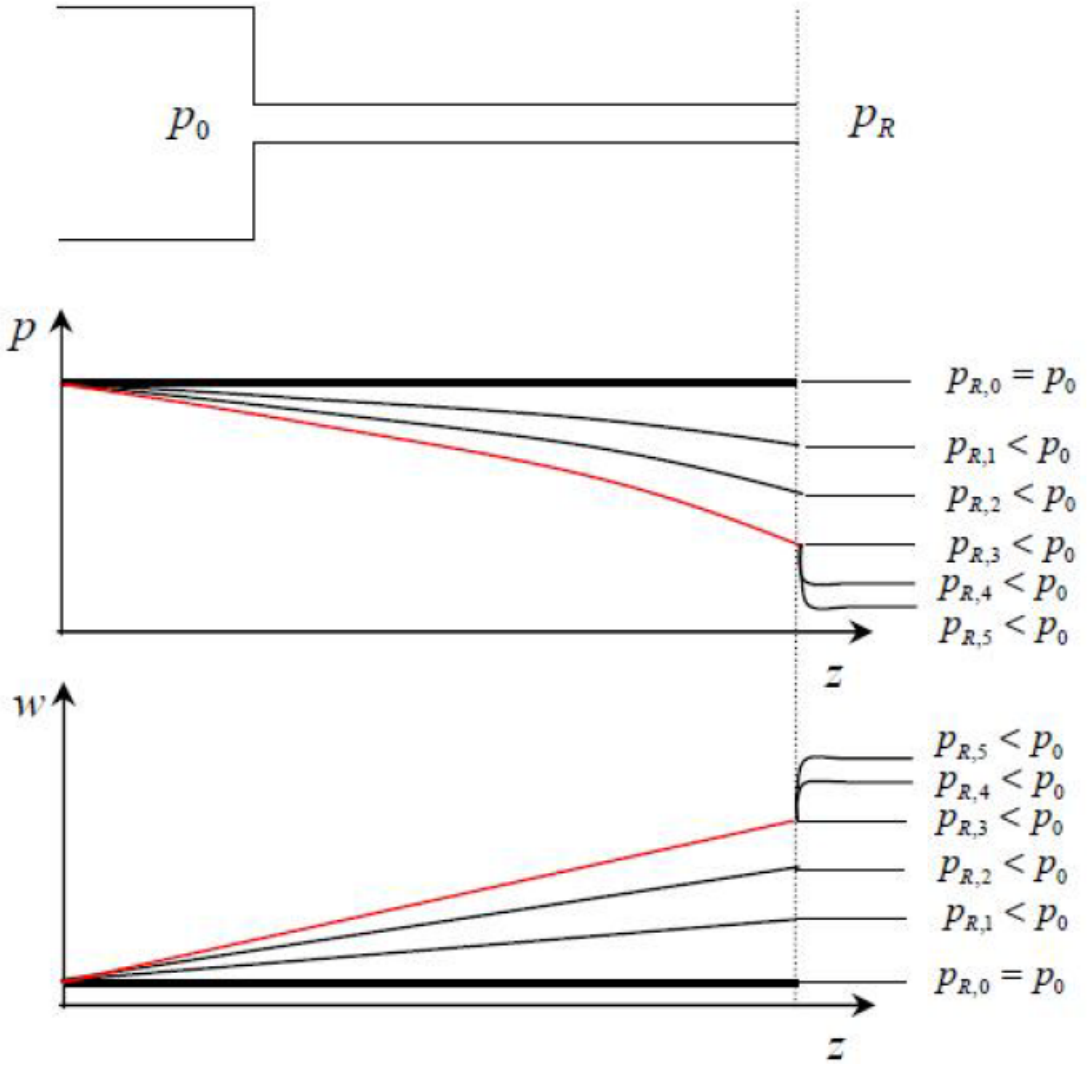

Figure 4.1 – Critical pressure and mass flow (velocity) behavior under critical conditions

The critical mass flow rate depends only on stagnation parameters. As can be seen from the figure above, when downstream pressure p_R decreases the fluid velocity w increases. However, the variations take place up to a point when the increasing in downstream pressure does not affect the process behavior. It can be seen in Figure 4.1 that the downstream

pressures $p_{R,3}$, $p_{R,4}$, and $p_{R,5}$ have identical impact on velocity of medium. This situation occurs since the choking occurs above pressure $p_{R,3}$ (defined as critical pressure)

The single-phase critical mass flow rate criterion can be theoretically derived by the combination of the energy balance and the perfect gas law, under the assumption of isentropic expansion. It can be retrieved in several textbooks, e.g. [4.4]. The final formulation is reported as follows:

$$W_c = \rho_c v_c A = A \frac{p_0}{\sqrt{T_0}} \sqrt{\frac{k}{R} \sqrt{\left(\frac{2}{k+1}\right)^{\frac{k+1}{k-1}}}} \quad (4.1)^1$$

To determine whether the single phase flow is at critical condition only requires to compare the fluid velocity with the speed of sound defined as above.

The determination of a choking criterion in two-phase flow is much more complicated. The main reasons can be summarized as follows:

- Two-phase critical flow cannot be uniquely determined: there are two existing phases so that means there are, in principle, two different speeds of sound (liquid and vapor). For two-phase releases, the choked flow condition of Mach number equal to unity does not hold because the concept of single sound speed for a mixture of phases does not make sense. Generally, more than one sound speed can be defined, typically one for each phase and one for the mixture depending on the flow pattern and geometry or quality of the mixture.
- The complicated character of two-phase flow (different flow regimes, different phase properties…) makes the assumptions not straightforward and the calculations not easy.

To overcome mentioned obstacles some modeling approximations need to be employed.

Therefore, the evaluation of critical flow for two-phase releases is typically carried out using specific theoretical or semi-empirical models based on certain assumptions for what concerns the mechanical and thermal equilibrium between the liquid and the vapor phase.

Normally, in two-phase choked flow evaluation, an appropriate model must be selected to evaluate the critical pressure and the mass flow rate through the break. The different models available are usually suitable for specific ranges of process properties (pressure, mass flow rates…) and geometry (tube diameter, tube length, break shape…), so an appropriate selection must be done according to the problem.

Several two-phase critical flow models present in literature refer to circular ducts; it is possible to apply these models to a layout more representative of a tube break, like an orifice or an irregular-shaped break.

Two-phase critical flow models can be classified according to the following criteria:

[1] ρ_c = Fluid density; v_c = Critical velocity; A = Flow section; p_0 = Fluid pressure; T_0 = Fluid temperature; $k = c_p/c_v$; R = Perfect Gas Constant;

- Derivation technique: theoretical or semi-empirical models
- Formulation: number of equations (balance, state) and parameters required
- Assumptions: simplifications with respect to reality (multi-dimensionality, non-homogeneities…)
- Output: model applicability

These criteria can be summarized in the standard classification provided for two-phase critical flow models, as reported in Figure 4.2 [4.5].

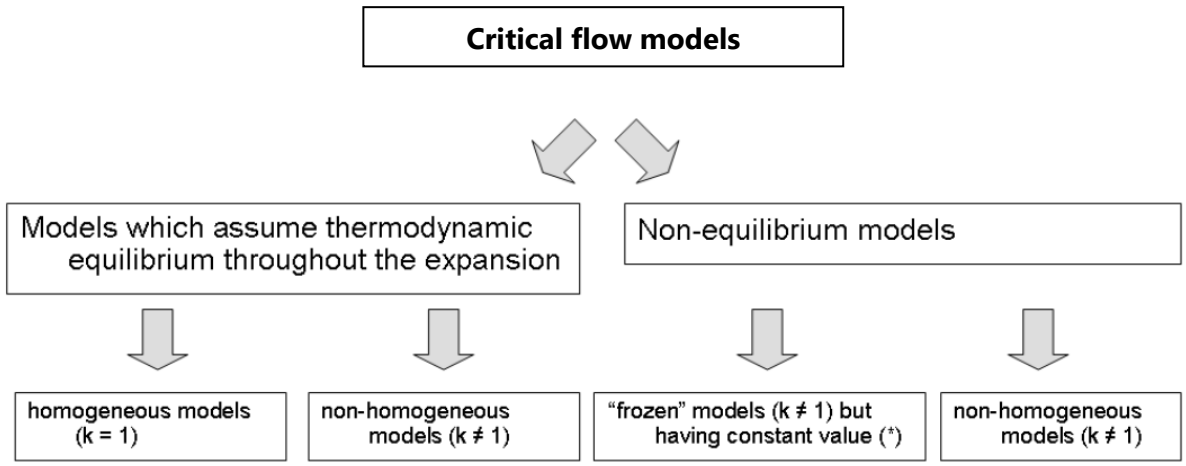

Figure 4.2 – Classification of two-phase critical flow models

The main divisions make a difference between models that assume thermodynamic equilibrium through the expansion line and models that assume non-thermodynamic equilibrium. The first mentioned category can be divided into homogeneous and non-homogeneous models ("frozen"). The non-equilibrium theory can be divided into frozen theories and non-homogeneous models.

4.1.1 Equilibrium models

Equilibrium models foresee, as hypotheses, that pressure and temperature for liquid and vapor phases are supposed to be equal, and always linked through the steam tables saturation curves (mono-variant system). The basic assumption of these models is the existence of thermal-dynamic equilibrium between liquid and vapor phases, taken any section of the flow duct. Mixture quality change along the duct length is supposed to happen at infinite velocity[2].

As sub-category, homogeneous models assume equal velocities for the liquid and the vapor phases (Slip ratio S = 1), while non-homogeneous models foresee different velocities between the two phases.

[2] Quality change would be in contrast with T and p equalities through the phases, being condensation and evaporation depending upon T and p differences between phases.

At low pressures, the velocity difference is normally relevant because of the pronounced density difference between the two phases.

The simplest equilibrium homogeneous model is the HEM:

- The average velocities for the phases are equal
- Thermodynamic equilibrium exists between the phases
- The expansion is isentropic
- Water properties correspond to the Equation of State represented by the water-steam tables

The HEM provides a reasonably good estimation of the critical pressure but tends to underestimate the throat mass flux, especially at low pressures.

A better approximation is represented by the Homogeneous Frozen Model (HFM):

- The average velocities for the phases are not equal
- No heat or mass transfer occurs between the phases, so the quality remains constant during the expansion (hence the "frozen" definition)
- The vapor phase expands isentropically (as a perfect gas)
- The kinetic energy is due solely to the vapor expansion

The HFM (simplest non-homogeneous model) results in a good prediction for the throat mass flux but underestimates the critical pressure.

4.1.2 Non-equilibrium models

Non-equilibrium models are based on the following assumptions:

- Thermal non-equilibrium (different properties between phases)
- Mechanical non-equilibrium (Slip ratio > 1)
- Chemical non-equilibrium (phases' density changes during expansion)

The first sub-category in non-equilibrium models are frozen theories with constant values of S. Frozen means that there is no heat or mass transfer between the faces. Constant S denotes that there are no velocity changes through the expansion line.

The second sub-category of non-equilibrium models are non-homogeneous models with slip ratio different than 1 and not constant during expansion. These models are the most complicated than all mentioned models. Within the last decades, many models have been derived. However, the most important ones have been recognized in the Henry-Fauske [4.6] and Ransom-Trapp [4.7].

4.2 Application of different two-phase critical flow models to the MYRRHA PHXTR

A PHX tube rupture must be postulated in the most challenging configuration concerning the position and the shape.

The most severe break is the one causing the highest amount of water release in the reactor primary pool, thus the one presenting the largest flow section. The "classical" double-ended guillotine tube is assumed the one causing the highest releases. Such assumption implies the release of water/steam mixture from the two broken tube ends, which must be computed separately to evaluate the total release.

Concerning the break flow section size, the following considerations can be made:

- At the PHX tubes lower end, an orifice is present to increase flow stability in the tube bundle. Such orifice restricts the flow section, thus becoming the "limiting" factor for the water flowing from the bottom. The orifice section represents the upper limit for the size used to compute the critical flow relative to the "bottom section".
- The "top section" critical flow must be evaluated according to the break section, since the upper limit is the tube section itself.

For the following analysis, the maximum tube break size is considered (double-ended guillotine break). No influence of the break shape has been considered here, assuming that the maximum break is defined by two circular sections (orifice and tube).

The tube break can occur at any axial position, meaning that water will flow through part of the tube in choked conditions before being released[3]. A specific break position will define the maximum flow. A sensitivity analysis defines the most challenging break for the system, basing on the break position along the tube height; such break is considered as reference for the analysis.

Table 4.1 and Table 4.2 show the geometrical input used for the critical flow evaluation following a PHXTR event:

Table 4.1 – Geometrical data used for critical flow analysis

Parameter	Unit	Value
Tube internal diameter	m	0.014
Tube orifice internal diameter	m	0.003
Tube flow section	m^2	1.539E-04
Tube orifice flow section	m^2	8.042E-06
Tube total length	m	10.920
Tube active length	m	2.1

[3] The limit case being the break occurring at one of the tube plate's level: in this case, one side it treated like an "orifice break".

Table 4.2 – SCS process data used for critical flow analysis

Parameter	Unit	Value
Water inlet temperature	°C	200
Water outlet temperature	°C	201.4
Water mass flow rate per tube	kg/s	0.069
Water inlet pressure	bar	16
Water outlet quality	-	0.3
Water outlet void fraction	-	0.9
Water outlet velocity	m/s	3.3
Steam outlet velocity	m/s	18.63
Water side pressure drop	bar	0.95

4.2.1 Stand-alone critical flow evaluation

Due to the phenomenological complexity of the two-phase choked flow, uncertainties of the empirical models are relatively wide. In order to find a critical mass flow rate value that can be considered accurate with enough reliability, several models have been chosen and tested among the ones showing the highest reliability and an applicability range best fitting the MYRRHA conditions [4.4], [4.5].

It is important to focus on the fact that MYRRHA SCS operates at 16 bar (considered "low pressure" for the typical LWR standards), with a phase density difference of ~100. Because of this, a certain degree of non-homogeneity and non-equilibrium should be considered.

A complete matrix with selected two-phase critical flow models results has been developed, comparing the critical mass flow rate values according to the different models (Table 4.3).

Table 4.3 – Two-phase critical flow models

Model	Class	Flow (kg/s)
HEM	Homogeneous Equilibrium	0.349
HFM - Moody	Homogeneous Frozen	0.581
HFM - Fauske	Homogeneous Frozen	0.557
Fauske	Non-Homogeneous Equilibrium	1.8
Burnell	Non-Homogeneous Non-Equilibrium	4.563
Henry-Fauske	Non-Homogeneous Non-Equilibrium	0.89
Leung-Grolmes	Homogeneous Non Equilibrium	0.961
Interpolated Moody	Homogeneous Non Equilibrium	1.09
Ransom-Trapp	Non-Homogeneous Non-Equilibrium	0.69

The results show a reasonable degree of similarity (except the pure HEM model, too simple, and the Burnell model, the first historical attempt at a full non-homogeneous non-equilibrium model [4.5]), which makes possible to derive a conservative value for the water release flow in the primary pool.

A reasonable estimation of the critical flow can be based on an average of the results from the different models considered (excluding the two values, which are clearly "distant"). This simple method provides a value of 0.94 kg/s. However, the two-phase critical flow models are affected by a certain degree of uncertainty (normally ± 30%), which makes the assumption of a precise value not realistic. The best approach would consist thus in adopting a conservative value according to the purpose of the analysis.

It is interesting to remind that the nominal flow through a PHX tube (designed to be close to the limits normally adopted in process industry in terms of fluid velocities) is ~13 times lower than the critical flow.

4.2.2 RELAP5-3D critical flow evaluation

An evaluation performed with an advanced thermal-hydraulic analysis numerical tool has also been performed, to confirm the validity of the previous evaluations and to be able to extend the simulation in time and have a first estimation of the PHXTR transient evolution in terms of Primary System pressurization and SCS emptying time.

The RELAP5-3D System Thermal-Hydraulics (STH) code [4.8] has been selected for this verification, due to the proven reliability of such tool and its extended use for the MYRRHA system design and safety studies [4.9].

RELAP5-3D does not support any fluid mixture involving two different liquid phases[4]. It is thus impossible to directly simulate the water release in the Primary System pool. However, due to the critical flow independence by the downstream conditions, part of the evaluation can still be performed. Specifically, such assumptions are considered to run the simulation starting from the MYRRHA Reference Model [4.10]:

- SCS starting from Steady State conditions
- Primary System simulated through a component sized as the MYRRHA cover gas volume full of non-condensable gas (Nitrogen) at the pressure of 1 bar and temperature of 325 °C (Steady State cover gas conditions)
- No power generation in the Primary System
- Only one SCS loop present

Some additional features have been added in the model:

- A separated single PHX tube, identical to the others, parallel to the rest of the bundle, to simulate the water release from one tube only
- Two junctions connecting the SCS tube to the Primary System volume, simulating the double-end guillotine break

A schematic representation of the RELAP5-3D model used for the critical flow test is provided in Figure 4.3 (derived from the MYRRHA Reference Model [4.10]):

[4] RELAP5-3D can support up to one fluid species in two-phase plus a non-condensable and soluble boron concentration (for the last two species, simplified balance equations are applied).

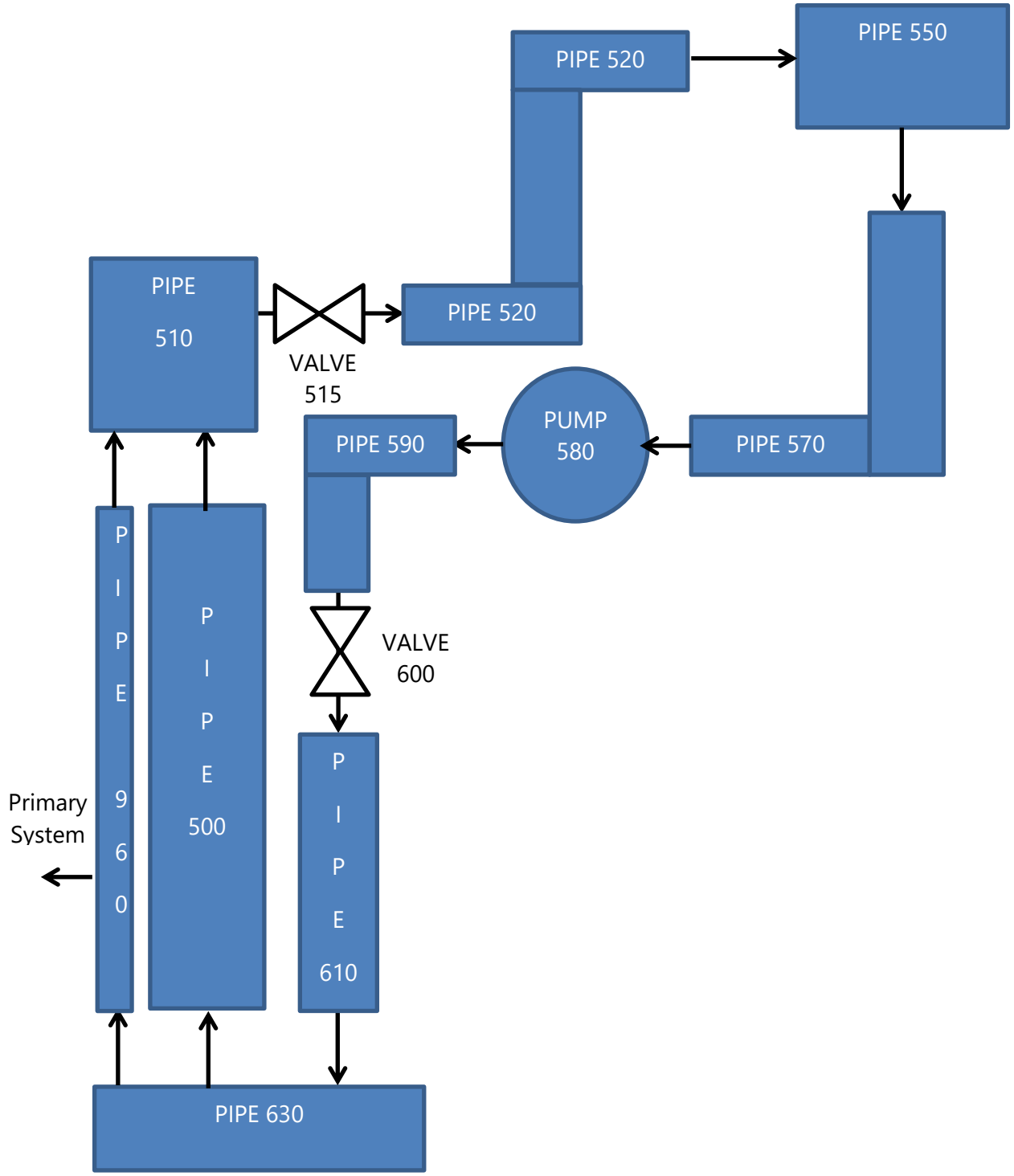

Figure 4.3 – RELAP5-3D model for critical flow evaluation

RELAP5-3D code supports the Ransom-Trapp model (as default) and the Henry-Fauske model for the choked flow predictions, as recognized to be the most reliable in the broadest ranges. The nodalization has been run with both models to compare the results with the values evaluated before through "stand-alone" applications.

Here below the RELAP5-3D results from the application of both choked flow models are reported:

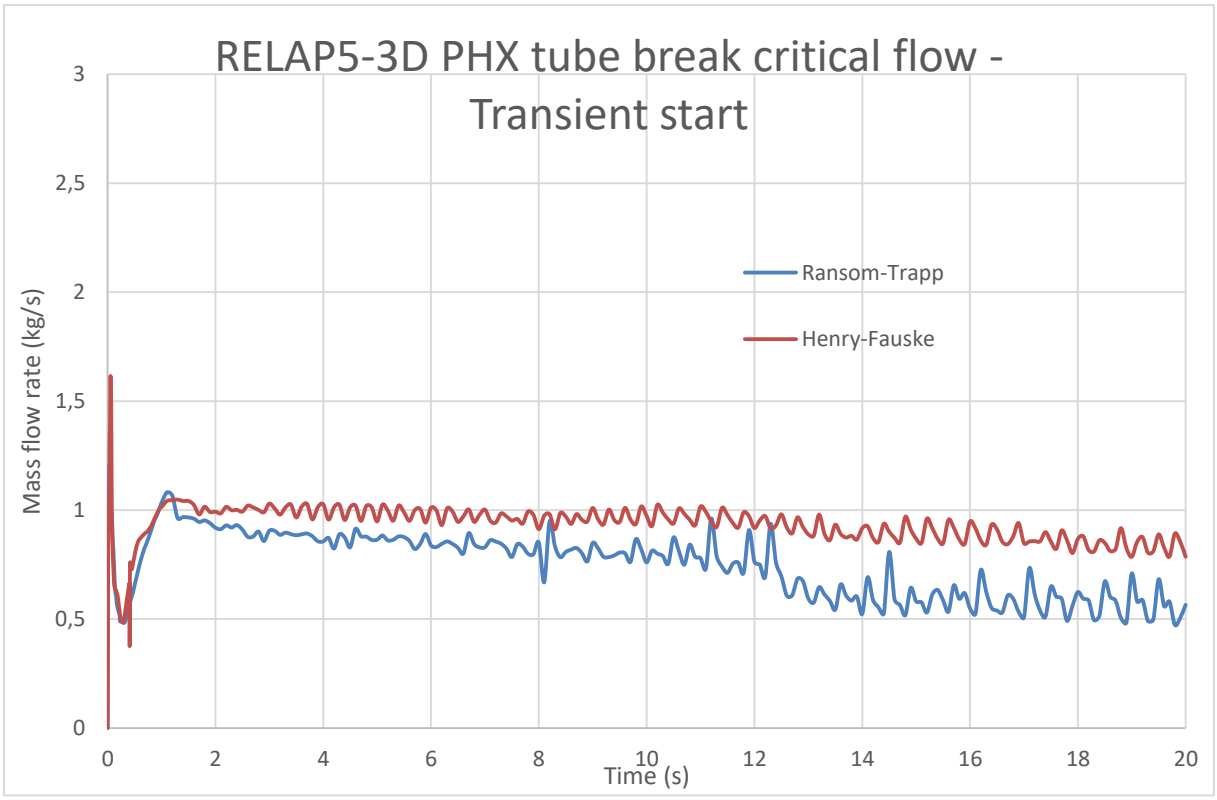

Figure 4.4 – RELAP5-3D critical flow (beginning of transient)

After a short transient (~1.5 s), the flow rate through the breaks reaches the critical flow, according to both models. The predicted value is not perfectly constant because of the changes involving the fluid upstream the break; however, considering the average value of the first 20 s (excluding the initial "settling" phase), the RELAP5-3D critical flow models provide the following predictions:

- Ransom-Trapp: 0.74 kg/s
- Henry-Fauske: 0.94 kg/s

As known from literature [4.3], the RT model tends to slightly underestimate the critical flow compared to HF. However, given the complexity of the involved phenomenology, such deviations are considered acceptable.

During the transient, the mass released in the Primary Vessel is estimated in Figure 4.5.

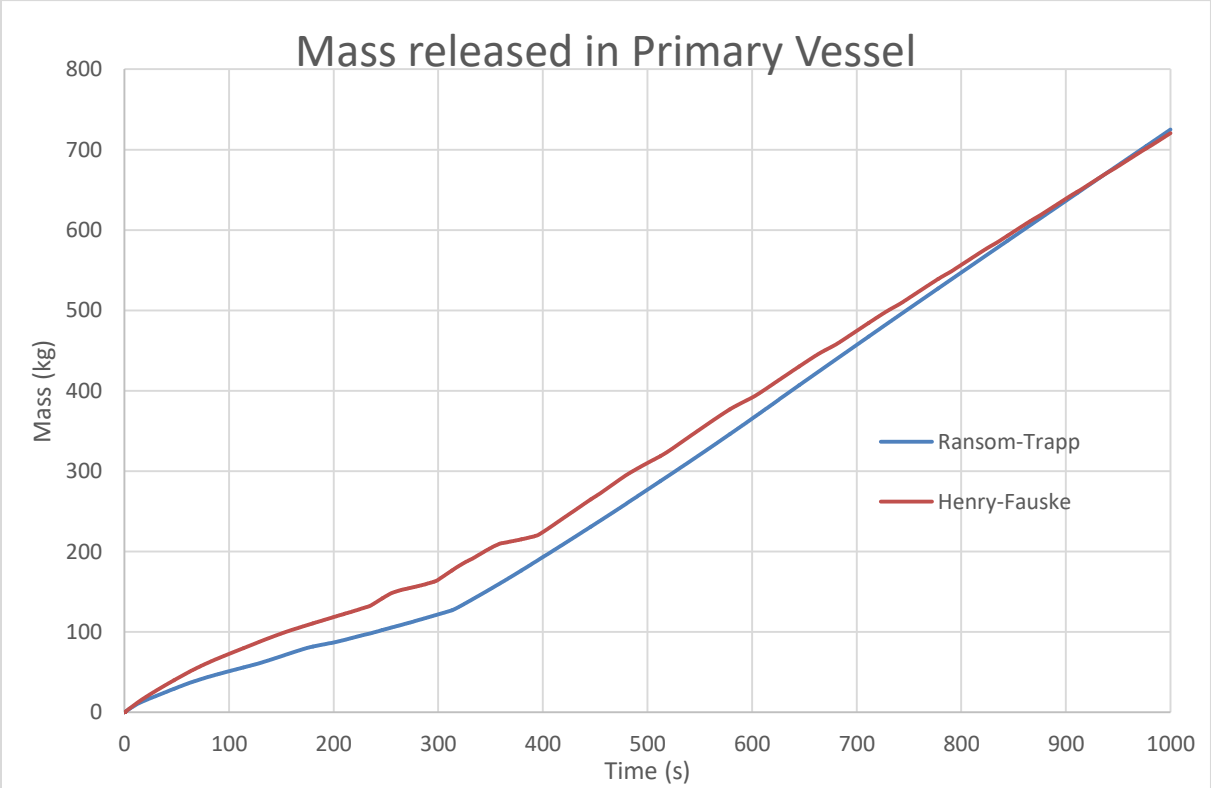

Figure 4.5 – RELAP5-3D evaluation of the mass released in Primary Vessel

It is possible to note again that the HF model predicts a higher mass release compared to the RT model; however, once the choking phase is concluded, the two predictions tend to converge on a mass flow release of ~0.85 kg/s. The flow remains in a choked state for ~200 s from the tube break, then the pressure differences between the two sides tend to reduce. The complete emptying of the SCS requires ~8 hours.

Concerning the enthalpy flow discharged in the Primary Vessel, the estimation provided by the code is reported in Figure 4.6. The trend is qualitatively very similar to the mass flow rate release, showing the connection between the amount of mass and energy.

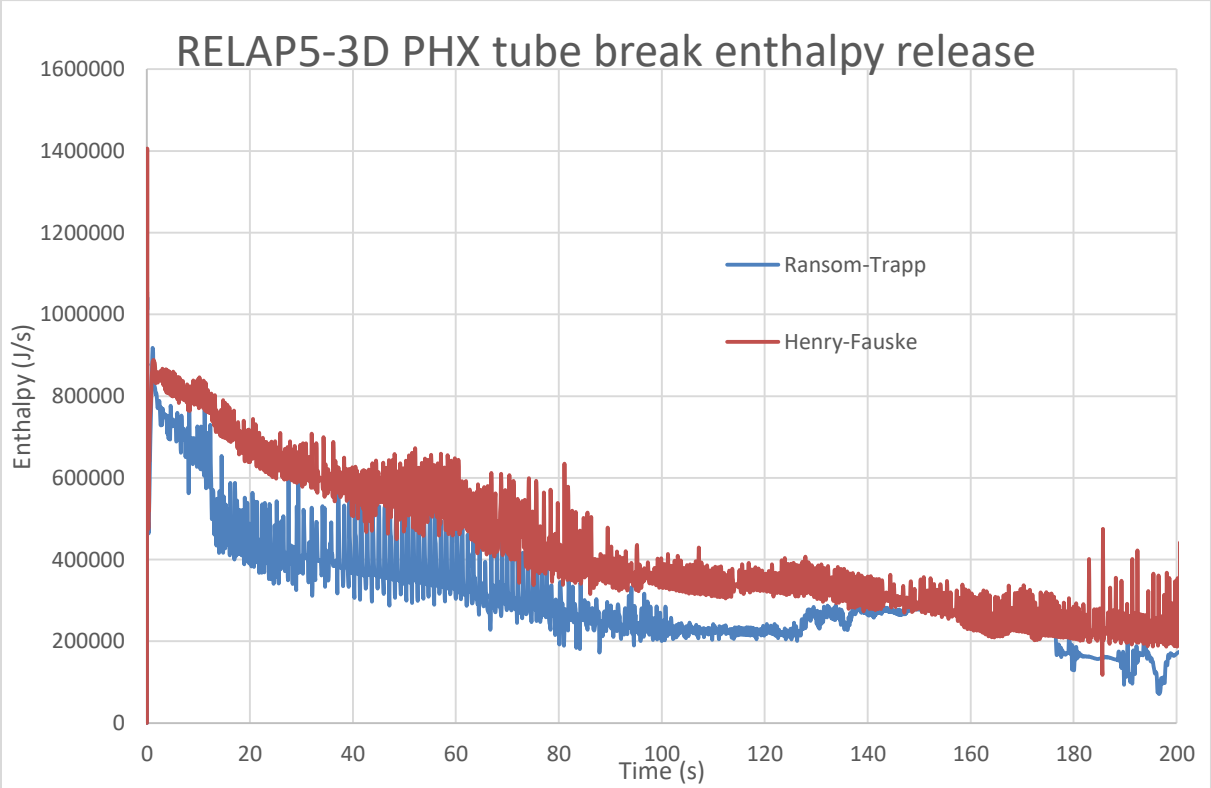

Figure 4.6 – RELAP5-3D enthalpy release

The comparison between the RELAP5-3D results and the stand-alone simulations provides quite similar results, especially if considering the non-equilibrium models, remarking how the low SCS pressure, causing the pronounced density difference between phases, is an important factor. In particular, the Henry-Fauske, Leung-Grolmes, Interpolated Moody and Ransom-Trapp models provide the value closest to the RELAP5-3D estimations. Considering the uncertainties typically associated to two-phase critical flow models, it is possible to state that the predictions of the application of suitable models provide the same result as RELAP5-3D code.

From a sensitivity on the break position along the PHX tube performed with the RELAP5-3D model (by shifting the position of the two junctions simulating the break), it appears that the critical flow is relatively independent of the break position. However, a rupture in proximity of the lower tube plate results the most challenging in terms of water release.

4.2.3 Comparison with EU FP7-MAXSIMA WP6 results

A similar study has been performed in the frame of the EU FP7-MAXSIMA project [4.11], Task 6.2. The complete set of results is described in the Deliverable D6.3 [4.12].

While a general agreement between the Task 6.2 activities and the results here showed could be surely identified, some differences appear clearly:

- A peak flow rate of ~1.3 kg/s at transient start has been found: this slightly higher value (compared to 0.94 kg/s) can be explained by the lack of orifice model in the

PHX tube (the orifice represents the limiting geometrical factor, and the choking section, for the water flowing from the lower end of the break).

- The assumption of a sudden evaporation of the complete water mass inventory released in the Primary Vessel represents a strong (conservative) approximation (see Chapter 5), while a relevant fraction of the water released could not boil until reaching the LBE free level.

It is important to mention that, in EU projects, it is often required to provide a "frozen" configuration of the system object of study. Thus, the final project results can be based on obsolete configurations and assumptions.

References

[4.1] T.-N. Dinh, "Multiphase Flow Phenomena of Steam Generator Tube Rupture in a Lead-Cooled Reactor System: A Scoping Analysis," in *ICAPP 2007*, Nice, 2007.

[4.2] D. Castelliti, "Preliminary Design Description of the Secondary Cooling System (SCS) and Tertiary Cooling System (TCS)," SCK•CEN Internal Report, Mol, 14 December 2016.

[4.3] L. Sokolowski, T. Kozlowski and A. Calvo, "Assessment of Two-Phase Critical Flow Model Performance in RELAP5 and TRACE Against Marviken Critical Flow Tests," U.S. NRC, February 2012.

[4.4] N. Todreas and M. Kazimi, Nuclear Systems Volume 1 - Second Edition, CRC Press Taylor & Francis Group, 2012.

[4.5] F. D'Auria and P. Vigni, Two-Phase Critical Flow Models, OECD-NEA Technical Addendum, 1980.

[4.6] R. E. Henry and H. K. Fauske, "The Two-Phase Critical Flow of One-Component Mixtures in Nozzles, Orifices, and Short Tubes," *Journal of Heat Transfer,* 1971.

[4.7] J. A. Trapp and V. H. Ransom, "A choked-flow calculation criterion for non-homogeneous, non-equilibrium, two-phase flows," *International Journal of Multiphase Flow,* vol. 8, no. 6, pp. pp. 669-681, December 1982.

[4.8] RELAP5-3D Code Manual Revision 4.3, Idaho Falls: DOE/NE Idaho Operations Office, October 2015.

[4.9] E. Bubelis and M. Schikorr, FP7 Central Design Team Deliverable 2.3 - FASTEF safety analysis - Critical and sub-critical mode, 2012.

[4.10] D. Castelliti, "RELAP5-3D MYRRHA ver. 1.6 description tables," SCK•CEN Internal Report, Mol, April 2016.

[4.11] "EU FP7-MAXSIMA Grant Agreement n. 323312," November 2012.

[4.12] D. Bisogni, "EU FP7-MAXSIMA D6.3: MYRRHA containment analysis," SCK•CEN, Mol, March 2016.

Chapter 5: Water phase behavior in liquid metal pool

Once the water-steam mixture flow rate released in the MYRRHA reactor Primary System pool, following a PHXTR event, has been characterized, the consequences on the reactor internals must be assessed. The event will evolve through different stages [5.1]:

- Rupture induced pressure wave and liquid displacement and sloshing
- Potential steam explosion
- Gradual primary vessel pressurization
- Bubble transport in the cover gas or in the reactor core

The different phenomena are not well separated each other, but they tend to overlap and to have mutual influences. The approach for the analysis consists in following the bubble distribution evolution through different calculation models and to identify and evaluate the consequences from several points of view.

As a conservative assumption, the real mass flow rate (as function of time, estimated by RELAP5-3D code) has not been assumed as the input term. The maximum value has been instead considered, underthe hypothesis that it remains constant over time.

5.1 Realistic water/steam input in Primary Vessel

The literature available concerning two-phase water-steam mixture released from a tube break in a superheated liquid metal environment is not extended, and it is normally based on the assumption that the mixture will immediately flash into pure steam because of the depressurization and the contact with the hot liquid. The attention has then been turned on evaluating the phenomenology determining the number of bubbles and their relative velocity in the flowing primary coolant.

Some code simulations and experiments have been recently performed [5.2], [5.3], but the initial liquid content has been usually neglected, assuming a pure vapor bubble (full evaporation since beginning).

However, experimental activities have proven this approach not fully correct [5.4]: the two-phase mixture is not completely flashing after the throat expansion, and then the following evaporation, due to the contact with the HLM, is not immediate, especially if initial liquid bubble radius is not in the lower end of the distribution (10^{-4} m - 10^{-3} m). This results in a vapor fraction progressively increasing, but not necessarily reaching the state of full vapor before the bubble reaches the reactor free level.

In the present study, the initial liquid content is not neglected, but it is indeed considered and quantitatively estimated, starting from the critical mass flow rate evaluated in Chapter 4. This is considered as the input term for the bubbles life estimation.

5.1.1 Residual liquid content

The throat expansion is characterized by high fluid velocities and low pressure. In the case of a two-phase mixture, the void fraction is, in general, different with respect to the upstream value.

Such change is not easy to quantify and is normally estimated through semi-empirical models based on experimental data providing distributions of bubble number and bubble mass for different bubble radiuses [5.4]. This allows an estimation of the residual void fraction after the throat expansion.

Moreover, based on the total liquid water release, the number of bubbles and their mass distribution is also estimated: this is important to analyze the PHXTR event evolution and the potential consequences in terms of plant safety and radiological releases.

The critical mass flow rate evaluated in Chapter 4 concluded that an initial value of 0.94 kg/s can be assumed from the following evaluations:

- Simple average of the values provided by the most reliable choked flow models
- Time-average value evaluated by RELAP5-3D code in the first 20 seconds

A preliminary step consists in evaluating the impact of the pre-existing two-phase mixture on the break release: a certain steam quality must be considered as input. In other words, the mass flow rate entering the primary vessel is not pure liquid water. An estimation of the water

input quality and void fraction can be given by the weighted average of the two break flows simulated in the RELAP5-3D model[1]:

$$x_{out} = \frac{m_1 \cdot x_1 + m_2 \cdot x_2}{m_1 + m_2} \qquad (5.1)$$

$$\alpha_{out} = \frac{1}{1 + \frac{1 - x_{out}}{x_{out}} \cdot \frac{\rho_g}{\rho_l}} \qquad (5.2)$$

These relations result in the following values:

x_{out} = 0.083;

α_{out} = 0.964;

As a consequence of the two-phase conditions in the tube (upstream the break), a steam mass fraction equal to x_{out} enters the throat, leaving a liquid mass fraction equal to (1-x_{out}) = 0.917.

A second step implies the consideration of the fluid expansion in the break throat. According to the experimental data measurements on the residual void fraction after the throat expansion [5.4], 92% of the water-steam mixture is assumed to not undergo any flashing, but to remain in liquid phase.

In conclusion, the liquid water input value is defined as a fraction of the original mass flow rate provided by the critical flow estimation:

$$m_{water} = 0.917 \cdot 0.92 \cdot m_{choked} \qquad (5.3)$$

This relation provides a liquid water input flow equal to 0.793 kg/s, equal to ~84% of the initial release. This is in agreement with the data experimentally found in [5.1] and [5.4].

The residual water mass considered to enter the primary vessel as vapor, equal to 0.147 kg/s (corresponding to a volumetric flow of 0.049 m^3/s), can cause liquid metal sloshing phenomena at very beginning of the transient.

5.1.2 Liquid droplets distributions

The real liquid mass flow rate input is thus determined. It would be possible to assume that the liquid droplets generated by such flow are limited, in diameter, only by the break size, in this case assumed as circular and equal to the tube internal diameter (d_{in} = 0.014 m).

Very little experimental evidence of liquid droplet distributions in a HLM pool is available. One experiment performed in similar conditions [5.4] has observed a certain liquid droplets distribution in terms of number and mass (Figure 5.1 and 5.2). These distributions can be applied to the MYRRHA PHXTR case in order to evaluate the initial droplet distributions. It will be then possible to follow each droplet evolution and to evaluate the consequences of its path and progressive collapse into steam bubble.

[1] Considering a value averaged in time during the first 20 seconds.

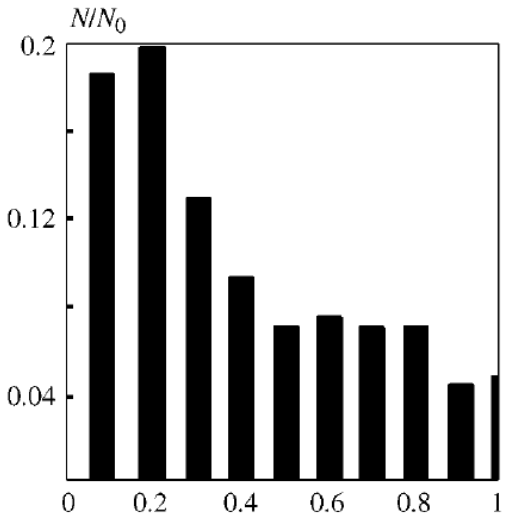

Figure 5.1 – Water droplet number distribution

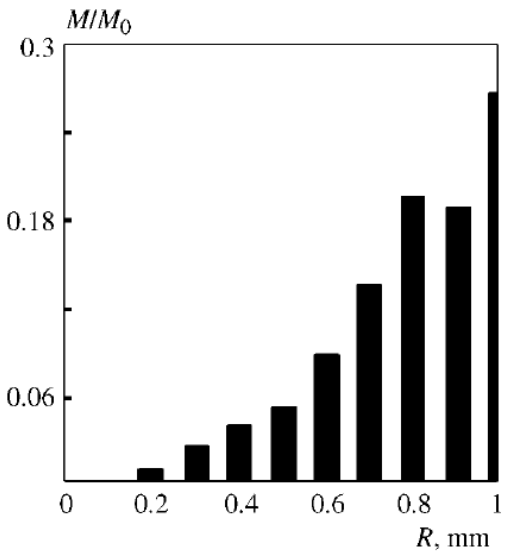

Figure 5.2 – Water droplet mass distribution

If applied to the MYRRHA case, it is possible to estimate the droplet flow distribution (in kg/s). The results are reported in Figure 5.3 and 5.4.

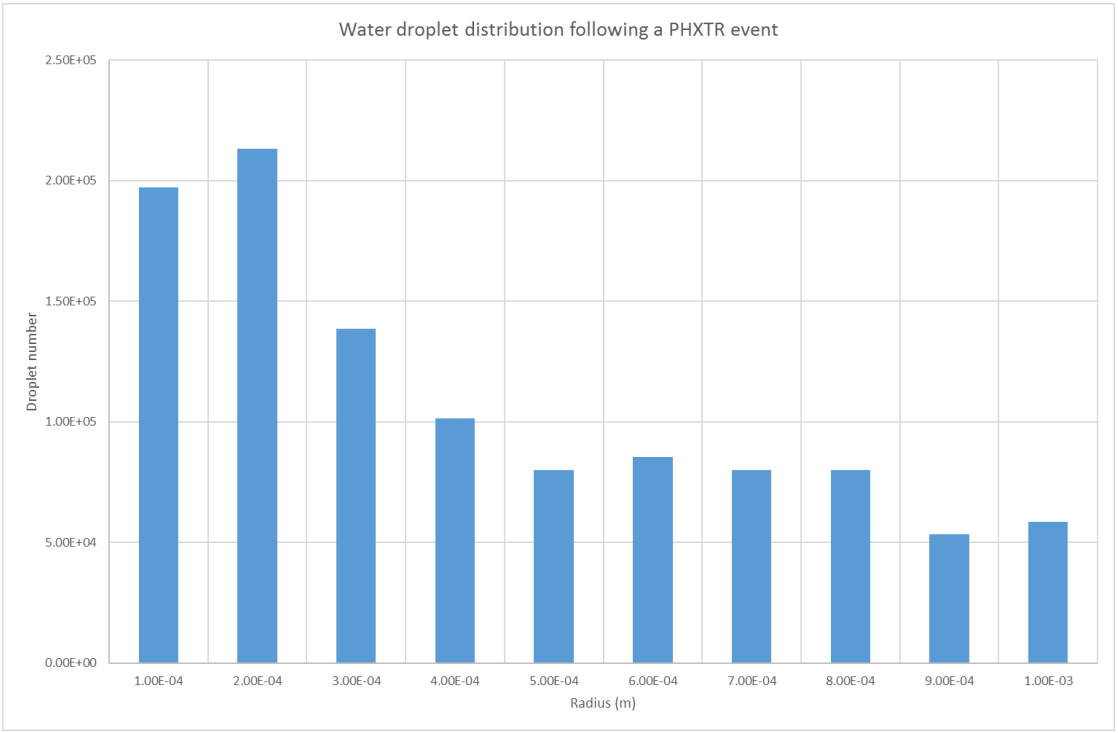

Figure 5.3 – Water droplet number distribution following a PHXTR event

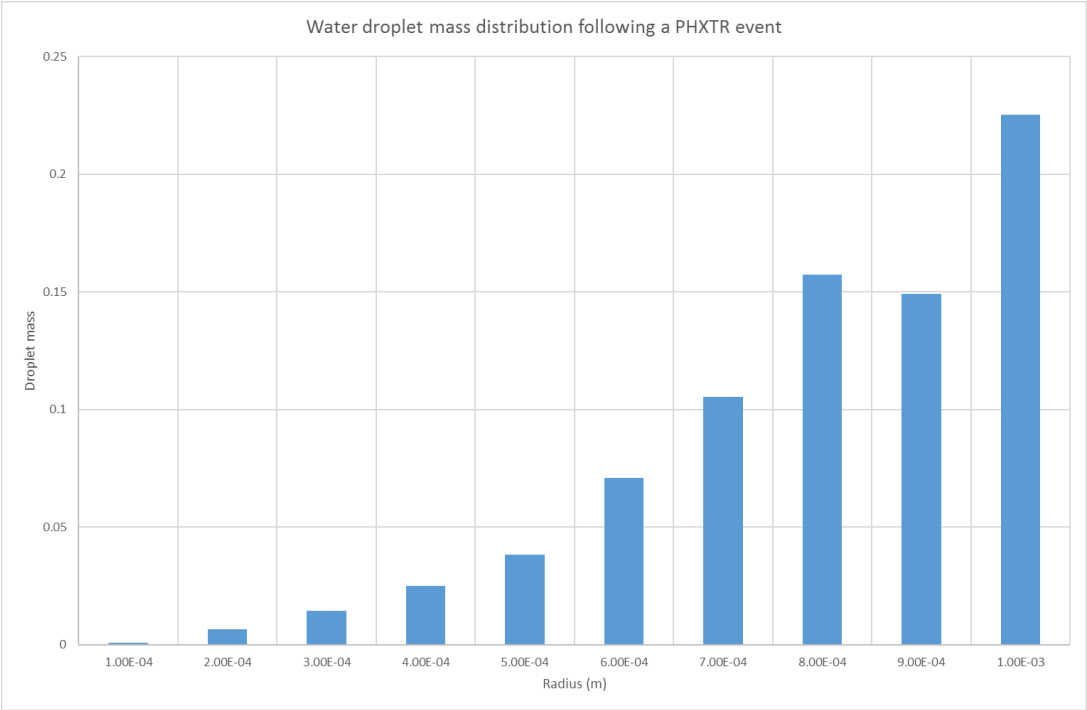

Figure 5.4 – Water droplet mass distribution following a PHXTR event

This represents the definitive input term considered for a PHXTR event in MYRRHA. Starting from these distributions it will be possible to estimate the evolution of the water droplets in the Primary Vessel and the consequences for the plant.

5.1.3 Droplet shape

Once injected in the primary pool, the amount of water must be characterized. It is possible to determine the droplet shape, and according to the problem boundary conditions by referring to the Morton and the Bond number, usually applied to characterize the shape of drops moving in a surrounding fluid or continuous phase:

- Morton number: viscous forces vs. interfacial forces in LBE → Bubble shape $[\frac{g*\mu_c^4*\Delta\rho}{\rho_c^2*\sigma^3}]$
- Bond number: gravity forces vs. interfacial forces $[\frac{\Delta\rho*g*d}{\sigma}]$

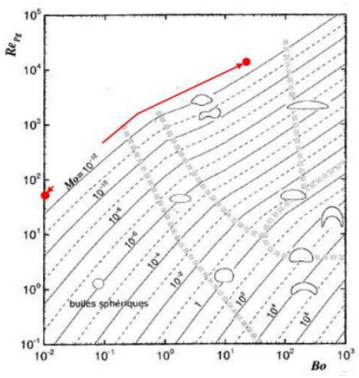

Figure 5.5 – Relation between Morton, Bond and Reynolds bubble numbers [5.2].

5.2 Water droplets evolution

The water droplet distributions evaluated represent the input term for the evaluation of the consequences of a PHXTR event.

As mentioned, no calculation tool is currently able to fully represent the complete multiphase phenomenology involving the transport of a water droplet in a superheated liquid metal. It is thus important to have a calculation tool able to consider the multiple aspects of the problem through a correct set of physical models, assumptions and approximations.

5.2.1 Calculation approach description

It has been chosen to represent the multiphase problem through basic balance equations, coupled with suitable sets of physical properties and closure relationships (pressure drops, mass/heat transfer correlations). The water droplet evolution, while in the liquid metal, is then described by a set of differential equations, each one representing a single water droplet: no interaction between the different droplets has been considered during the multiphase transport.

The effect of the global release is then considered for the consequences on reactor internals and for the pressurization fo the cover gas.

The differential equation system has been programmed in a MATLAB R2106b [5.5] script, the expected outcome consisting in a series of water bubble parameters and physical properties evolution over time. The results have then been used, in the same script, as an input for specific calculation models focused on deriving other quantities more directly related to the consequences of the PHXTR event.

The following assumptions have been considered:

- The vapor generated behaves like a perfect gas
- The pressure in the vapor phase is equal to the pressure in the liquid phase (but temperature is assumed different)
- When compared to liquid density, the vapor density is assumed negligible (true when absolute pressure is low)
- Surface temperature of the LBE remains constant
- The vapor film thickness is uniform, with a perfect regular spherical shape
- The initial vertical velocity of liquid droplet is zero

In the following paragraphs the complete mathematical model used for the analysis, including the assumptions mentioned, is described.

5.2.2 Differential equations used in MATLAB model[2]

Any water injection in Primary System will bring moisture from a pressurized, relatively cold environment (SCS) to a hot pool at nearly atmospheric pressure. As a result, the water will tend to assume a new thermodynamic state according to the new conditions, which will be superheated. Such state, if assumed for liquid water (thermal non-equilibrium hypothesis), is not stable and the (initially) liquid droplet will undergo a transient in terms of geometrical and state properties (radius, pressure, density, temperature).

A specific differential equation system has been developed to follow the water bubble growth [5.6]. Thermal non-equilibrium hypothesis is assumed (different temperatures for liquid and vapor phases).

The system includes five equations. Solving the system provides time evolution of the following variables:

- Droplet liquid radius
- Bubble vapor pressure
- Bubble vapor density
- Droplet (saturation) temperature
- Droplet velocity

A series of other variables (vertical position in the vessel, vapor volume fraction…) can then be derived from these quantities.

The model follows the evolution of one single droplet. Once the solution for a single droplet is available, this can be extended to the rest of the distribution to have a complete overview on the parameters' evolution. Knowing the history of all water droplets in the pool represents the starting point to evaluate plant consequences.

It is important to remind that no interaction for the bubbles has been considered: each single bubble history is followed on its own.

The equation system has been solved using the "ode45" Ordinary Differential Equation solver, a pre-defined MATLAB function allowing to solve systems of ordinary differential equations of any order.

The script has been run for all the different droplet initial dimensions, thus providing the solution for the complete dimension distribution considered.

[2] Legend for the following equations: σ_0 = Stefan-Boltzmann constant; T_1 = LBE temperature; T_2 = Droplet temperature; Abs = Droplet absorptivity; ε_1 = LBE emissivity; ρ_l = liquid density; ρ_g = vapor density; R_{in} = Initial droplet radius; R_d = Droplet radius; k_v = vapor conductivity; h_{fg} = latent heat; g = gravitational constant; p_v = vapor pressure; p_{LBE} = LBE pressure; σ = Surface tension; μLBE = LBE viscosity; R_g = Universal gas constant; T_3 = Vapor temperature; m_d = Droplet mass; vel_d = Droplet velocity; ρ_m = volume-averaged water density; Vol_d = Droplet volume; C_d = Bubble drag coefficient; vel_{LBE} = LBE velocity (constant); A = Bubble diametral section.

5.2.2.1 Droplet surface energy balance

The first equation [5.4] represents the energy balance over the droplet surface:

$$\sigma_0 \cdot (T_1^4 - T_2^4) \cdot \left\{ \frac{1}{Abs} + \left(\frac{1}{\epsilon_1} - 1\right) \cdot \left[\left(\frac{\rho_l}{\rho_v} + 1\right) \cdot \frac{R_{in}^3}{R_d^3} - \frac{\rho_l}{\rho_v} \right]^{-\frac{1}{3}} \right\}^{-1} + 0.255 \cdot \sqrt{\frac{k_v \cdot h_{fg} \cdot (T_1 - T_2)}{2 \cdot R_d}} \cdot \sqrt[4]{R_d \cdot g \cdot \rho_l \cdot \rho_v} = -h_{fg} \cdot \rho_l \cdot \frac{dR_d}{dt} \quad (5.3)$$

This equation provides a quantification of the vaporization of water in hot LBE pool. The droplet radius will progressively decrease until reaching the bubble collapse. Figure 5.6 provides a schematic representation of the three layers involved in the analysis (hot LBE, vapor layer, liquid droplet)[3].

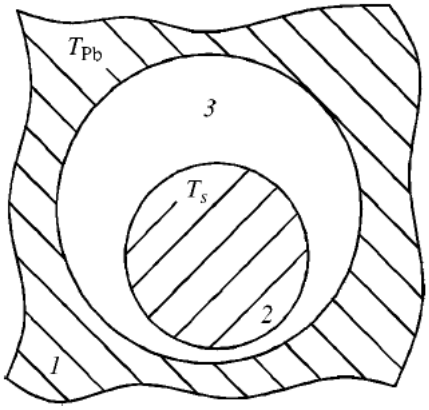

Figure 5.6 – Schematic representation of vapor layer growing from a superheated liquid bubble surrounded by LBE

5.2.2.2 Mechanical equilibrium on bubble surface (Rayleigh-Lamb-Plesset equation)

The second equation [5.7] represents the mechanical equilibrium on the bubble surface:

$$\rho_l \cdot \left[\frac{d^2 R_d}{dt^2} + \frac{3}{2} \cdot \left(\frac{dR_d}{dt} \right) \right] = p_v - p_{LBE} - \frac{2 \cdot \sigma}{R_d} - \frac{4 \cdot \mu_{LBE}}{R_d} \cdot \frac{dR_d}{dt} \quad (5.4)$$

This equation provides a balance of the internal vapor pressure with the external LBE pressure (defined by the hydrostatic head), the effect of surface tension and the viscosity.

5.2.2.3 Clausius – Clapeyron equation

The third equation represents the water two-phase state equation:

$$ln \frac{p_v}{p_l} = -\frac{h_{lg}}{R_g} \cdot \left(\frac{1}{T_v} - \frac{1}{T_l} \right) \quad (5.5)$$

[3] The LBE emissivity has been derived by [5.15].

It describes the relationship between pressure and temperature along liquid and vapor phase boundary, when the system is monovariant (the definition of one parameter will univocally define the second).

5.2.2.4 Ideal gas state equation

The fourth equation represents the ideal gas state equation:

$$p_v = R_g \cdot \rho_v \cdot T_3 \qquad (5.6)$$

It describes the well-known relationship between pressure, specific volume and temperature in a perfect gas. The vapor phase behavior is assumed equal to a perfect gas.

5.2.2.5 Bubble momentum balance

The fifth equation represents the momentum balance on the bubble/droplet:

$$m_d \cdot \frac{dvel_d}{dt} = (\rho_{LBE} - \rho_m) \cdot g \cdot Vol_d - \frac{C_d \cdot \rho_{LBE} \cdot (vel_d - vel_{LBE})^2 \cdot A}{2} \qquad (5.7)$$

It consists in a force balance: the bubble acceleration is defined by the balance between the buoyancy force and the drag force.

The drag coefficient has been subject of experimental analysis at the TALL-3D facility at KTH, which conclusions are described in the Deliverable 4.8 [5.8] of the EU FP7-MAXSIMA project [5.9]. Despite a notable effort in the setup of the facilities and the measurements defices, the results are currently not yet fully post-processed. The data about bubble drag coefficient has this been taken from [5.3].

5.2.3 Main results

The differential equation system can be numerically solved to provide the trend, in function of time, of several parameters related to the bubble evolution in the Primary Vessel pool.

Figure 5.7 shows the evolution of the liquid droplet radius in function of time for the different initial droplet radii.

Figure 5.8 shows the vertical position occupied by the droplet in the Primary Vessel, while progressively moving in the HLM pool. The "0" point has been assumed to be located at the bottom of the PHX tube bundle, where the tube rupture is postulated. The profiles shown in this figure never exceeds 3.7 m because this is supposed to be the vertical distance between the tube rupture location and the LBE free surface level.

Figure 5.9 shows the droplet velocity until reaching the LBE free level (if not collapsing before).

It can be noted that the droplet with the smallest diameter takes short time (~1 s) to collapse, definitaly not sufficient to reach the LBE free surface. The two trends are comparatively shown in Figure 5.9, where it is possible to see how the droplet collapse happens while still well into

the primary pool. The water mass is thus entirely vaporized, contributing to the LBE displacement (see below).

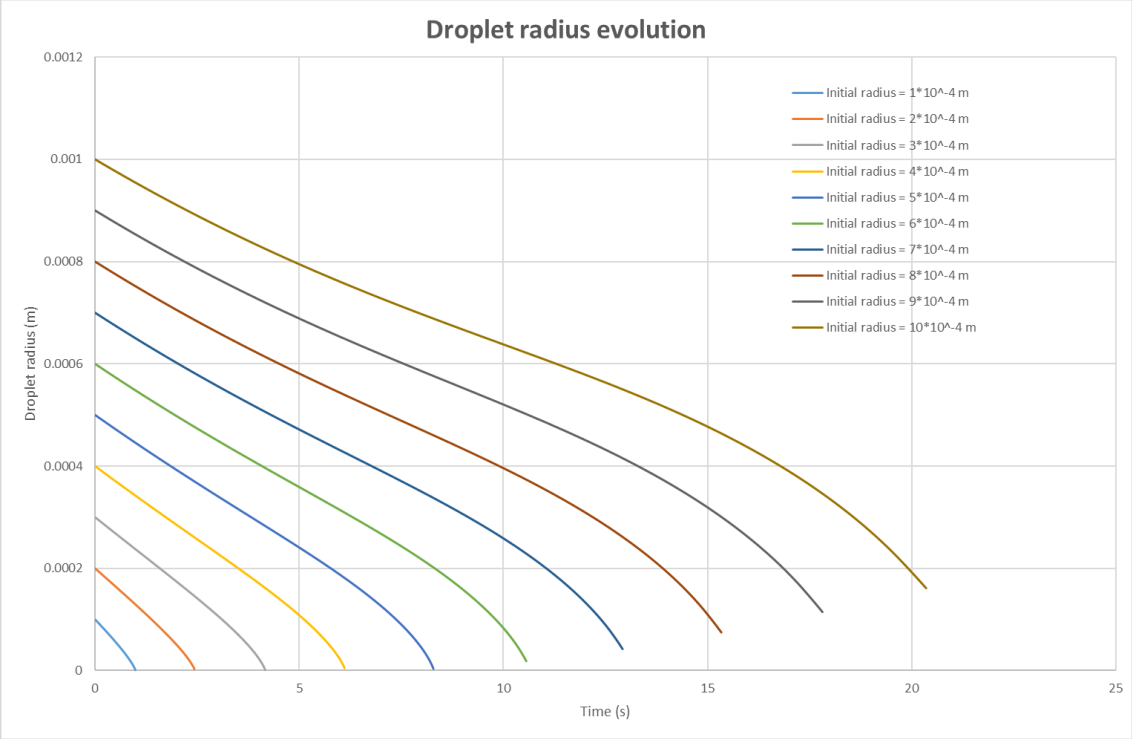

Figure 5.7 – Evolution of liquid droplet radii

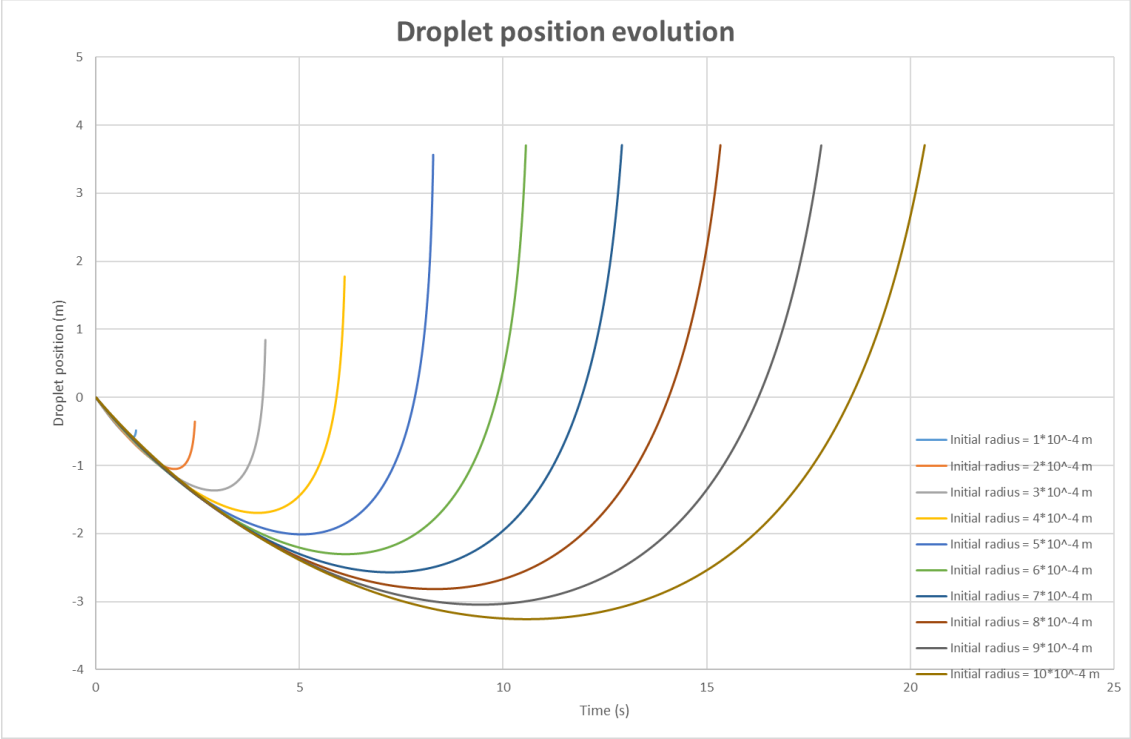

Figure 5.8 – Evolution of liquid droplet position in Primary Vessel

A qualitatively similar behavior is also seen in droplets with an initial radius of $5*10^{-4}$ m: despite the collapse requiring ~8 s, this time still proves not enough for the droplet to survive until reaching the LBE free surface.

This can also be explained by the fact that, initially, the water droplets are entrained downwards by LBE flow (the nominal LBE velocity in the PHX tube bundle is ~0.95 m/s), requiring some time to develop a certain upward velocity (Figure 5.9).

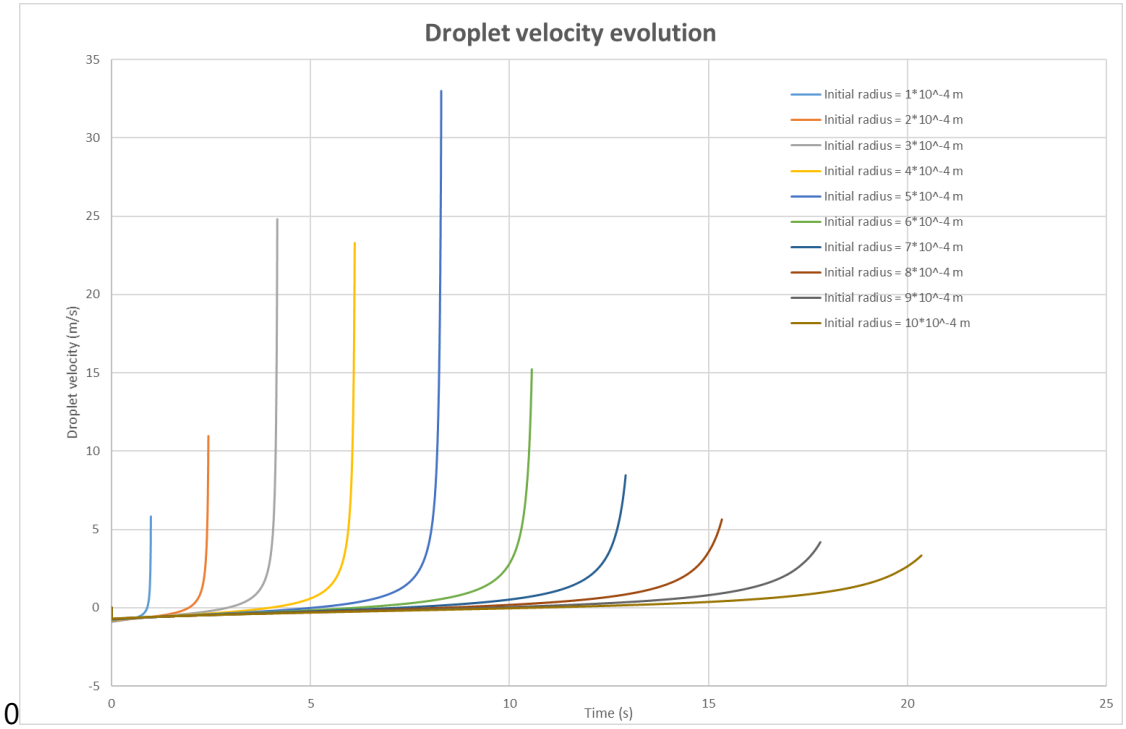

Figure 5.9 – Evolution of liquid droplet velocity

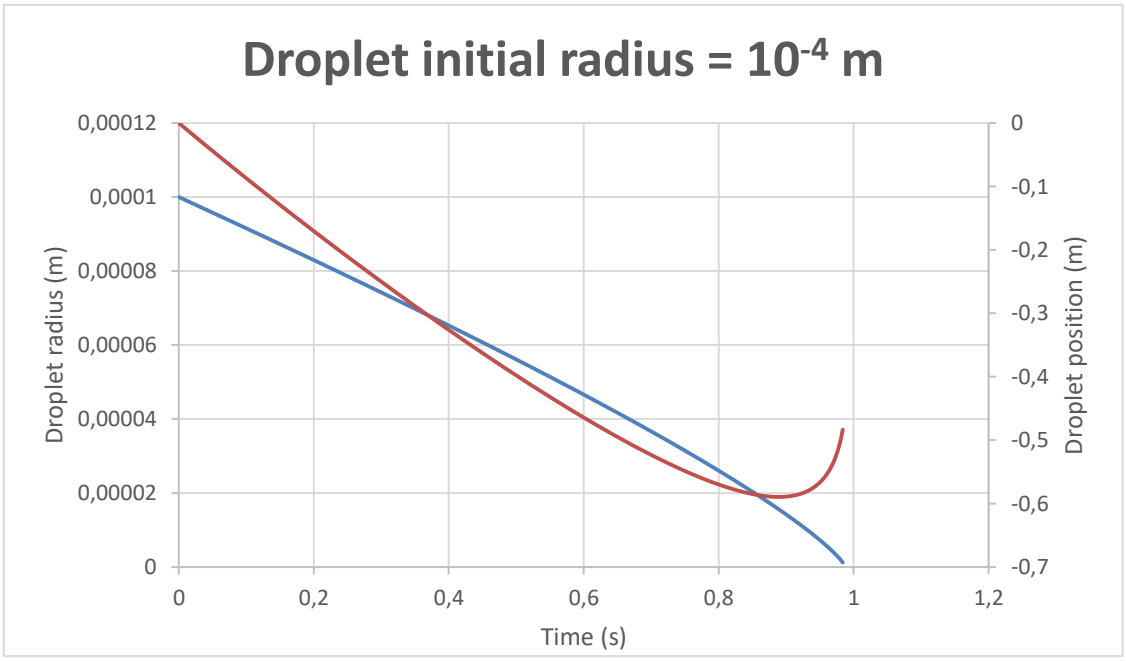

Figure 5.10 – Comparison between radius and position evolution of a bubble with 10^{-4} m as initial diameter

If the initial radius is greater than $5*10^{-4}$ m, then the original water droplet does not completely collapse before reaching the LBE free surface (Figure 5.11). This has a positive impact on the LBE displacement, because part of the droplet volume does not evaporate within the liquid metal, thus not contributing to the LBE movement.

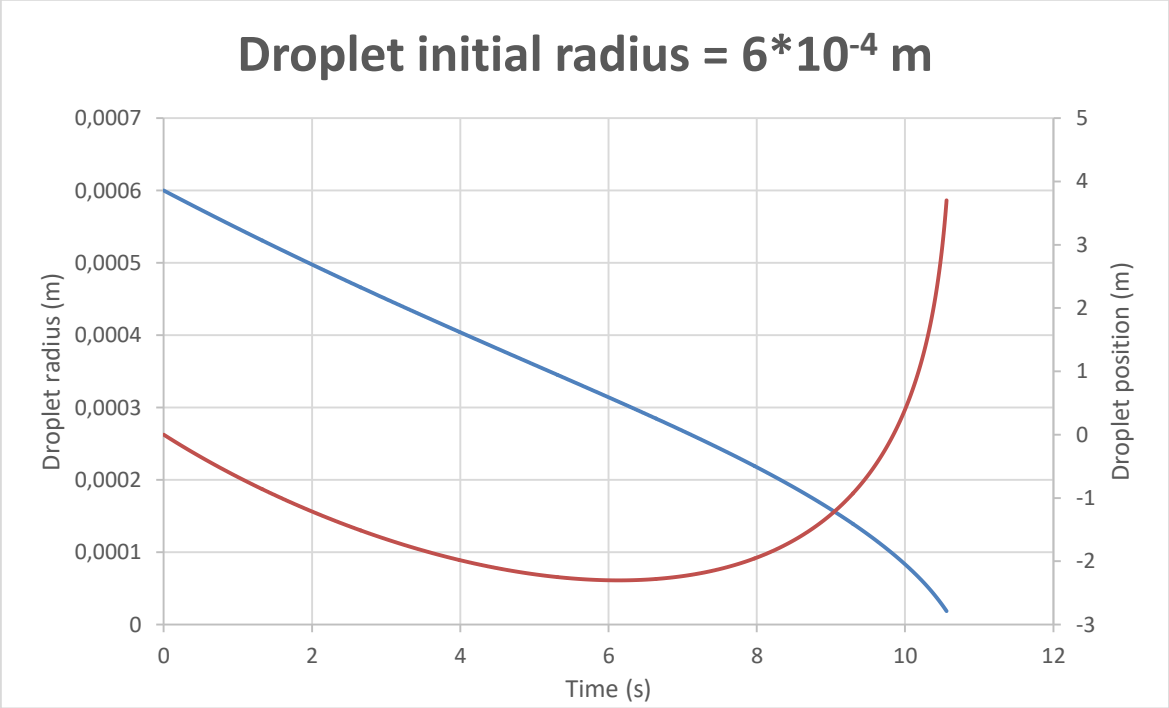

Figure 5.11 – Comparison between radius and position evolution of a bubble with 10^{-4} m as initial diameter

5.2.3.1 Potential core void insertion

According to the position reached by the droplets (Figure 5.7), only a small fraction of droplets (the ones with the largest radius) could effectively pass through the Primary Pump box and outlet channel to reach the Lower Plenum (distance between tube break and PP outlet: ~3 m), from where it could be possible to reach the core with potential void insertion: the heaviest droplets will spend ~5 s more than 3 m below the break.

However, the model here described is 1-D and, most importantly, does not consider the presence of reactor internals or, in general, obstacles to the fluid motion.

It is thus safe to conclude that a minor void fraction ($2.6*10^{-4}$ m^3/s) could have a chance to be entrained in the core during a reduced time frame, without considering any structure. In practice, due to the complex 3-D shape of the pump box, a void insertion in the core appears to be unrealistic.

A confirmation will be provided by the SIMMER-III simulations.

5.3 Liquid displacement and sloshing

Another important phenomenon to evaluate when assessing PHXTR consequences on the plant is the primary coolant displacement caused by the steam expansion in the primary pool.

As mentioned, vapor expansion should not be assumed to completely happen at the very beginning of the event, but progressively evolving from the release until the complete droplet collapse.

The only vapor term that should be considered in the Reactor Vessel since the beginning of the event is the initial vapor fraction flow entrained with the flow through the break, which has been already evaluated (Paragraph 5.1.1, initial liquid content) and quantified in 0.049 m^3/s. The volume increase due by this contribution can be assumed almost immediate.

Figure 5.12 shows the progressive vapor volume growth per second (m^3/s) for the droplet radiuses distribution considered.

This value, added to the initial vapor flow, represents the amount of liquid metal that is displaced per second, potentially causing damages to the vessel internals.

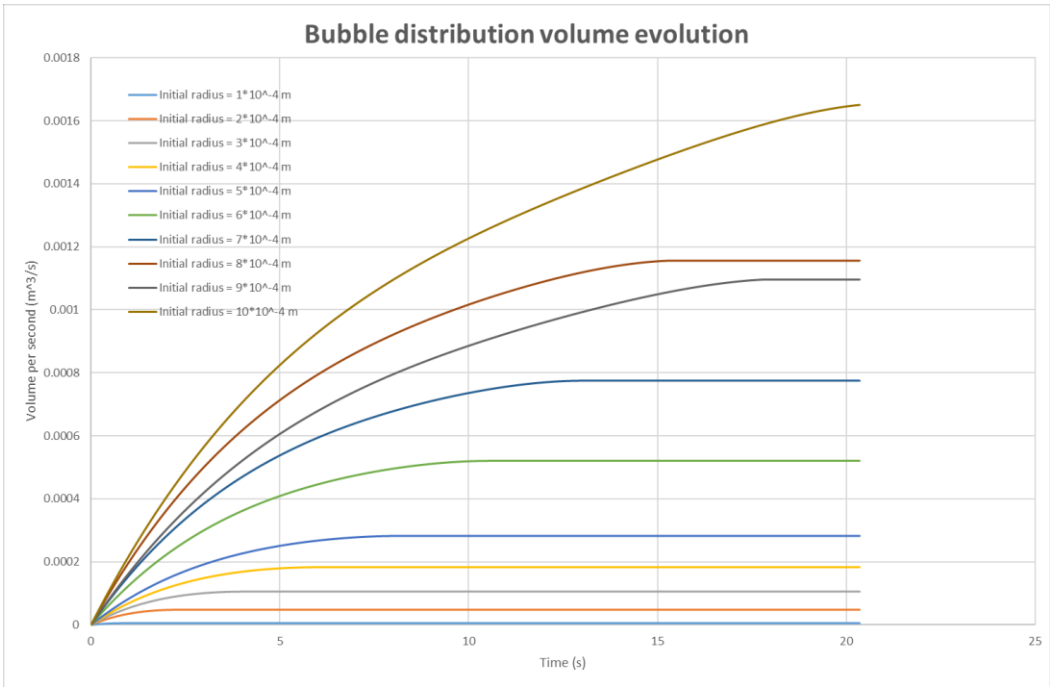

Figure 5.12 – Bubble distribution volume increase per second

In total, a volume increase of $5.82*10^{-3}$ m^3/s is expected from the vapor generation in the LBE pool during the bubble residence time. This, summed to the initial vapor flashing, provides a total volume increase of $5.48*10^{-2}$ m^3/s.

As evaluated before, the time required for the largest droplet to reach the LBE free surface level is ~21 s. The steam volume present in the Primary Vessel in a sort of "steady state" regime is ~1.15 m^3. By comparing this value with the total LBE value present in the pool (~740 m^3), the swelling caused by a PHXTR event results to be ~0.15% of the total volume.

This value is very small, especially compaared to the LBE volume flowing through the Primary Pump in the same time frame (~28 m^3), generating a larger sloshing effect on the reactor internals.

The evaluation does not account for structural obstacles on the pathway of bubble expansion and HLM motion. Nonetheless, with respect to dynamics of overall steam volume expansion, the reference case serves a reasonable approximation: the liquid metal is subject to the same expansion regardless of the exact layout. Moreover, also the bubble actual number and shape do not play a significant role: even when interfacial instabilities lead to fragmentation of a large bubble, the steam volume is conserved.

In general, it is possible to conclude that the HLM displacement caused by a PHXTR does not represent an issue for the Primary System internals, as the vapor volume swelling is very limited compared to other characteristic volumes.

5.4 Potential steam explosion risk

As mentioned above, a large fraction (~84%) of the injected mass from the secondary circuit remains in the liquid state in the form of sub-millimeter and 1-mm-range droplets, dispersed over a mixing zone. The main reason for water/steam dispersal into a fine mixture is because the liquid mass is jetted into the vessel's (heavy-liquid) lead pool under a very high (sonic) velocity from a small breach site. Therefore, it is physically reasonable to expect a low likelihood for large liquid drops to form in the mixing zone in the early time period. In other words, the PHXTR-relevant flow regime suggests that the triggering mechanism due to a collapse of a large steam bubble (containing large liquid drop), described in [5.10], is not relevant here.

Postulating a triggered pressure wave, the CCI explosion potential can be evaluated.

Apparently, the dispersed configuration, as shown in, preconditions the pre-mixture to a high CCI efficiency. Being in reverse of FCI, the CCI potential can be characterized by the amount of energy that can be transferred from melt to a single water droplet, according to the following relation:

$$E_{CCI} = \left(C_{p,l} \cdot \Delta T_{sub} + h_{fg}\right) \cdot m_d$$

Which provides value in the range of 0.008 J to 8 J for the typical 0.1 and 1 mm water droplets, respectively. The whole mixture's energy potential is estimated in the range of 9 kJ/s to 9 MJ/s, accounting for the total mass flow rate at the break.

Thus, the energetic potential of a postulated CCI in a LFR SGTR event is two orders of magnitude less than a postulated FCI in a LWR severe accident [5.1]. So, the amount of energy released in a PHXTR event is considered not dangerous for the reactor internals.

5.5 SIMMER simulations

The PHXTR event is a multiphase 3-D problem that would require advanced calculation tools to be correctly evaluated by accounting for the complete phenomenology.

However, the PHXTR includes a great number of various multiphase interactions involving different reactor disciplines and components: a "complete" code predicting all the possible implications (thermal-hydraulical, mechanical, neutronic, chemical) is beyond current possibilities: no tool can account for every single aspect, which is the reason why a dedicated software has been developed: this allows to follow all phenomenological aspects, but lacks the spatial definition.

Because of this, it has been chosen to simulate the PHXTR accident through SIMMER-III code.

This code series allows representing with reasonable simulation times the pressurized water partially flashing into the LBE pool and the further evolution of the bubbles, also considering potential core reactivity insertion consequences

In comparison with other calculation tools widely used in nuclear industry (STH, CFD), SIMMER-III represents a compromise: it features a coarse-mesh 2-D (r-z) solver with the ability to simulate the multiphase interactions (LBE-water-steam), which represents a clear advantage in comparison to classical STH codes (e.g.: RELAP5-3D), but no turbulence models are included, and the geometrical definition is not comparable to the level commonly reached by CFD codes. On the other hand, CFD codes could not properly follow the two-phase water mixture evolution in a hot liquid metal environment[4].

The calculation time required for SIMMER-III is quite extended compared to STH codes, but normally less demanding than CFD.

In conclusion, SIMMER-III represents a reasonable compromise for the PHXTR simulation, which is interesting to explore.

5.5.1 SIMMER-III simulations

A set of preliminary SIMMER-III simulations [5.11] have been performed at SCK•CEN on the MYRRHA Primary System design version finalized in the frame of FP7-CDT project [5.12]. The main conclusions have been illustrated in Chapter 3.3.2.1.

The main parameters monitored, the cover gas pressurization, the mass flow rate through the rupture disk and the total steam mass lost, are reported here.

[4] CFD simulations are normally limited to gas bubbles injection, where no phase change is involved.

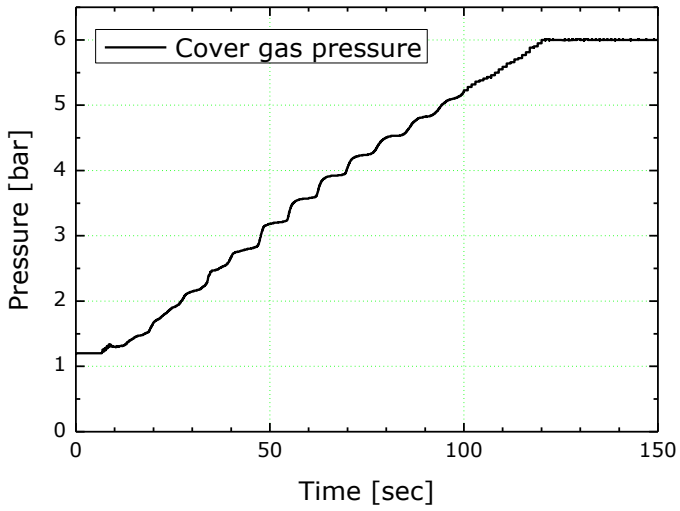

Figure 5.13 – Cover gas pressurization during PHXTR – MYRRHA CDT design

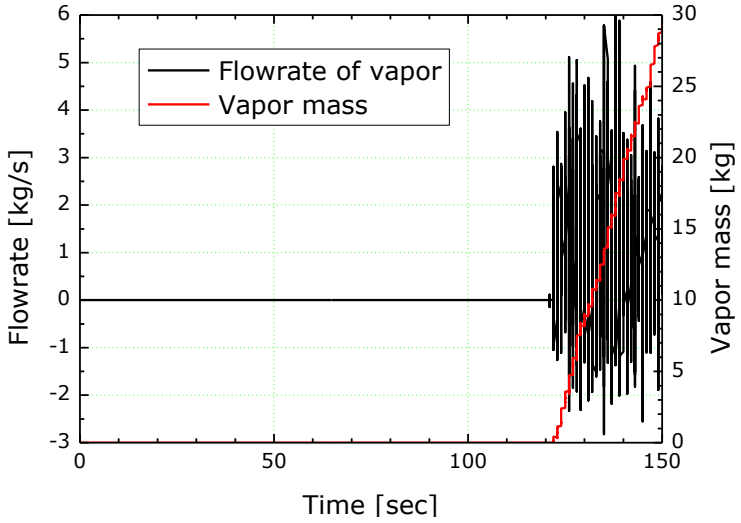

Figure 5.14 – Vapor mass flow rate through the rupture disk during PHXTR – MYRRHA CDT design

After the finalization of the Design Revision 1.6, the SIMMER-III model previously used has been updated according to the new Primary System dimensions, thermal-hydraulic specifications and requisites [5.13]. The main model modifications can be summarized as follows:

- Reactor vessel diameter considerably larger (~33%) and reactor internals position adjusted accordingly
- Two rupture disks implemented:
  - First rupture disk opening pressure modified (from 6 bar to 5 bar)
  - Second rupture disk opening pressure set at 7 bar
- Water mass flow rate flowing out of the tube break modified (from 2.3 kg/s to 0.94 kg/s)[5]

[5] The previous critical flow value was based on an estimation [5.16] performed without considering the presence of the orifice at the tube bundle inlet.

- First rupture disk no more releasing directly into reactor hall but in the PRS; second rupture disk releasing in reactor hall.

A scheme of the 2-D SIMMER-III model used for this simulation has been reported in Figure 5.15.

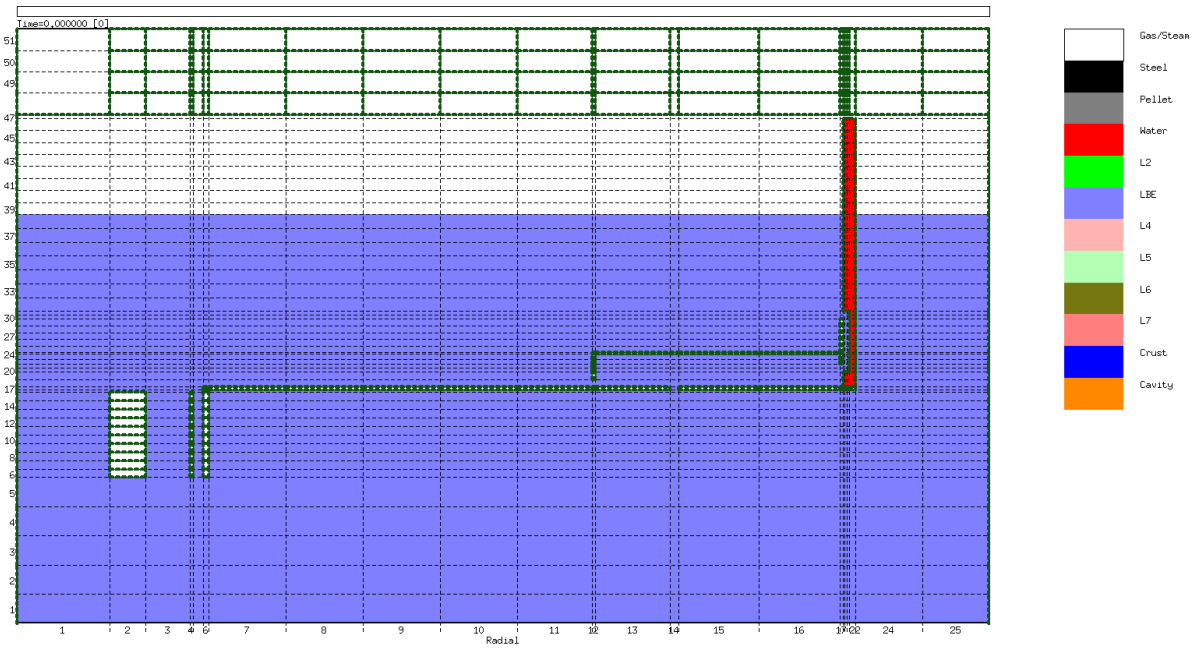

Figure 5.15 – MYRRHA Primary System SIMMER-III model

The first rupture disk is assumed not to fail. In accord with the safety case, the simulation of a triple simultaneous tube rupture has been assumed as boundary case. The results of the simulation have been reported.

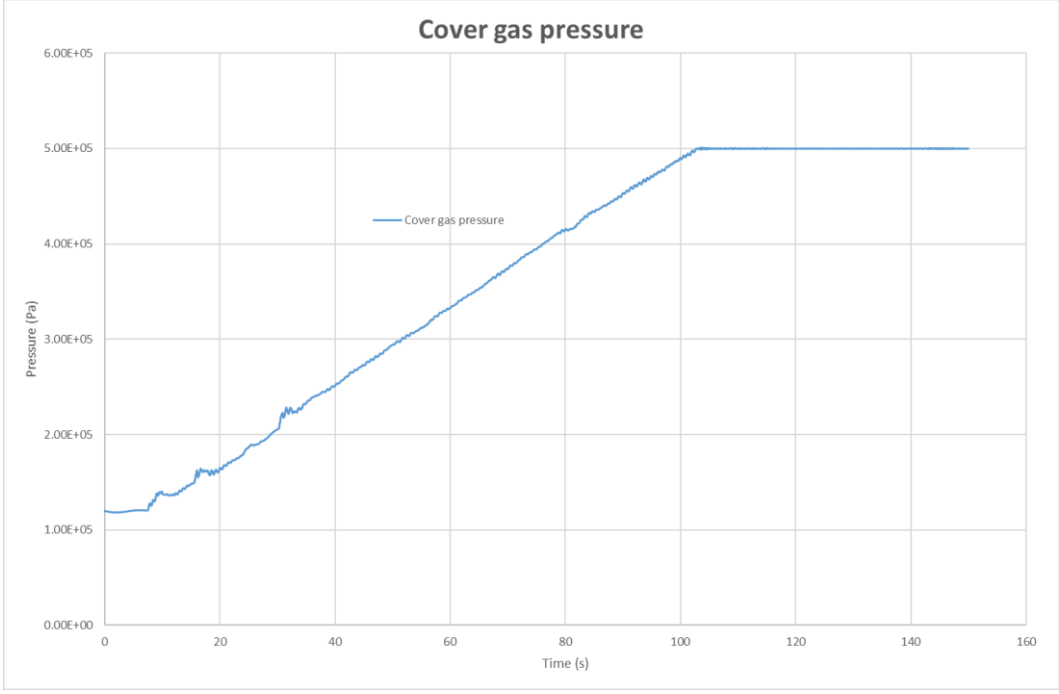

Figure 5.16 – Cover gas pressure

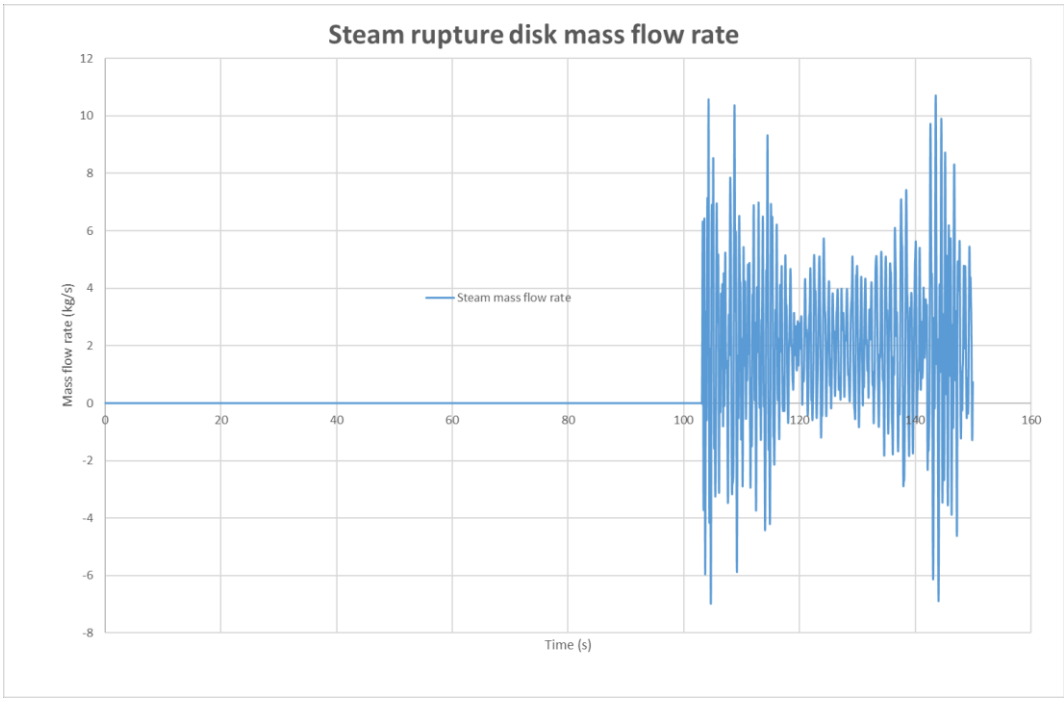

Figure 5.17 – Rupture disk steam mass flow rate

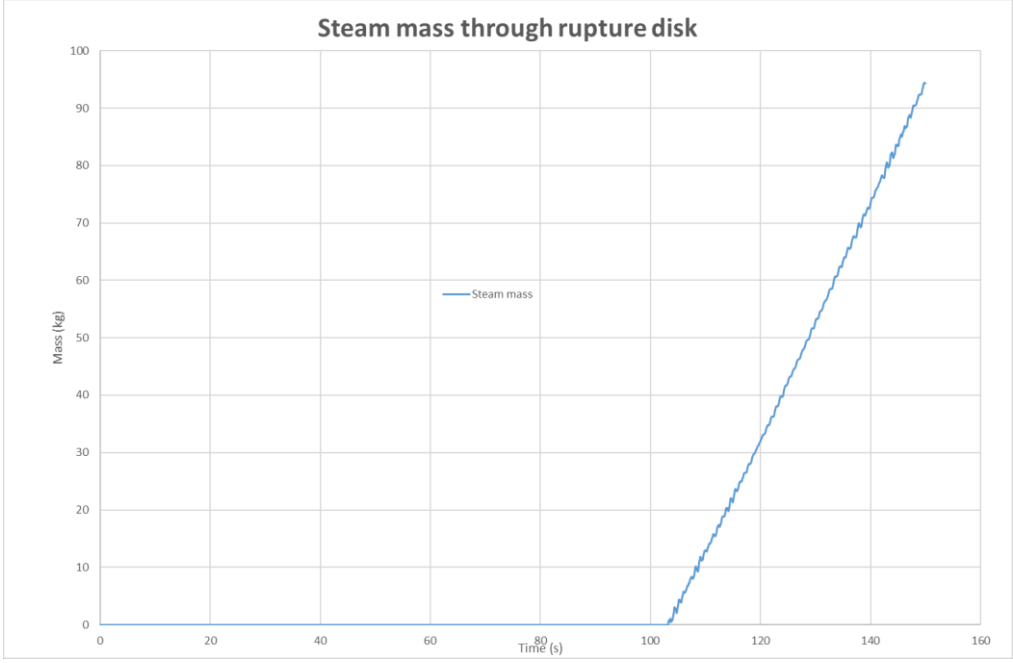

Figure 5.18 – Steam mass expelled through the rupture disk

The following considerations can be derived:

- The rupture disk opens at 103 s, earlier than in the previous version (120 s); this can be explained by the fact that the rupture disk opening pressure has been lowered.
- The PRS must be dimensioned in order to be able to dump the full amount of water released through the PHX tube break (potentially the full SCS water inventory).

- No void fraction is reported to pass through the Primary Pump and to reach the core. Any reactivity insertion transient caused by void insertion associaed to PHXTR can thus be excluded.

5.5.2 FP7-MAXSIMA Task 4.1 conclusions

In the frame of EU FP7-MAXSIMA project, Task 4.1, an experimental simulation of a real scale PHXTR has been performed in the CIRCE facility, at ENEA-Brasimone [5.14]. The test section, consisting in 31 tubes submerged in the CIRCE LBE pool, simulated the MYRRHA PHX tube bundle in its CDT design version[6]. SCK•CEN has carefully followed the design phase to guarantee the correspondence with the MYRRHA reactor.

Four tests have been performed: two simulating a tube rupture at the bundle bottom, and two representing the case with a middle-height rupture.

The results, fully illustrated in Deliverable 4.3 [5.14], shown that there is no risk of damage for neighboring tubes or other internals due to the LBE sloshing of the potential steam explosion. Moreover, no sign of water entrainment towards the bottom has been noticed.

This confirms that the geometrical and thermal-hydraulic features of the MYRRHA reactor do not represent a configuration that could be subject to issues due to a PHXTR event.

[6] Very similar to the official version.

References

[5.1] P. Kudinov and T. N. Dinh, "Approach to Steam Generator Tube Rupture and Leakage in Lead Cooled Systems," Division of Nuclear Power Safety, KTH, Stockholm, January 2010.

[5.2] S. Buckingham and L. Koloszar, "DEMOCRITOS PHASE 3 Final Report," VKI, Brussels, July 2014.

[5.3] M. Jeltsov, "Application of CFD to Safety and Thermal-Hydraulic Analysis of Lead-Cooled Systems," Royal Institute of Technology (KTH), Stockholm, June 2011.

[5.4] A. V. Beznosov, S. S. Pinaev, D. V. Davydov, A. A. Molodtsov, T. A. Bokova, P. N. Martynov and V. I. Rachkov, "Experimental studies of the characteristics of contact heat exchange between lead coolant and the working body," vol. 98, no. 3, 2005.

[5.5] "http://www.mathworks.com," [Online].

[5.6] D. Castelliti, G. V. d. Eynde and G. Lomonaco, "MYRRHA Primary Heat Exchanger Tube Rupture: Phenomenology and Evolution," in *NURETH-17*, Xi'An, September 2017.

[5.7] M. Furuya, K. Matsumura and I. Kinoshita, "A Linear Stability Analysis of a Vapor Film in Terms of the Triggering of Vapor Explosions," *Journal of Nuclear Science and Technology,* vol. 39, no. 10, pp. pp. 1026 - 1032, October 2002.

[5.8] A. Konovalenko, P. Sköld, P. Kudinov, D. Grishchenko and S. Bechta, "Bubble transport experiments and simulation," KTH, June 2017.

[5.9] "EU FP7-MAXSIMA Grant Agreement n. 323312," November 2012.

[5.10] Y. Sibamoto, Y. Kukita and H. Nakamura, "Simultaneous measurement of fluid temperature and phase during water jet injection into high temperature melt," Avignon, 2005.

[5.11] T. Sugawara and D. Castelliti, "Analysis for heat exchanger tube rupture in FASTEF by SIMMER-III," SCK•CEN Internal Report, Mol, 2011.

[5.12] "FP7 Central Design Team (CDT) for a Fast-spectrum Transmutation Experimental Facility - Grant Agreement," SCK•CEN, Mol, 2009.

[5.13] R. Fernandez, "Mechanical design of the primary system," SCK•CEN Internal Report, Mol, September 2015.

[5.14] A. Pesetti, "Final Report on the SGTR event in HLM pool and Post Test Analysis," ENEA, Bologna, June 2017.

[5.15] K. B. Panfilovich, I. L. Golubeva and V. V. Sagadeev, "Thermal Radiation of Liquid Metal Alloys," *Heat Transfer Research,* vol. 36, no. 6, 2005.

[5.16] G. Bandini, P. Meloni and M. Polidori, "Analysis of the heat exchanger tube rupture accident in the XT-ADS reactor with SIMMER-III code," in *Actinide and Fission Product Partitioning and Transmutation*, OECD, 2012.

Chapter 6: Primary Heat Exchanger Design Evolution

The MYRRHA Design Version 1.6 [6.1] represents the reference for the design status of the MYRRHA reactor, object of the safety analyses submitted to FANC, the Belgian Agency for Nuclear Control, for pre-licensing activities.

Following a critical review of such design, partially inspired by comments received by FANC, several aspects requiring a modification have been identified.

Concerning the Primary Heat eXchanger (PHX) and the PHXTR event, a new water-LBE interaction, causing a potential increased risk for Polonium release, has been discovered [6.2].

In light of this, the PHX design has been deeply reevaluated: the PHXTR, previously classified as DBC2 event, must now be shifted to DBC4 (or higher) class, with a return time low enough (10^{-6} events/year or less) to consider it very unlikely to happen during the reactor lifetime. This safety requirement can be achieved through a radical design modification.

Moreover, the reassessment of the Primary System thermal balance, due to the new requirements on primary coolant chemical control, imposed an increase in PHX heat transfer surface, which in turn implies a modification in the PHX dimensions.

One solution potentially able to respond to the new challenges consists in the adoption of a double-walled tube design coupled with a leak monitoring system. This is currently considered as a design evolution option, which will be subject of the complete set of thermal-hydraulic and mechanical analyses performed on the official PHX concept.

6.1 MYRRHA design modifications and improvements

The MYRRHA reactor, in its evolution towards a new design version, is modified in several aspects.

The modifications involving the PHX design represent the direct consequence of three specific issues that must be addressed. In particular:

- Improvement of reactor safety, with special reference to the mitigation of the Primary Heat Exchanger Tube Rupture (PHXTR) consequences
- Redefinition of Primary System thermal balance
- Reduction of Reactor Vessel diameter

6.1.1 Heat Exchanger Tube Rupture exclusion

Among the initiating events potentially generated in the PHX, the tube rupture accident shows dangerous consequences in terms of Polonium release, especially in the light of recent studies showing a higher volatility of Po and its water-based compounds [6.2].

In this perspective, it has been decided to take the required measures leading to the exclusion of such event. Specifically, the PHX design has been modified by adopting a double-walled tube structure. The underlying idea consists in excluding any direct contact between the two coolants by interposing two physical barriers separating reactor primary coolant from Secondary Cooling System water. The failure of a single barrier would be then detected and necessary countermeasures taken, before any direct contact.

Such design modification introduces some disadvantages representing a further challenge for the component design:

- The increase of the heat transfer surface due to the worsening of the overall Heat Transfer Coefficient (HTC) across the tube will cause the increase of the overall dimensions (height and/or diameter)
- Hydraulic and mechanical complication of the tube design

Despite the evolution towards new design has brought radical modifications to the PHX design, a number of features remained unchanged:

- Relevant two-phase pressure drop in the tube bundle, with potential risk of dynamic instabilities and consequent need to design a suitable orifice to generate enough pressure drop in the monophasic (inlet) zone
- The notable tube length could lead to important mechanical stresses due to the bundle vibrations
- The tube bundle is in contact with the free surface leading to possible problems due to differential thermal expansion and level fluctuations (thermal fatigue)

The double wall configuration can be obtained by means of different techniques. A pioneering study on this type of components is described in [6.3]. Following an evaluation of

the different possible double wall configurations, a specific solution has been identified and developed to further stages.

6.1.2 Redefinition of Primary System thermal balance

The MYRRHA design general update foresees modifications in Primary System thermal balance, mostly due to oxygen solution chemical control requiring lower temperatures compared to what previously considered.

From the thermal-hydraulic process perspective, the overall Primary System thermal balance is changed by lowering the average LBE temperature by ~50 °C. This leads to the following overall variations in thermal hydraulic characteristics (Table 6.1):

Table 6.1 – Updated primary system thermal balance

Parameter	Unit	Revision 1.6	Update
Reactor design maximum power	MW	110	110
Average lower plenum temperature	°C	270	220
Average upper plenum temperature	°C	325	275
Total primary system mass flow rate	kg/s	13800	13800

The overall Primary System temperature decrease (and the consequent decrease of the mean temperature difference between primary and secondary systems) has an impact on the PHX size, increasing the heat transfer surface required to remove the nominal power.

The required PHX efficiency can be recovered by increasing the number of tubes and/or by enlarging the tube diameter and/or by extending the tube length.

6.1.3 Reduction of Reactor Vessel diameter

The updated requirements, originating from safety and design, are both concurring in increasing the PHX heat transfer surface:

- The adoption of double wall tube structure increases the tube wall thermal resistance, thus decreasing thermal efficiency and requiring an increase in heat transfer surface
- The average Primary System LBE temperature lowered by ~50 °C requires a matching increase in heat transfer surface

Heat transfer surface increase can be translated in overall PHX tube bundle diameter increase, which will cause an increase of the Reactor Vessel diameter. This is in open contrast with one of the main plant targets, the reduction of Reactor Vessel diameter. Therefore, the only feasible solution consists in extending the tube bundle actively contributing to the heat transfer (“active length”).

The concept of an "active" and "non-active" tube bundle length has been preserved in the design update as well (see Chapter 2). It is in fact not possible to avoid such solution while having a LBE free level and with the need to bring secondary fluid outside the primary vessel.

The "active" length is defined as the part of tube bundle actually taking part in the counter-current flow heat transfer. It is conventionally defined as the tube bundle fraction extending below the inlet window.

The "non-active" length, extending from the inlet window up to the first tube plate, is present with the purpose of carrying the water-steam mixture outside the PHX towards the SCS riser line.

Despite representing a relevant fraction of the total tube bundle length, the amount of heat transfer involving the non-active length is considered negligible compared to the power transferred in the active portion.

In order to implement the necessary design updates without incurring in radial dimension increase, a relaxation on the relative distance between the active core and the PHX active length geometrical center is allowed[1], provided the natural circulation onset and the associated DHR function is not jeopardized.

Such requirement relaxation allows the PHX tube bundle axial extension.

[1] In Design Revision 1.6, it was required for this distance to be at least 1 m.

6.2 Innovative Primary Heat Exchanger tube bundle thermal-hydraulic assessment

The MYRRHA PHX design evolution adopts a shell-and-tube configuration with a double-walled structure for the tubes. The primary LBE flows downward in the shell side, while the secondary water/steam mixture flows upward in the tubes.

The configuration chosen for the double-walled PHX tube bundle design is the so-called "bayonet". Generally speaking, a bayonet tube is a component made of several coaxial tubes. The bayonet tube adopted in MYRRHA can be described as follows (Figure 6.2):

- A downcomer channel
- A downcomer tube separating the downcomer from the riser annulus
- A riser annulus, where the actual heat transfer takes place
- A first tube (the inner tube of the double-walled structure)
- A gap
- A second tube (the outer tube of the double-walled structure)

The secondary coolant (water) flows from the top to the bottom of the PHX through the downcomer tube, then it redirects upward in the annular channel between the downcomer tube and the first outer tube. The reactor primary coolant heats water in the annular channel[2].

The mixture then enters the steam collector of the upper head (see Figure 6.1) to exit the PHX towards the Steam Separator of the SCS.

Secondary water enters the downcomer in a slightly subcooled state (provided by the height difference between the SCS Steam Separator [6.4] and the PHX inlet) at a temperature corresponding to the saturation temperature in the Steam Separator (~ 200 °C).

After entering the Riser annulus, the nearly saturated water reaches saturation temperature (p ~ 16 bar) and starts boiling. Water assumes a two-phase state in almost the totality of the Riser length, thus enhancing the heat transfer with the primary LBE.

At full power, the mixture reaches a quality of ~0.3 (and a void fraction of ~0.9) at the riser outlet. The riser temperature, once the saturation is reached, remains almost constant through the whole riser length[3]. This aspect currently remains unchanged with respect to the official design, since no change to the SCS has still be decided [6.5].

The riser temperature differs from the down-comer temperature by only ~3 °C so the down-comer tube, normally insulated to avoid undesired regenerations, in this case is limited to a single steel layer because the regenerative effect is considered negligible.

[2] The fluid heated in the annular channel will, in turn, heat the water in the down-comer tube; this second regenerative heat transfer mechanism generally deteriorates the efficiency of the bayonet, but this represents a minor issue for MYRRHA as the temperature difference between the downcomer water and the water-steam mixture is very limited (~3 °C) reducing regenerating effects to a minimum. Moreover, the production of steam is not part of the application catalogue.

[3] In reality, it experiences minor variations as the pressure is decreasing due to the pressure drops.

6.2.1 Double wall bayonet tube concept: main features

The main improvements deriving from the adoption of such design solution, with respect to Design Revision 1.6, are the following:

- Effective mitigation of a PHX tube rupture event
- Removal of the water collector below the primary LBE surface
- Removal of the large feed water pipe located in the center
- Removal of the lower tube sheet (no tube sheet weldings below LBE free surface)
- Simpler geometry and primary flow distribution at the outlet
- Higher aspect ratio providing a better counter-current flow development through the bundle and a better bundle efficiency
- Simplified tube plugging procedure
- Higher operability with reduced maintenance time

An overall view of the new PHX concept is shown in Figure 6.1.

Concerning the reactor safety, it is important to remark how the removal of the feedwater pipe and bottom collector below the LBE free level are also important safety improvements of the new PHX design, since these solutions inherently prevent ruptures of these structures inside the LBE. Such feature drives the PHX design towards the reduction of the water inventory inside the Primary Vessel; in particular, the component sections whose failure would have translated in a sudden and complete release of water inventory in Primary System (with dangerous consequences [6.6]) are now not included anymore in the design.

Moreover, the adoption of a double walled tube structure requires modification in the upper head of the PHX: three tube-sheets, creating three different chambers, are needed.

6.2.2 PHX tube double wall configuration

Among the possible double-walled bayonet tube configurations, the selected solution consists in two concentric tubes with a conductivity-enhanced gap in the middle. Figure 6.2 shows the general layout under study.

The gap between the first and the second outer tube, and its filling medium, must satisfy the following requisites:

- A thermal efficiency avoiding excessive increase of the tube bundle heat transfer surface
- The ability to remove decay heat in passive mode after applicable DBC events (safety function)
- Possibility of detection of a leaking inner or outer tube (safety function)
- Gap easy filling
- Chemical compatibility with PHX materials

By increasing the active length (extending the PHX tube bundle towards the bottom of the reactor vessel), both the design and the safety requirements have been achieved without enlarging the external diameter, despite the loss in thermal performance caused by the adoption of the double wall structure.

Figure 6.1 – Updated PHX overall view

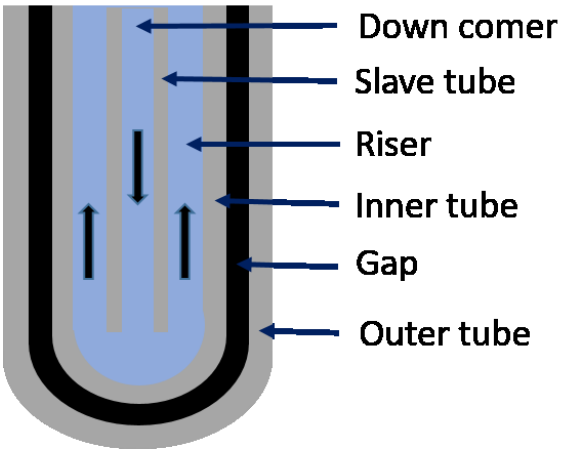

Figure 6.2 – Bayonet tube configuration

6.2.3 Tube bundle calculation results

The temperature profiles resulting from the new PHX design configuration are reported in the following figures:

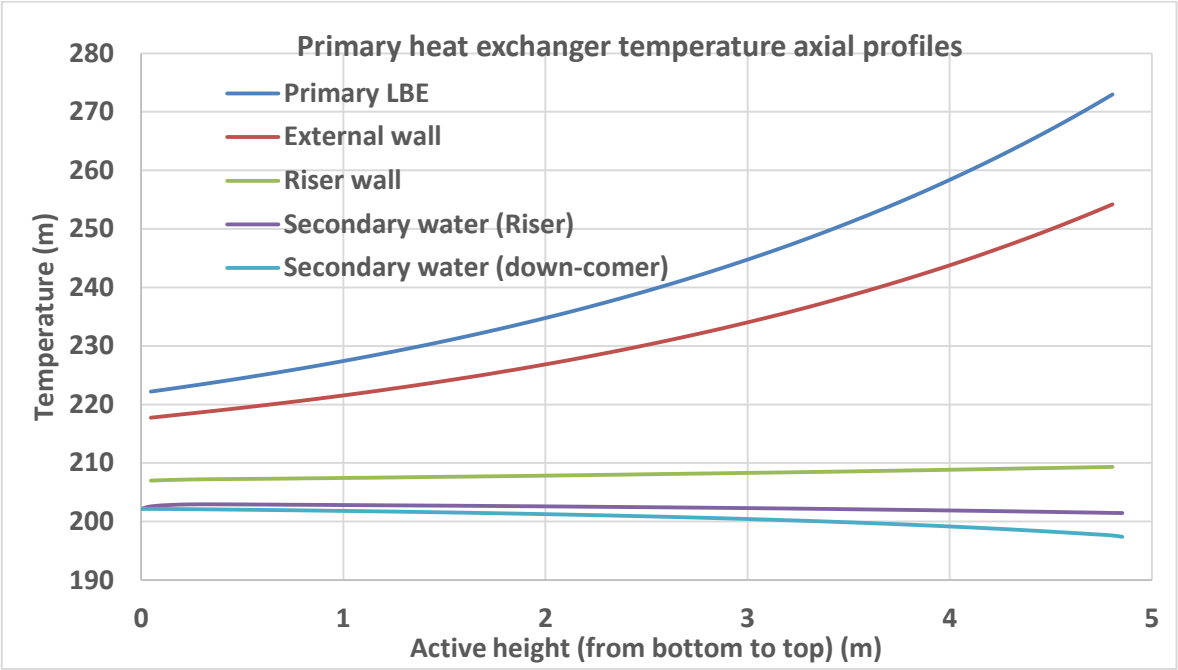

Figure 6.3 – PHX temperatures axial profile

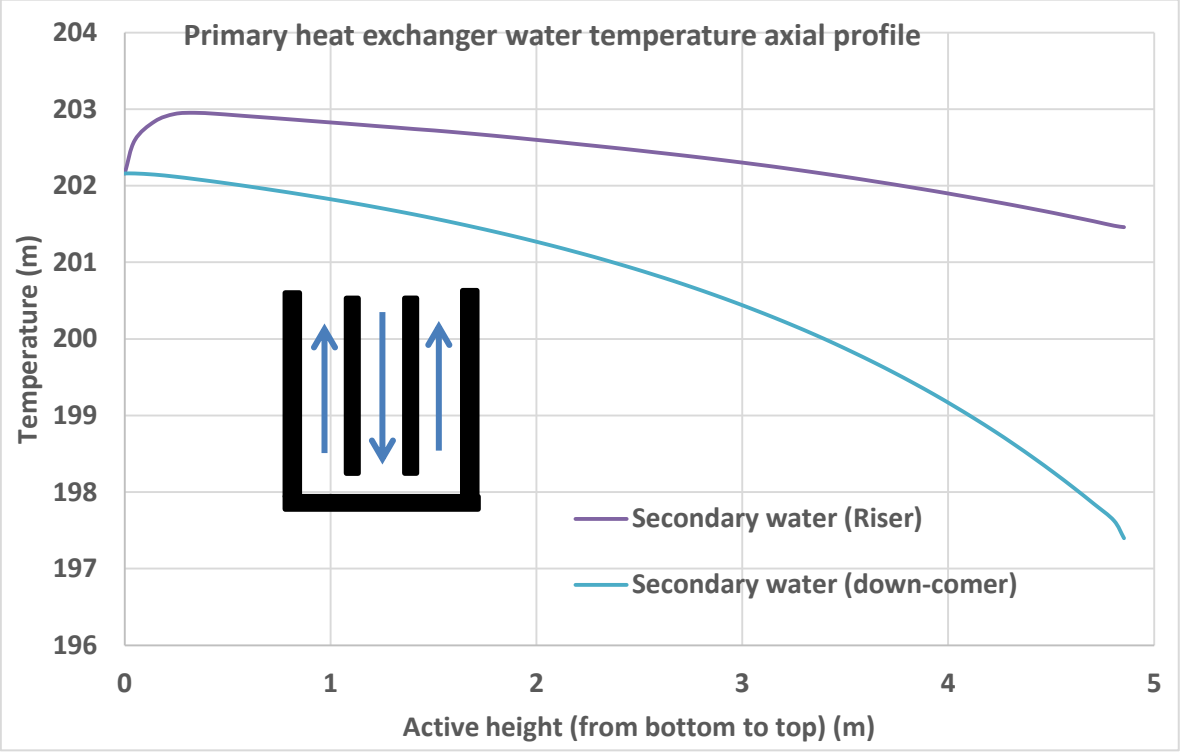

Figure 6.4 – PHX temperatures axial profile (detail on water temperature evolution)

Figures 6.3 and 6.4 show the axial profiles of the temperatures characterizing the PHX thermal-hydraulic design:

- Primary LBE bulk temperature
- External double tube wall temperature
- Internal double tube wall temperature
- Secondary water temperature

From these figures, it is possible to follow in detail the path of the water from the downcomer inlet to the riser outlet. Subcooled water enters the downcomer (T ~197.5 °C) and, because of the slight regeneration effect involved, it reaches the bottom of the bayonet tube at a temperature of ~202.5 °C. In the riser annulus, after reaching the saturation, the temperature starts decreasing as function of the pressure drops.

The flow quality is evolving very similarly to the former PHX configuration: from 0 (slight subcooling) at the tube riser inlet, evolving toward ~0.3 at the active length outlet. The void fraction is rising from 0 to ~0.9 almost monotonically, with a limited discontinuity in the transition point between Slug and Annular flow regime caused by the mechanical non-equilibrium model implementation in RELAP5-3D.

The main geometrical results are depicted in Table 6.2, while the most relevant thermal-hydraulic parameters are specified in Table 6.3.

Table 6.2 - Proposed PHX configuration: geometry

Parameter	Unit	Value
Tube bundle active length	m	4.9
Shroud internal diameter	m	0.8
Tube number	-	748
Tube diameter	mm	21
Overall heat transfer surface	m^2	238
Shell hydraulic diameter	mm	20.02

Table 6.3 - Proposed PHX configuration: thermal-hydraulics

Parameter	Unit	Value
LBE velocity	m/s	1.35
Downcomer water velocity	m/s	1.89
Riser water velocity	m/s	17.077
LBE friction pressure losses	bar	0.42
Downcomer friction pressure losses	bar	0.70
Riser friction active length pressure drop	bar	0.33
Riser friction non active length pressure drop	bar	1.73
Average LBE HTC	$W/m^2/K$	11962
Average overall HTC	$W/m^2/K$	2674.1

The PHX tube bundle diameter is unchanged with respect to the Design Revision 1.6, while the heat exchanging length of the tube bundle is maximized: such modifications are suitable for the plant to fulfill the new requirements in terms of layout and thermal balance. The limits on maximum fluid velocities (for LBE, liquid water and steam) are also respected.

The pressure drops, in both primary and secondary systems, are increased. This is due to the extended length and the different bundle layout. This will need to be considered from the safety perspective.

6.2.4 Considerations on tube bundle instabilities

The updated PHX configuration must be tested against instabilities, following the same procedure performed on the current configuration. A similar RELAP5-3D model has been set up and the same procedure has been followed (see Chapter 2).

Concerning Ledinegg instabilities, the behavior is similar to the reference design: the unstable regime appears at very low mass flow rate values, outside of any operating range.

The conclusions about the density-wave instabilities are, on the other hand, considerably different: the single-phase downcomer tube is providing enough pressure drops to stabilize the riser flow in normal operation. Moreover, if the water subcooling is higher than nominal conditions (colder water), thermal regeneration will occur across the coaxial downcomer tube, so that the riser inlet temperature is always similar, regardless of the subcooling at the downcomer inlet.

Flow regime transition instabilities are present also in this configuration, but to a lesser extent. However, such phenomena are not avoidable since caused by physical changes in water flow pattern.

The tube bundle presents thus a strong resistance to instabilities: no orifice will be required.

The instability analysis will be refined once the design update will be completed[4].

6.2.5 Considerations on the Heat Transfer Coefficient

Regardless of the configuration considered, the global HTC of MYRRHA PHX is quite stable and relatively independent of reactor power level. This feature is present in the reference design and can be retrieved in the update as well.

For what concerns the LBE side, the HTC variation experienced between 100% and 10% power is in the range of 60% (from ~11000 W/(m^2*K) to ~4000 W/(m^2*K)). Such a variation, accounting the high value of the HTC itself, generates limited variations of the overall PHX heat transfer, thus making the component relatively independent from LBE mass flow rate variations.

[4] A SCS concept review is also planned: several analyses requiring a broader specification of boundary conditions have been put on hold until the global frame is more defined.

The choice to have a two-phase water mixture as secondary operating fluid (with water entering in a slight subcooled state) provides the advantage to have a very high (~25000 $W/(m^2*K)$) HTC on the water side, due to the boiling flow regimes established into the PHX water tubes. In particular, the water-side HTC is not suffering any considerable variation because of quality change.

The variation of the tube thickness and gap thermal resistance is almost independent from temperature. Moreover, the thermal resistance offered by the double wall (two steel layers plus the gap) is, proportionally, much more relevant than the convective resistances on the primary and secondary tube side. This results in the radial temperature difference being mostly located in the wall thickness, making the HTC variations even less relevant.

As a result, the overall HTC does not experience appreciable variations at different reactor power loads.

6.3 Primary Heat Exchanger design implications towards DHR function

As for the reference PHX, one of the functional requirements consists in the ability to remove the Decay Heat, transmitting the decay power from the primary LBE to the SCS in active mode or, if necessary, in passive mode (natural circulation).

The improved PHX design maintains the features of the reference concept in terms of safety function:

- Small variability of the HTC with flow conditions in the two loops
- Resistance against a Primary Vessel break event

6.3.1 Implications of Primary Heat Exchanger design modifications on natural circulation

In order to fulfill the new design and safety requirements (adoption of lower Primary System temperatures and shift of the PHXTR event to at least DBC4 class), one of the design condition adopted in the current version has been relaxed: the distance between the geometrical centers of the core and the PHX active lengths ("ΔH_{geom}") is no more fixed to 1 m.

While it could appear that removing the distance between the centers of gravity could bring to the impossibility of the natural circulation onset, this has been proven not true [6.7]: actually, the onset of natural circulation is related, through direct proportionality, to the distance between the thermal centers of gravity of the core and of the PHX ("ΔH_{ther}").

ΔH_{geom} is different from ΔH_{ther}: while the former is strictly related to the geometry and it cannot change, the latter is the difference between the points of average temperature of the components, which is a function of the temperature profile in core and PHX and may change if the working conditions of the system are subject to changes.

Specifically, the active core thermal center is almost coincident with the geometrical center and it is not subject to considerable variations in function of power (the profile shape remains cosinusoidal), while the PHX thermal center may experience sensible changes according to power modifications (profile shape is logarithmic). Moreover, in the PHX the difference between thermal and geometrical centers of gravity may experience a greater variation than the active core.

It is thus expected that, considering ΔH_{ther}, the natural circulation onset becomes possible, especially in lower power (DHR) conditions where the PHX experiences most of its thermal gradient in the uppermost region of the bundle (thus increasing ΔH_{ther} to the maximum value allowed by the component position).

A dedicated RELAP5-3D model has been developed to quantify the variations of ΔH_{ther} during operation at different power levels.

6.3.2 PHXTR event: approach modification

The innovative PHX design option has been conceived assuming the PHXTR event shift to DBC4 (or higher) class as a requisite. Thus, it is obvious that the approach to this specific accident must be completely different.

The results of the studies on the innovative PHX concept and the actual possibility to detect the rupture of one of the two tube external walls will define the PHXTR DBC class. Three potential scenarios are then possible:

- PHXTR as DBC4 event: the number of Strong Lines of Defense[5] required to withstand the event will be lowered from 2 to 1, but a complete accident analysis, including the associated uncertainties, will be still required.
- PHXTR as DBC5 event: only a Medium Line of defense will be required, and the event analysis will be conducted assuming Best Estimate conditions.
- PHXTR as DBC6 event: the event will be excluded.

It is indeed possible that Belgian Safety Authority will just require the demonstration of the exclusion criterion, without any need for the complete transient evolution and consequences analysis. However, the studies reported in this work can provide a strong insight on the PHXTR event, whose evolution will be similar in both design configurations, as no driving plant parameters variation is wide enough to cause a substantial deviation.

[5] Line of Defense with a failure probability lower than 10^{-6}.

6.4 R&D programme

An R&D programme to demonstrate the thermal-hydraulic and mechanical performance of the double-walled bayonet-tube heat exchangers was initiated in 2016 and consists of four work packages.

These four work packages will allow to qualify the proposed double-walled heat exchanger design from a thermal hydraulic, mechanic and leak monitoring point of view.

Such experimental campaigns primarily aim at assessing:

- The bayonet tube manufacturability assessment
- The bayonet tube gap conductance
- The potential uprising of mechanical issues
- The LBE Heat Transfer Coefficient (at first not in bundle geometry)

The analyses on the double-walled tube will primarily involve two experimental facilities located in SCK•CEN domain, in Mol: COMPLOT and HEXACOM.

6.4.1 COMPonent LOop Testing (COMPLOT)

The COMPLOT facility (Figure 6.5) [6.8] is a large-scale closed-loop LBE experimental facility, designed to characterize the hydraulic behavior of numerous MYRRHA reactor components at full-scale, in flowing LBE, representative of the reactor conditions. Test sections of up to 10 meters in length are allowed. A wide range of flow rates (2 - 36 m^3/h) is obtained with a variable speed pump, combined with a throttle valve and bypass.

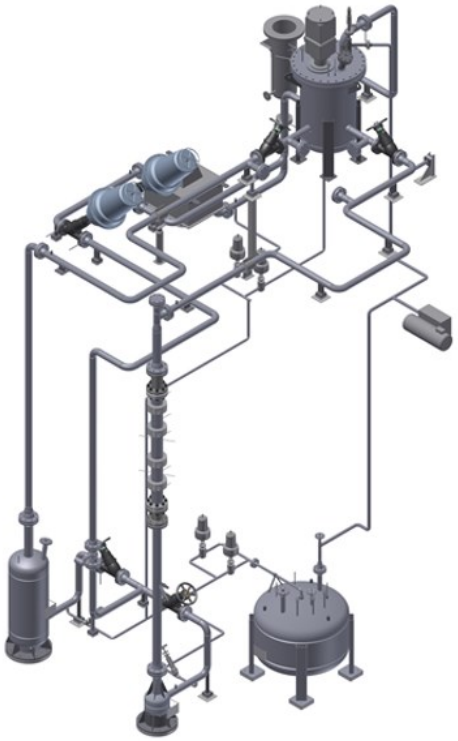

Figure 6.5 – COMPLOT facility 3-D layout

Originally, the COMPLOT loop was conceived to perform isothermal experiments (up to a maximum of 400 °C). To allow heat transfer tests, the loop is modified to include a 100 kW heater.

6.4.2 Heat EXchanger At COMplot (HEXACOM)

The HEXACOM facility (Figure 6.6) [6.9] is a two-phase water-steam cooling circuit that provides temperatures and flow conditions representative of the MYRRHA Secondary Cooling System (16 bar, nearly saturated water inlet) [6.6] and is able to reject 100 kW of heat to the environment.

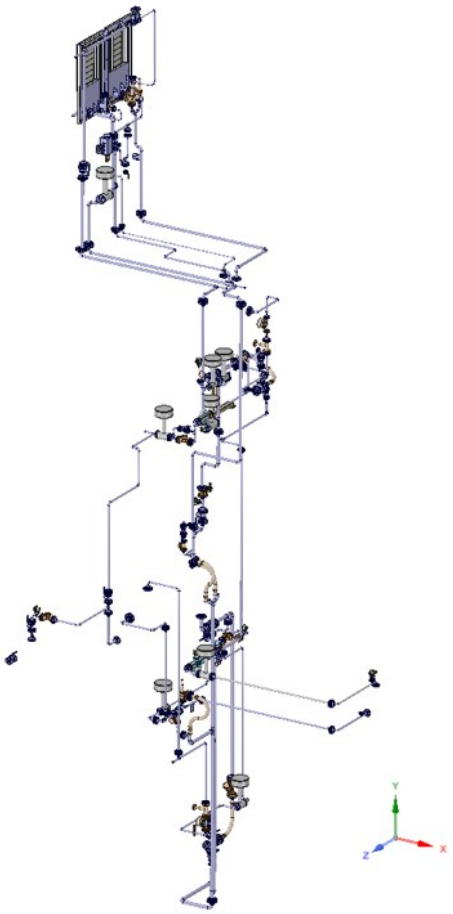

Figure 6.6 – HEXACOM facility 3-D layout

The HEXACOM facility can be effectively used for several purposes, thanks to its flexibility. Initially conceived to remove the power generated in COMPLOT, it will be used to perform a series of tests to prove the MYRRHA SCS concept and validate the calculation tools. For this purpose, the HEXACOM design mimics quite carefully the SCS layout[6], which is represented in scale 1:1: this is necessary because the behavior of a two-phase mixture cannot be scaled without losing representativeness.

[6] At least for what concerns the first sub-loop. Aero-Condenser loop is not perfectly representative.

In addition to that, a valve has been added (Valve 727 in Figure 6.7) in the riser line directing the water-steam mixture towards the Steam Separator. This valve, called "Diego's Valve", has the purpose of providing a jet of two-phase water mixture for testing purposes. One of the foreseen applications consists in studying the interaction of the jet with hot LBE. This would represent an interesting benchmark for the theories expressed in this work (hence the name).

Because of some delays in procurement and commissioning phase, HEXACOM loop will not be operative before beginning of 2019.

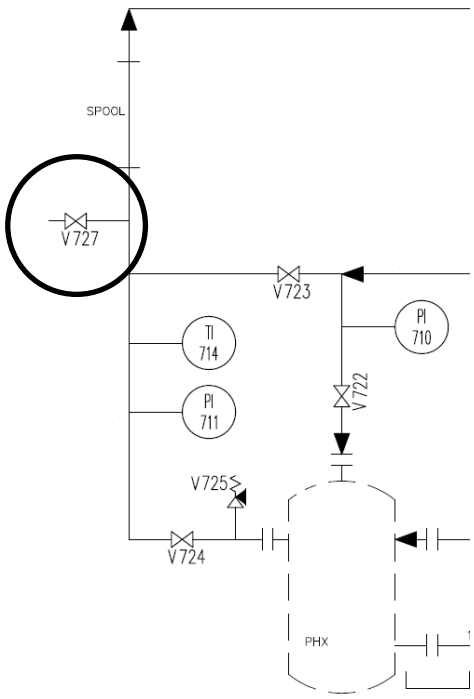

Figure 6.7 – "Diego's Valve" location

6.4.3 Test section and experimental campaign

The thermal hydraulic and mechanical behavior of a single double-walled heat exchanger tube at full scale will be experimentally investigated in MYRRHA-representative conditions in the COMPLOT facility at SCK•CEN.

It will be coupled, via the COMPLOT test section itself, to the secondary cooling loop, simulated by HEXACOM.

The test section is at the interface between COMPLOT and HEXACOM and hosts a single double-walled heat exchanger tube at full scale. The LBE-channel (round tube) dimensions are chosen to provide flow conditions as close as possible to the MYRRHA configuration (hexagonal lattice) with respect to Reynolds number and Nusselt number.

The main objective of the experiment is to determine the contribution of the double-walled tube, with specific reference to the gap, to the overall heat transfer coefficient between LBE and water. It is thus important to establish the correct radial temperature profile and to measure this as accurately as possible. For this purpose, thermocouples will be placed at the

inner and outer surface of the tube and in the LBE and in the water channel, at different axial heights along the active length of the heat exchanger tube, allowing to infer local and global values of the wall thermal resistance.

Next, the study will focus on the investigation of the sensitivity of heat transfer and pressure loss to the chemical conditions in the bulk of the LBE and the surface of the heat exchanger tube. In particular, the influence of oxygen dissolved in the primary fluid will be tested.

Finally, in order to investigate the performance of the complete heat exchanger tube bundle (instead of limiting the study to one single tube), an extension of the experiment is envisaged in which an integral heat exchanger test, with a larger but limited number of tubes, is planned in a large-scale LBE facility. The number of tubes should be sufficient to have fully representative flow conditions on the LBE-side for as many tubes as possible while keeping a reasonable test section size. This will make the thermal and mechanical assessment (including vibrations and spacer grids) of the tube bundle performance possible.

A series of additional features are required to the COMPLOT and HEXACOM facilities for this experimental campaign:

- Possibility to operate the facility at power levels beyond 100% (reference case)
- Flexibility to modify the water mass flow rates in order to achieve outlet steam quality ranging from 0.1 to 0.5
- Ability to simulate operational transients like Start-up, Shut-down and in-situ dry-out and refilling during maintenance

References

[6.1] R. Fernandez, "Mechanical design of the primary system," SCK•CEN Internal Report, Mol, September 2015.

[6.2] B. G. Prieto, Evaporation of polonium from lead-bismuth eutectic nuclear coolant, KU Leuven: SCK•CEN, Ph.D. thesis, June 2015.

[6.3] D. D. D. Fur, LMFBR Steam Generator Development: DUPLEX Bayonet Tube Steam Generator, vol. 2, Chattanooga, Tennessee (USA) (CENC-1238): Combustion Engineering Incorporated, 1975.

[6.4] D. Castelliti, "Secondary Cooling System and Tertiary Cooling System Design Basis," SCK•CEN Internal Report, Mol, December 2015.

[6.5] D. Castelliti, "Preliminary Design Description of the Secondary Cooling System (SCS) and Tertiary Cooling System (TCS)," SCK•CEN Internal Report, Mol, 14 December 2016.

[6.6] G. Bandini, P. Meloni and M. Polidori, "Analysis of the heat exchanger tube rupture accident in the XT-ADS reactor with SIMMER-III code," in *Actinide and Fission Product Partitioning and Transmutation*, OECD, 2012.

[6.7] D. Castelliti and F. Mirelli, "HLD04 - MYRRHA Primary Heat Exchanger design status towards Design Revision 1.7," SCK•CEN Internal Report, Mol, 2017.

[6.8] K. V. Tichelen and G. Kennedy, "COMPLOT and E-SCAPE: Facilities for Liquid-Metal, Pool-Type Thermal Hydraulic Investigations and their Associated R&D Program in the Frame of the MYRRHA Project," in *The 10th International Topical Meeting on Nuclear Thermal-Hydraulics, Operation and Safety (NUTHOS-10)*, Okinawa, Japan, December 14-18, 2014.

[6.9] D. Rozzia, F. Mirelli and K. V. Tichelen, "Assessment of the HEXACOM loop by RELAP-5," SCK•CEN Internal Report, Mol, January 2017.

Final considerations, recommendations and future developments

MYRRHA (Multi-purpose hYbrid Research Reactor for High-tech Applications) is a pool-type Material Testing Accelerator Driven System (ADS), cooled by Lead-Bismuth Eutectic (LBE) with the ability to operate also as a critical reactor. The plant main targets include to perform fast-spectrum irradiations, to demonstrate the Minor Actinides transmutation concept, to prove the ADS concept and to act as GEN-IV European Technology Pilot Plant for Lead Fast Reactor.

A key component in the MYRRHA reactor design is the Primary Heat eXchanger (PHX), which represents the main thermal connection between the Primary System and the Secondary Cooling System. The PHX main function is to deliver the power generated in the reactor core to the Secondary Cooling System, including accidental conditions. Because of this, passive mode operation for Decay Heat Removal is part of the functional requirements.

The PHX design is based on a countercurrent shell and tube concept with primary LBE flowing downward in the shell side and secondary two-phase water mixture flowing upward in the tubes. Four identical PHX units are located in the Reactor Vessel.

A complete thermal-hydraulic and mechanical assessment of the PHX has been finalized, including a detailed analysis on pressure drops and on hydraulical instabilities, and then reported as part of the complete file describing the MYRRHA Design Revision 1.6.

The MYRRHA reactor has entered the pre-licensing phase after the finalization of the Design Revision 1.6, the first design version to be officially submitted to the Belgian Safety Authority (FANC).

In addition to the conceptual design, a series of safety studies must be submitted to the Safety Authority, to prove that no major threat for the reactor safety has been neglected and no event can jeopardize the reactor barriers integrity and lead to unacceptable radiological release to the environment.

Among the safety studies, one of the most relevant for the reactor safety case, originating in the PHX, is the Primary Heat eXchanger Tube Rupture (PHXTR), classified as DBC2 (return time > 10^{-2} event/year). The accident evolution is supposed to be less challenging in comparison with other Heavy Liquid Metal (HLM) reactor concepts, thanks to the lower Secondary Cooling System (SCS) pressure adopted in MYRRHA (16 bar). Nevertheless, it is important to study the complete transient evolution and all the potential consequences:

- Water release in the Primary Vessel
- Pressure wave
- Heavy Liquid Metal displacement and sloshing
- Potential Coolant-Coolant Interaction and steam explosions risk
- Multiphase transport

The MYRRHA Design Revision 1.6 has proven to be very resistant to this specific Initiating Event. In particular, despite the conservative assumption of complete SCS water inventory release in the Primary Vessel at the maximum possible mass flow rate (critical flow), the

pressure wave magnitude evaluated has a very low intensity, not enough to induce the failure of the neighboring tubes nor to have a negative impact on other reactor internals.
The HLM displacement also revealed to be not a real issue, as the volume per second of steam released in the primary pool is negligible compared to the total LBE volume and the fluid motion generated by the Primary Pump operation.

The Coolant-Coolant Interaction and consequent potential steam explosion has also been found to not represent a problem, as the amount of energy released by such interaction is low enough to avoid any damage to internals.

Finally, both 1-D multiphase evaluations and 2-D SIMMER-III simulations has shown that no void will find its way towards the reactor core, so any reactivity insertion transient caused by void insertion associated to PHXTR can be excluded.

The MYRRHA reactor is thus resistant to a PHXTR event.

However, due to the newly discovered chemical interaction of water with the Polonium dissolved in the LBE, the consequences of a PHXTR, especially during reactor maintenance periods with the Cover open, are not acceptable. The PHXTR event should thus be pushed at least in DBC4 class.

At the same time, due to chemical interaction of LBE with cladding material, it has been decided to lower the Primary System temperatures.

Therefore an evolution of the current MYRRHA design is necessary.

One of the first and most relevant components interested in the design update is the PHX. A completely new design, able to fulfill the new requirements in terms of safety and thermal balance while not increasing the overall reactor dimensions, has been conceived. It is based on the adoption of a double-walled tube structure with enhanced conductivity. Moreover, the majority of the water inventory present in the PHX has been removed by eliminating the water plena.

This innovative PHX design is currently in testing phase in SCK•CEN domain, and it will be implemented in the next MYRRHA official design revision.

From the point of view of the PHXTR event, it remains a complex accidental sequence to be studied under all possible perspectives. In case it will prove to be impossible to completely exclude such event from the MYRRHA safety case, a demonstration will be required. A multiphisics assessment, based on 3-D calculation tools able to consider the real reactor geometry and all the involved phenomenology (phase change, metastable phases, different bubble interaction in function of dimensions…), including potential mechanical damage to other reactor internals, would represent the best approach. This could be achieved by improved CFD simulations coupled with mechanical module (which is already available) and a complete multiphase module (which is still missing). However, it is expected a notable effort in terms of calculation time and a serious commitment to a series of experimental activities to validate such calculation tool.

Appendix 1: RELAP5-3D System Thermal Hydraulics code [A1.1]

RELAP5 code series has been developed at the end of '70 in past century, at Idaho National Laboratory (INL) and has been economically supported by U.S. Department of Energy (DOE) and by Nuclear Regulatory Commission (NRC). The RELAP code series can still count on a strong users and developers' network, organized in various international programs such as the International Code Assessment and Application Program (ICAAP), the Code application and Maintenance program (CAMP), and the International RELAP5 Users Group (IRUG).

The specific code applications include various transient simulations in light water reactors (LWR) such as loss of coolant accidents, anticipated transients without scram (ATWS), and transients like loss of feedwater, station blackout and turbine trip.

RELAP5, in its mod 3.3 version, is a generic system code which, other than being able to evaluate the behavior of a reactor coolant system during a transient, can also be used for the simulation of a wide range of thermal-hydraulic transients in both nuclear and conventional plants where various phenomena with mixtures of liquid, vapor, non-condensable gases and non-volatile solutes can happen.

The purpose of RELAP5 code developing program has been to obtain a code version that can prove to be suitable for the analysis of all transients and accidents that have been hypothesized for LWR systems, including LBLOCA, SBLOCA and all operational transients.

The thermal-fluid-dynamic simulation with the RELAP5 code is obtained thanks to a non-homogeneous and non-equilibrium model for two-phase systems, which is solved by a fast, semi-implicit numerical scheme, allowing fast transient calculations.

Since the beginning of its development, the purpose of the RELAP5 code has been to create a suitable tool that would be able to include all the most important effects needed for an accurate prediction of system transient evolutions and, at the same time, simple and efficient enough to be able to allow parametric studies and sensitivity analyses.

The code also includes several general component models that can be used to simulate various system parts. The pre-defined models include pumps, valves, tubes, jet-pumps, turbines, steam separators, pressurizers, feedwater heaters, hydraulic accumulators, and control system components.

The RELAP5 code allows the user to properly simulate the heat transmission through the adoption of complex heat exchange models for conduction, convection and irradiation regimes. The modeling of such phenomena is obtained thanks to 1-D "heat structures", with several configuration options available for the user.

The power generation can be imposed from table input data or it can be calculated by a dedicated point neutron kinetics model or by the interaction with 3-D neutron kinetics PARCS code.

Moreover, some special models are included for particular situations such as loss of form, flux in abrupt area changes, multiple junctions, choked flow, boron tracking, and non-condensable gases transport.

The RELAP5 code includes wide input control capabilities, in order to support the user in recognizing and correcting input errors and model inconsistencies.

The RELAP5 model development began its evolution with the first numerical schemes (1976) until today. Current versions are the sum of all the previous experiences in modeling the plant behavior during accidental events, in various processes involving two-phase flow and for several features of LWR reactor. The code development has been greatly helped by the wide and extended comparison with experimental data that have been obtained in a great number of programs and experimental facilities like LOFT, Semiscale and NRU.

A1.1 RELAP5-3D Input Deck for the PHX instability analysis

A sample RELAP5 input deck used for the analysis of the Primary Heat Exchanger tube bundle instabilities is shown hereafter.

```
=mirups
100 newath  transnt
101 run
102 si  si
105 5.0 6.0
110 air argon
115 1.0 0.0
120 380010000   0.0 bipb    pri
121 420010000   4.6641  h2o sec1

201 1.0 5.00e-12    0.00125 7007    200 2000    4000
202 50.0    5.00e-10    0.00125 7007    200 2000    4000
203 500.0   5.00e-10    0.00125 7007    200 2000    4000
*   trip
411 time    0   gt  null    0   0.0 n
431 time    0   gt  null    0   1000000.0   n
451 time    0   gt  null    0   2000.0  n

*   primary system

*   inlet tdv
2600000 intdv   tmdpvol
2600101 7.329930e-04    0.05    0.0 0.0 0.0 0.0 0.0 0.0 0000010
2600200 003
2600201 0.0 2.610930e+05    513.15

*   flow boundary condition
2800000 flowbc  tmdpjun
2800101 260010000   300000000   0.0 00000000
2800200 1
2800201 0.0 0.0 0.0 0.0
2800202 10.0    0.0 0.0 0.0
2800203 50.0    10.0877193  0.0 0.0
2800204 1000000.0   10.0877193  0.0 0.0

*   primary heat exchanger 1
3000000 phx1    annulus
3000001 10
3000101 7.329930e-04    10
3000301 0.214   10
3000401 0.0 10
3000601 -90.0   10
3000801 1.00e-06    0.029165    10
3000901 0.0 0.0 9
3001001 0000000 10
3001101 00001000    9
3001201 003 2.801710e+05    513.15  0.0 0.0 0.0 1
3001202 003 2.805220e+05    513.15  0.0 0.0 0.0 2
3001203 003 3.018570e+05    513.15  0.0 0.0 0.0 3
3001204 003 3.232060e+05    513.15  0.0 0.0 0.0 4
3001205 003 3.445680e+05    513.15  0.0 0.0 0.0 5
3001206 003 3.659410e+05    513.15  0.0 0.0 0.0 6
3001207 003 3.664210e+05    513.15  0.0 0.0 0.0 7
3001208 003 3.878160e+05    513.15  0.0 0.0 0.0 8
```

```
3001209 003 4.092210e+05    513.15  0.0 0.0 0.0 9
3001210 003 4.306350e+05    513.15  0.0 0.0 0.0 10
3001300 1
3001301 0.0 0.0 0.0 9
3001401 0.029165    0.0 1.0 1.0 9

*   phx outlet junction 1
3400000 phxout1 sngljun
3400101 300010000   350000000   0.0 2.0 2.0 00001100
3400201 1   0.0 0.0 0.0
3400110 0.038223    0.0 1.0 1.0

*   ingresso pompa 1
3500000 pumpin1 snglvol
3500101 7.329930e-04     0.05     0.0 0.0 -90.0    -0.05    1.00e-06     0.0
0000000
3500200 003 4.306350e+05    513.15

*   phx outlet junction 2
3600000 phxout2 sngljun
3600101 350010000   380000000   0.0 0.0 0.0 00001000
3600201 1   0.0 0.0 0.0
3600110 0.0 0.0 1.0 1.0

*   outlet tdv
3800000 outtdv  tmdpvol
3800101 7.329930e-04    0.05    0.0 0.0 0.0 0.0 0.0 0.0 0000010
3800200 003
3800201 0.0 4.306350e+05    495.55

*   secondary cooling system

*   phx inlet tdv
4000000 phxintdv    tmdpvol
4000101 1.0e+06 0.0 1.0e+06 0.0 0.0 0.0 0.0 0.0 0000010
4000200 003
4000201 0.0 1.60e+06    473.15

*   secondary flow boundary condition
4100000 secflobc    tmdpjun
4100101 400010000   420000000   0.0 00000000
4100200 1
4100201 0.0 0.137426901 0.0 0.0
4100202 1000000.0   0.137426901 0.0 0.0

*   heat exchanger lower plenum 1
4200000 hxlplen1    snglvol
4200101 0.000307877 0.10    0.0 0.0 90.0    0.10    1.00e-06    0.0 0000000
4200200 003 1.60e+06    473.15

*   giunzione 1 uscita lower plenum hx
4300000 jun1olp valve
4300101 420010000   500000000   0.000153939 0.4003  0.994   00000100
4300110 0.014   0.0 1.0 1.0
4300201 1   0.0 0.0 0.0
4300300 srvvlv
4300301 201

*   giunzione 2 uscita lower plenum hx
4310000 jun2olp valve
4310101 420010000   505000000   0.000153939 0.4003  0.994   00000100
```

```
4310110 0.014   0.0 1.0 1.0
4310201 1   0.0 0.0 0.0
4310300 trpvlv
4310301 411

*   phx first tube active length
5000000 act1    pipe
5000001 10
5000101 0.000153939 10
5000301 0.214   10
5000401 0.0 10
5000601 90.0    10
5000801 1.00e-06    0.014   10
5000901 0.0 0.0 9
5001001 0000000 10
5001101 00000000    9
5001201 003 1.60e+06    473.15  0.0 0.0 0.0 1
5001202 003 1.60e+06    473.15  0.0 0.0 0.0 2
5001203 003 1.60e+06    473.15  0.0 0.0 0.0 3
5001204 003 1.60e+06    473.15  0.0 0.0 0.0 4
5001205 003 1.60e+06    473.15  0.0 0.0 0.0 5
5001206 003 1.60e+06    473.15  0.0 0.0 0.0 6
5001207 003 1.60e+06    473.15  0.0 0.0 0.0 7
5001208 003 1.60e+06    473.15  0.0 0.0 0.0 8
5001209 003 1.60e+06    473.15  0.0 0.0 0.0 9
5001210 003 1.60e+06    473.15  0.0 0.0 0.0 10
5001300 1
5001301 0.0 0.0 0.0 9
5001401 0.014   0.0 1.0 1.0 9

*   tube intermediate junction 1
5010000 intjun1 sngljun
5010101 500010000   502000000   0.0 0.0 0.0 00000000
5010201 1   0.0 0.0 0.0
5010110 0.014   0.0 1.0 1.0

*   phx first tube non-active length
5020000 noact1  pipe
5020001 99
5020101 0.000153939 99
5020301 0.088686869 99
5020401 0.0 99
5020601 90.0    99
5020801 1.00e-06    0.014   99
5020901 0.0 0.0 98
5021001 0000000 99
5021101 00000000    98
5021201 003 1.60e+06    473.15  0.0 0.0 0.0 1
5021202 003 1.60e+06    473.15  0.0 0.0 0.0 2
5021203 003 1.60e+06    473.15  0.0 0.0 0.0 3
5021204 003 1.60e+06    473.15  0.0 0.0 0.0 4
5021205 003 1.60e+06    473.15  0.0 0.0 0.0 5
5021206 003 1.60e+06    473.15  0.0 0.0 0.0 6
5021207 003 1.60e+06    473.15  0.0 0.0 0.0 7
5021208 003 1.60e+06    473.15  0.0 0.0 0.0 8
5021209 003 1.60e+06    473.15  0.0 0.0 0.0 9
5021210 003 1.60e+06    473.15  0.0 0.0 0.0 10
5021211 003 1.60e+06    473.15  0.0 0.0 0.0 99
5021300 1
5021301 0.0 0.0 0.0 98
5021401 0.014   0.0 1.0 1.0 98
```

```
*   phx second tube active length
5050000 act2    pipe
5050001 10
5050101 0.000153939 10
5050301 0.214   10
5050401 0.0 10
5050601 90.0    10
5050801 1.00e-06    0.014   10
5050901 0.0 0.0 9
5051001 0000000 10
5051101 00000000    9
5051201 003 1.60e+06    473.15  0.0 0.0 0.0 1
5051202 003 1.60e+06    473.15  0.0 0.0 0.0 2
5051203 003 1.60e+06    473.15  0.0 0.0 0.0 3
5051204 003 1.60e+06    473.15  0.0 0.0 0.0 4
5051205 003 1.60e+06    473.15  0.0 0.0 0.0 5
5051206 003 1.60e+06    473.15  0.0 0.0 0.0 6
5051207 003 1.60e+06    473.15  0.0 0.0 0.0 7
5051208 003 1.60e+06    473.15  0.0 0.0 0.0 8
5051209 003 1.60e+06    473.15  0.0 0.0 0.0 9
5051210 003 1.60e+06    473.15  0.0 0.0 0.0 10
5051300 1
5051301 0.0 0.0 0.0 9
5051401 0.014   0.0 1.0 1.0 9

*   tube intermediate junction 2
5060000 intjun2 sngljun
5060101 505010000   507000000   0.0 0.0 0.0 00000000
5060201 1   0.0 0.0 0.0
5060110 0.014   0.0 1.0 1.0

*   phx second tube non-active length
5070000 noact2  pipe
5070001 99
5070101 0.000153939 99
5070301 0.088686869 99
5070401 0.0 99
5070601 90.0    99
5070801 1.00e-06    0.014   99
5070901 0.0 0.0 98
5071001 0000000 99
5071101 00000000    98
5071201 003 1.60e+06    473.15  0.0 0.0 0.0 1
5071202 003 1.60e+06    473.15  0.0 0.0 0.0 2
5071203 003 1.60e+06    473.15  0.0 0.0 0.0 3
5071204 003 1.60e+06    473.15  0.0 0.0 0.0 4
5071205 003 1.60e+06    473.15  0.0 0.0 0.0 5
5071206 003 1.60e+06    473.15  0.0 0.0 0.0 6
5071207 003 1.60e+06    473.15  0.0 0.0 0.0 7
5071208 003 1.60e+06    473.15  0.0 0.0 0.0 8
5071209 003 1.60e+06    473.15  0.0 0.0 0.0 9
5071210 003 1.60e+06    473.15  0.0 0.0 0.0 10
5071211 003 1.60e+06    473.15  0.0 0.0 0.0 99
5071300 1
5071301 0.0 0.0 0.0 98
5071401 0.014   0.0 1.0 1.0 98

*   uscita scambiatore 1
5100000 phxout1 sngljun
5100101 502010000   520000000   0.0 0.994   0.4999  00000000
```

```
5100110 0.014   0.0 1.0 1.0
5100201 1   0.0 0.0 0.0

*   uscita scambiatore 1
5110000 phxout1 sngljun
5110101 507010000   520000000   0.0 0.994   0.4999  00000000
5110110 0.014   0.0 1.0 1.0
5110201 1   0.0 0.0 0.0

*   upper plenum
5200000 upplen  snglvol
5200101 0.000307877 0.10    0.0 0.0 90.0    0.10    1.00e-06    0.0 0000000
5200200 002 1.60e+06    0.30

*   giunzione uscita scambiatore
5300000 phxexit sngljun
5300101 520010000   550000000   0.000307877 0.5 1.0 00000000
5300110 0.0 0.0 1.0 1.0
5300201 1   0.0 0.0 0.0

*   phx outlet tdv
5500000 phxoutdv    tmdpvol
5500101 0.000307877 0.10    0.0 0.0 0.0 0.0 0.0 0.0 0000010
5500200 002 0   quale   520010000
5500201 0.0 1.5076e+06  0.0
5500202 0.0 1.5076e+06  0.3

*   heat structures

*   primary heat exchanger single tube
15001000    10  5   2   1   7.00e-03
15001100    0   2
15001101    1.00e-05    1   5.00e-04    3   4.00e-05    4
15001201    1   1
15001202    2   3
15001203    1   4
15001301    0.0 4
15001400    0
15001401    583.16  5
15001501    500100000   -10000  101 1   0.214   10
15001601    300010000   10000   111 1   0.214   10
15001701    0   0.0 0.0 0.0 10
15001800    0
15001801    0.0 100.0   100.0   0.0 0.0 0.0 0.0 1.0 10
15001900    1
15001901     0.04179 100.0    100.0    0.0 0.0 0.0 0.0 1.0 2.10     1.1 2.16
10

*   primary heat exchanger rest of bundle
15011000    10  5   2   1   7.00e-03
15011100    0   2
15011101    1.00e-05    1   5.00e-04    3   4.00e-05    4
15011201    1   1
15011202    2   3
15011203    1   4
15011301    0.0 4
15011400    0
15011401    583.16  5
15011501    505100000   -10000  101 1   0.214   10
15011601    300010000   10000   111 1   0.214   10
15011701    0   0.0 0.0 0.0 10
```

```
15011800    0
15011801    0.0 100.0   100.0   0.0 0.0 0.0 0.0 1.0 10
15011900    1
15011901     0.04179 100.0    100.0    0.0 0.0 0.0 0.0 1.0 2.10     1.1 2.16
10

*   control variables

*   tube bundle inlet pressure drop
20500500    tbinpd  sum 1.0 0.0 1
20500501    0.0 1.0 p   420010000
20500502    -1.0    p   500010000
20500503    0.05    rho 420010000
20500504    0.0428  rho 500010000

*   tube bundle active pressure drop
20500600    tbacpd  sum 1.0 0.0 1
20500601    0.0 1.0 p   500010000
20500602    -1.0    p   500100000
20500603    0.0428  rho 500010000
20500604    0.0428  rho 500100000

*   tube bundle non active pressure drop
20500700    tbnacpd sum 1.0 0.0 1
20500701    0.0 1.0 p   502010000
20500702    -1.0    p   502990000
20500703    0.044343434 rho 502010000
20500704    0.044343434 rho 502990000

*   tube bundle outlet pressure drop
20500800    tboutpd sum 1.0 0.0 1
20500801    0.0 1.0 p   502990000
20500802    -1.0    p   520010000
20500803    -0.044343434    rho 502990000
20500804    -0.05   rho 520010000

*   phx primary mass flow rate
20501500    flowpri sum 1.0 0.0 1
20501501    0.0 1.0 mflowj  300050000

*   phx secondary mass flow rate 1
20501600    flowsec1    sum 1.0 0.0 1
20501601    0.0 1.0 mflowj  500050000

*   phx secondary mass flow rate 2
20501700    flowsec2    sum 1.0 0.0 1
20501701    0.0 1.0 mflowj  505050000

*   phx primary temperature difference
20503200    dtprim  sum 1.0 0.0 1
20503201    0.0 1.0 tempf   260010000
20503202    -1.0    tempf   350010000

*   phx secondary temperature difference 1
20503300    dtsec1  sum 1.0 0.0 1
20503301    0.0 1.0 tempf   502010000
20503302    -1.0    tempf   420010000

*   phx secondary temperature difference 2
20503300    dtsec2  sum 1.0 0.0 1
20503301    0.0 1.0 tempf   507010000
```

```
20503302    -1.0    tempf   420010000

*   phx 1 logarhythmic average temperature difference - part 1
20503500    dtlmp1  sum 1.0 0.0 1
20503501    0.0 1.0 tempf   260010000
20503502    -1.0    tempf   502010000

*   phx 1 logarhythmic average temperature difference - part 2
20503600    dtlmp2  sum 1.0 0.0 1
20503601    0.0 1.0 tempf   350010000
20503602    -1.0    tempf   420010000

*   phx 1 logarhythmic average temperature difference - part 3
20503700    dtlmp3  sum 1.0 0.0 1
20503701    0.0 1.0 cntrlvar    35
20503702    -1.0    cntrlvar    36

*   phx 1 logarhythmic average temperature difference - part 4
20503800    dtlmp4  div 1.0 0.0 0
20503801    cntrlvar    36  cntrlvar    35

*   phx 1 logarhythmic average temperature difference - part 5
20503900    dtlmp5  stdfnctn    1.0 0.0 1
20503901    abs cntrlvar    38

*   phx 1 logarhythmic average temperature difference - part 6
20504000    dtlmp6  stdfnctn    1.0 0.0 1
20504001    log cntrlvar    39

*   phx 1 logarhythmic average temperature difference - part 7
20504100    dtlmp7  div 1.0 0.0 0
20504101    cntrlvar    40  cntrlvar    37

*   phx inlet temperature
20504200    phxintem    sum 1.0 0.0 1
20504201    -273.15 1.0 tempf   260010000

*   phx outlet temperature
20504300    phxoutem    sum 1.0 0.0 1
20504301    -273.15 1.0 tempf   350010000

*   phx 1 power 1
20508000    primpow1    sum -1.0    0.0 1
20508001    0.0 1.0 q   300010000
20508002    1.0 q   300020000
20508003    1.0 q   300030000
20508004    1.0 q   300040000
20508005    1.0 q   300050000
20508006    1.0 q   300060000
20508007    1.0 q   300070000
20508008    1.0 q   300080000
20508009    1.0 q   300090000
20508010    1.0 q   300100000

*   phx 1 power total
20508300    primpow sum 1.0 0.0 1
20508301    0.0 1.0 cntrlvar    80

*   phx 1 power to secondary system 1
20509000    sec1pow1    sum 1.0 0.0 1
20509001    0.0 1.0 q   500010000
```

```
20509002    1.0 q   500020000
20509003    1.0 q   500030000
20509004    1.0 q   500040000
20509005    1.0 q   500050000
20509006    1.0 q   500060000
20509007    1.0 q   500070000
20509008    1.0 q   500080000
20509009    1.0 q   500090000
20509010    1.0 q   500100000

*   phx 1 power to secondary system total
20509300    sec1pow sum 1.0 0.0 1
20509301    0.0 1.0 cntrlvar    90

*   phx 2 power to secondary system 1
20509500    sec2pow1    sum 1.0 0.0 1
20509501    0.0 1.0 q   505010000
20509502    1.0 q   505020000
20509503    1.0 q   505030000
20509504    1.0 q   505040000
20509505    1.0 q   505050000
20509506    1.0 q   505060000
20509507    1.0 q   505070000
20509508    1.0 q   505080000
20509509    1.0 q   505090000
20509510    1.0 q   505100000

*   phx 2 power to secondary system total
20509800    sec2pow sum 1.0 0.0 1
20509801    0.0 1.0 cntrlvar    95

*   total power to water
20509900    waterpow    sum 1.0 0.0 1
20509901    0.0 1.0 cntrlvar    93
20509902    1.0 cntrlvar    98

*   phase change number 1 - power to mass flow rate ratio
20510100    npch1   div 1.0 0.0001  0
20510101    mflowj  430000000   cntrlvar    93

*   phase change number 2 - latent enthalpy
20510200    npch2   sum 1.0 0.0 1
20510201    0.0 1.0 sathg   400010000
20510202    -1.0    sathf   400010000

*   phase change number 3 - power / (mass flow rate * dhfg)
20510300    npch3   div 1.0 0.0 1
20510301    cntrlvar    102 cntrlvar    101

*   phase change number 4 - vapor specific volume
20510400    npch4   powerr  1.0 0.0 1
20510401    rhog    400010000   -1.0

*   phase change number 5 - liquid specific volume
20510500    npch5   powerr  1.0 0.0 1
20510501    rhof    400010000   -1.0

*   phase change number 6 - differential specific volume
20510600    npch6   sum 1.0 0.0 1
20510601    0.0 1.0 cntrlvar    104
20510602    -1.0    cntrlvar    105
```

```
*   phase change number 7 - final npch value
20510700    npch7   mult    1.0 0.0 1
20510701    cntrlvar    103
20510702    cntrlvar    106
20510703    rhof    400010000

*   subcooling number 1 - subcooling enthalpy
20512100    nsub1   sum 1.0 0.0 1
20512101    0.0 1.0 sathf   400010000
20512102    -1.0    hvmix   400010000

*   subcooling number 2 - subcooling enthalpy / latent enthalpy
20512200    nsub2   div 1.0 0.0 1
20512201    cntrlvar    102 cntrlvar    121

*   subcooling number 3 - final nsub value
20512300    nsub3   mult    1.0 0.0 1
20512301    cntrlvar    122
20512302    cntrlvar    106
20512303    rhof    400010000

*   servo valve control
20520100    vlvcntl1    function    1.0 1.0 0
20520101    time    0   555

*   general tables

20255500    reac-t  451
20255501    -1.0    1.0
20255502    0.0 1.0
20255503    0.1 0.292893219
20255504    0.2 0.0
20255505    0.3 0.292893219
20255506    0.4 1.0

*   material tables

20100100    tbl/fctn    1   1       *   oxyde layer
20100200    tbl/fctn    1   1       *   aisi 316l

*   oxide layer conductivity
20100101    3.0 1000000.00
20100102    5000.0  1000000.00

*   oxide layer heat capacity
20100151    3.0 1.00e+00
20100152    300.0   1.00e+00
20100153    350.0   1.00e+00
20100154    400.0   1.00e+00
20100155    450.0   1.00e+00
20100156    500.0   1.00e+00
20100157    550.0   1.00e+00
20100158    600.0   1.00e+00
20100159    650.0   1.00e+00
20100160    700.0   1.00e+00
20100161    750.0   1.00e+00
20100162    800.0   1.00e+00
20100163    850.0   1.00e+00
20100164    900.0   1.00e+00
20100165    950.0   1.00e+00
```

```
20100166    1000.0  1.00e+00
20100167    5000.0  1.00e+00

*   aisi 316l conductivity
20100201    3.00    1000000.00
20100202    293.16  1000000.00
20100203    323.16  1000000.00
20100204    373.16  1000000.00
20100205    423.16  1000000.00
20100206    473.16  1000000.00
20100207    523.16  1000000.00
20100208    573.16  1000000.00
20100209    623.16  1000000.00
20100210    673.16  1000000.00
20100211    723.16  1000000.00
20100212    773.16  1000000.00
20100213    823.16  1000000.00
20100214    873.16  1000000.00
20100215    923.16  1000000.00
20100216    973.16  1000000.00
20100217    1023.16 1000000.00
20100218    1073.16 1000000.00
20100219    5000.00 1000000.00

*   aisi 316l heat capacity
20100251    3.00    1.00e+00
20100252    293.16  1.00e+00
20100253    323.16  1.00e+00
20100254    373.16  1.00e+00
20100255    423.16  1.00e+00
20100256    473.16  1.00e+00
20100257    523.16  1.00e+00
20100258    573.16  1.00e+00
20100259    623.16  1.00e+00
20100260    673.16  1.00e+00
20100261    723.16  1.00e+00
20100262    773.16  1.00e+00
20100263    823.16  1.00e+00
20100264    873.16  1.00e+00
20100265    923.16  1.00e+00
20100266    973.16  1.00e+00
20100267    1023.16 1.00e+00
20100268    1073.16 1.00e+00
20100269    5000.00 1.00e+00

20800001    systms  1
20800002    systms  2
20800003    hvmix   -1
20800004    sathf   -1
20800005    sathg   -1
.
```

References

[A1.1] D. Castelliti, T. Hamidouche, G. Bandini and E. Bubelis, "FP7-MAXSIMA Deliverable 2.4: Transient Analysis Final Report," SCK•CEN, Mol, May 2017.

Appendix 2: SIMMER-III code [A2.1]

SIMMER-III is a two-dimensional (2D), multi-velocity-field, multi-phase, multi-component, Eulerian, fluid-dynamics code system with an integrated structure model including fuel-pins, hexcans and general structures, together with a space-, time- and energy-dependent transport theory neutron dynamics model. The overall fluid-dynamics solution algorithm is based on a time-factorization approach, in which intra-cell interfacial area source terms, heat and mass transfers, and the momentum exchange functions are determined separately from inter-cell fluid convection. In addition, an elaborate analytical equation-of-state (EOS) model is available to close and complete the fluid-dynamics conservation equations. The structure model represents the configuration and the time-dependent disintegration of fuel pins and subassembly can walls. In neutronics, the transient neutron flux distribution is calculated with the improved quasi-static method. For the space-dependent part, a TWODANT or THREEDANT based flux shape calculation scheme (transport theory) has been implemented. The equations of this integrated code are solved on three geometrical mesh levels (fluid dynamics, pin, neutronics) with three time-step hierarchies (neutronic flux shape, reactivity + heat transfer, nuclear power + fluid dynamics).

SIMMER-III are developed by JAEA in cooperation with KIT, CEA, IRSN, SCK.CEN, ENEA, Pisa Univ., Kyushu Univ., JRC and RSE.

The code has originally been allocated in the severe accident domain of fast sodium cooled reactors. However, the philosophy behind the SIMMER development was to generate a versatile and flexible tool, applicable for the safety analysis of various reactor types with different neutron spectra and coolants. Its flexibility also allows the application to non-reactor safety problems as e.g. criticality accidents (JCO) or simulating the interaction between lithium-lead and water in a fusion reactor blanket (BLAST, LIFUS).

Main application areas of SIMMER in Europe have been accelerator driven systems (ADS) loaded with fertile-free fuels and high Minor Actinide content. Recently again sodium cooled reactors have been moved in the center of interest. Other areas of application were Molten Salt Reactors, gas cooled reactors and water cooled reactors.

As can be seen from the application range, various coolant options were under investigation. In the past two large verification and validation efforts have been performed for SIMMER. The first effort, the Phase-I Assessment - SIMMER validation was mainly based on analyzing basic physical problems and single phenomena problems. This is in some respect unique for an accident codes, as usually reactor frameworks/structures and reactor phenomena are already hard-wired in the code. This first principle assessment guarantees a basic validation of the code. In the Phase-II assessment complex experiments (out-of pile and in-pile) and multi-phenomena problems have been analyzed. In these studies mostly sodium and water were used as coolants. After these two assessment efforts additional work on SIMMER validation has been performed in the different laboratories and institutions depending mostly on the application area. In addition some validation efforts have also performed more internationally as e.g. in IAEA CRPs. The various areas of application drive the code development on the short and intermediate time-scales.

A key application area of SIMMER has been in the ADS development and safety and related to this in heavy liquid metal (HLM) problems. There has been no coherent validation effort as

in Phase-I and Phase-II, but a considerable work has been performed related to problems that came up during the analyses for the various ADS systems. Much work was performed within the 5th, 6th and 7th Framework Programs of the EU and valuable information can be found in the many deliverables provided in these programs.

The current deliverable tries to collect some validation work and highlights the application areas related to HLM flows. Naturally, the 'validation' picture is not such structured and complete as in the Phase-I and Phase-II assessment phases. The focus is on special areas directly related to the work in the individual institutions and programs. The deliverable is based on literature openly available.

Again to mention, especially Phase-I and parts of Phase-II official assessment can be used as a basis, as fundamental problems and problems related to fuel/coolant interaction have been analyzed, independent of the reactor coolant.

Based on the SIMMER applications, the following main areas, where validation work has been performed, can be identified :

- Multi-phase flow in HLM
- Interaction of HLMs with water
- General flow problems.

It is important to note that within the official assessment the problem definition and the results were intensively discussed with all participants and partly recalculated by other groups. In addition the input is given in the reports for further checking. By this a high level of validation could be reached and code 'user effects' could be minimized. For later validation efforts in the individual laboratories for individual needs this level of information (e.g. the input data sets) are not available.

Under sodium cooled fast reactor accident conditions high density fuel or steel multi-phase flow conditions need to be simulated. In heavy liquid metal coolants similar flow conditions under gas or steam ingress into the flow may occur. In addition the reaction between Pb or LBE with water may produce two-phase flow conditions. This demonstrates the necessity for an adequate description of multi-phase flow processes for HLM conditions. Because of the high boiling point of HLMs, mostly single-phase situations in transient/accident conditions of an ADS are to be expected. However, it was realized that the multi-phase capability of SIMMER-III is required for simulating potential accident scenarios with gas release from breaching pins leading to coolant voiding. In most of the applications and verification tests of the SIMMER code sodium and water were used as coolants. Consequently, available models and correlations had to be checked if they are adequate for (HLM) flows. Some of the HLM flow characteristics are similar to the ones of lighter liquid metal flows: low Prandtl number, large surface tensions, and low dynamic viscosities. Furthermore, the shape regime maps for fluid particles as a function of the Eötvös, Morton, and Reynolds numbers can be used in order to determine the fluid particle shape. The specificity of HLMs in comparison with lighter metals is that Archimedes' force is larger and that therefore high Eötvös numbers are more easily obtained. As far as head loss coefficients in pipes are concerned, they have been extensively and successfully tested with such a wide range of materials that reasonable results can be expected with HLM. Closure laws for momentum exchange functions were

chosen as general as possible with regard to materials (Blasius law, drag coefficients etc.) and the original engineering correlations were not tuned to a specific experiment.

A2.1 SIMMER-III Input Deck for the PHXTR event evaluation

A sample SIMMER-III input deck used for the analysis of the Primary Heat Exchanger tube rupture event is shown hereafter.

```
START : FASTEF Light model  FOR S-III VER 3.E

 &XCNTL

  ALGOPT(24) =0,
  ALGOPT(25) =0,
  ALGOPT(59) =1,

  EDTOPT(15) =1,
  EDTOPT(20) =2,

  EOSOPT(41) = 1,
  EOSOPT(42) = 1,

  ERROPT(2) = 1,
 /
  ALGOPT(49) =1,

 &XMSH
  IB = 25, JB = 51, IGEOM = 0,
  DRINP(1) = 0.473926077, 0.183126552, 0.224762674, 0.015295098,
             0.05426481, 0.0266138, 0.392595193, 0.392595193,
             0.392595193, 0.392595193, 0.382522474, 0.013304811,
             0.382522474, 0.041467135, 0.411694771, 0.411694771,
             0.013305622, 0.011027285, 0.011027285, 0.011027285,
             0.031285705, 0.000709572, 0.00012053, 0.339960248,
             0.339960248,

  DZINP(1) = 5*6.85600E-01, 10*2.00000E-01, 6.50000E-02, 6.00000E-02,
             2*1.75000E-01,
             9.00000E-02,
             9.00000E-02,
             2*1.22500E-01, 3.00000E-02, 5*1.57000E-01,
             9.00000E-02,
             9.00000E-02,
             5*3.25000E-01,  2*3.27000E-01,  8*2.80750E-01,  1.00000E-01,  4*5.00000E-
01,
  ICL = 1, ICR = 25, JCB = 1, JCT = 51,
 /

 &XTME
  TCPU   = 3600000000.0, TWFIN  = 150.0,
  DTSTRT = 1.0E-5,       DTMAX  = 1.0E-2, DTMIN  = 1.0E-7,
  DTHINI = 1.0E-5,       DTHMAX = 1.0E-1, DTHMIN = 1.0E-5,
  NDT0   = 10,       IDTH   = 10,
 /

 <<<<< IRMAP >>>>>
 &XRGN
  LRGN = 0,
  IRMAP(1,1) =    19, 19, 19, 19, 19, 19, 19, 19, 19, 19, 19, 19, 19, 19, 19, 19,
19, 19, 19, 19, 19, 19, 19, 19, 19,
  IRMAP(1,2) =    19, 19, 19, 19, 19, 19, 19, 19, 19, 19, 19, 19, 19, 19, 19, 19,
19, 19, 19, 19, 19, 19, 19, 19, 19,
  IRMAP(1,3) =    19, 19, 19, 19, 19, 19, 19, 19, 19, 19, 19, 19, 19, 19, 19, 19,
19, 19, 19, 19, 19, 19, 19, 19, 19,
  IRMAP(1,4) =    19, 19, 19, 19, 19, 19, 19, 19, 19, 19, 19, 19, 19, 19, 19, 19,
19, 19, 19, 19, 19, 19, 19, 19, 19,
  IRMAP(1,5) =    19, 19, 19, 19, 19, 19, 19, 19, 19, 19, 19, 19, 19, 19, 19, 19,
19, 19, 19, 19, 19, 19, 19, 19, 19,
```

```
  IRMAP(1,6) =   19, 18, 19, 18, 19, 18, 19, 19, 19, 19, 19, 19, 19, 19, 19, 19,
19, 19, 19, 19, 19, 19, 19, 19, 19,
  IRMAP(1,7) =   19, 18, 19, 18, 19, 18, 19, 19, 19, 19, 19, 19, 19, 19, 19, 19,
19, 19, 19, 19, 19, 19, 19, 19, 19,
  IRMAP(1,8) =   19, 18, 19, 18, 19, 18, 19, 19, 19, 19, 19, 19, 19, 19, 19, 19,
19, 19, 19, 19, 19, 19, 19, 19, 19,
  IRMAP(1,9) =   19, 18, 19, 18, 19, 18, 19, 19, 19, 19, 19, 19, 19, 19, 19, 19,
19, 19, 19, 19, 19, 19, 19, 19, 19,
  IRMAP(1,10) =  19, 18, 19, 18, 19, 18, 19, 19, 19, 19, 19, 19, 19, 19, 19, 19,
19, 19, 19, 19, 19, 19, 19, 19, 19,
  IRMAP(1,11) =  19, 18, 19, 18, 19, 18, 19, 19, 19, 19, 19, 19, 19, 19, 19, 19,
19, 19, 19, 19, 19, 19, 19, 19, 19,
  IRMAP(1,12) =  19, 18, 19, 18, 19, 18, 19, 19, 19, 19, 19, 19, 19, 19, 19, 19,
19, 19, 19, 19, 19, 19, 19, 19, 19,
  IRMAP(1,13) =  19, 18, 19, 18, 19, 18, 19, 19, 19, 19, 19, 19, 19, 19, 19, 19,
19, 19, 19, 19, 19, 19, 19, 19, 19,
  IRMAP(1,14) =  19, 18, 19, 18, 19, 18, 19, 19, 19, 19, 19, 19, 19, 19, 19, 19,
19, 19, 19, 19, 19, 19, 19, 19, 19,
  IRMAP(1,15) =  19, 18, 19, 18, 19, 18, 19, 19, 19, 19, 19, 19, 19, 19, 19, 19,
19, 19, 19, 19, 19, 19, 19, 19, 19,
  IRMAP(1,16) =  19, 19, 19, 19, 19, 18, 19, 19, 19, 19, 19, 19, 19, 19, 19, 19,
19, 19, 19, 19, 19, 19, 19, 19, 19,
  IRMAP(1,17) =  19, 19, 19, 19, 19, 18, 18, 18, 18, 18, 18, 18, 18, 19, 18, 18,
18, 18, 18, 18, 18, 18, 18, 19, 19,
  IRMAP(1,18) =  19, 19, 19, 19, 19, 19, 19, 19, 19, 19, 19, 19, 19, 19, 19, 19,
19, 99, 99, 99, 99, 99, 18, 19, 19,
  IRMAP(1,19) =  19, 19, 19, 19, 19, 19, 19, 19, 19, 19, 19, 18, 19, 19, 19, 19,
19, 99, 99, 99, 99, 99, 18, 19, 19,
  IRMAP(1,20) =  19, 19, 19, 19, 19, 19, 19, 19, 19, 19, 19, 18, 19, 19, 19, 19,
19, 19, 19, 19, 99, 99, 18, 19, 19,
  IRMAP(1,21) =  19, 19, 19, 19, 19, 19, 19, 19, 19, 19, 19, 18, 19, 19, 19, 19,
19, 19, 19, 19, 99, 99, 18, 19, 19,
  IRMAP(1,22) =  19, 19, 19, 19, 19, 19, 19, 19, 19, 19, 19, 18, 19, 19, 19, 19,
18, 19, 19, 19, 99, 99, 18, 19, 19,
  IRMAP(1,23) =  19, 19, 19, 19, 19, 19, 19, 19, 19, 19, 19, 18, 19, 19, 19, 19,
18, 19, 19, 19, 99, 99, 18, 19, 19,
  IRMAP(1,24) =  19, 19, 19, 19, 19, 19, 19, 19, 19, 19, 19, 18, 18, 18, 18, 18,
18, 19, 19, 19, 99, 99, 18, 19, 19,
  IRMAP(1,25) =  19, 19, 19, 19, 19, 19, 19, 19, 19, 19, 19, 19, 19, 19, 19, 19,
18, 19, 19, 19, 99, 99, 18, 19, 19,
  IRMAP(1,26) =  19, 19, 19, 19, 19, 19, 19, 19, 19, 19, 19, 19, 19, 19, 19, 19,
18, 19, 19, 19, 99, 99, 18, 19, 19,
  IRMAP(1,27) =  19, 19, 19, 19, 19, 19, 19, 19, 19, 19, 19, 19, 19, 19, 19, 19,
18, 19, 19, 19, 99, 99, 18, 19, 19,
  IRMAP(1,28) =  19, 19, 19, 19, 19, 19, 19, 19, 19, 19, 19, 19, 19, 19, 19, 19,
18, 19, 19, 19, 99, 99, 18, 19, 19,
  IRMAP(1,29) =  19, 19, 19, 19, 19, 19, 19, 19, 19, 19, 19, 19, 19, 19, 19, 19,
18, 19, 19, 19, 99, 99, 18, 19, 19,
  IRMAP(1,30) =  19, 19, 19, 19, 19, 19, 19, 19, 19, 19, 19, 19, 19, 19, 19, 19,
19, 19, 19, 19, 99, 99, 18, 19, 19,
  IRMAP(1,31) =  19, 19, 19, 19, 19, 19, 19, 19, 19, 19, 19, 19, 19, 19, 19, 19,
19, 19, 19, 19, 99, 99, 18, 19, 19,
  IRMAP(1,32) =  19, 19, 19, 19, 19, 19, 19, 19, 19, 19, 19, 19, 19, 19, 19, 19,
19, 99, 99, 99, 99, 99, 18, 19, 19,
  IRMAP(1,33) =  19, 19, 19, 19, 19, 19, 19, 19, 19, 19, 19, 19, 19, 19, 19, 19,
19, 99, 99, 99, 99, 99, 18, 19, 19,
  IRMAP(1,34) =  19, 19, 19, 19, 19, 19, 19, 19, 19, 19, 19, 19, 19, 19, 19, 19,
19, 99, 99, 99, 99, 99, 18, 19, 19,
  IRMAP(1,35) =  19, 19, 19, 19, 19, 19, 19, 19, 19, 19, 19, 19, 19, 19, 19, 19,
19, 99, 99, 99, 99, 99, 18, 19, 19,
  IRMAP(1,36) =  19, 19, 19, 19, 19, 19, 19, 19, 19, 19, 19, 19, 19, 19, 19, 19,
19, 99, 99, 99, 99, 99, 18, 19, 19,
  IRMAP(1,37) =  19, 19, 19, 19, 19, 19, 19, 19, 19, 19, 19, 19, 19, 19, 19, 19,
19, 99, 99, 99, 99, 99, 18, 19, 19,
  IRMAP(1,38) =  19, 19, 19, 19, 19, 19, 19, 19, 19, 19, 19, 19, 19, 19, 19, 19,
19, 99, 99, 99, 99, 99, 18, 19, 19,
  IRMAP(1,39) =  20, 20, 20, 20, 20, 20, 20, 20, 20, 20, 20, 20, 20, 20, 20, 20,
20, 99, 99, 99, 99, 99, 18, 20, 20,
```

```
  IRMAP(1,40) =  20, 20, 20, 20, 20, 20, 20, 20, 20, 20, 20, 20, 20, 20, 20, 20,
20, 99, 99, 99, 99, 99, 18, 20, 20,
  IRMAP(1,41) =  20, 20, 20, 20, 20, 20, 20, 20, 20, 20, 20, 20, 20, 20, 20, 20,
20, 99, 99, 99, 99, 99, 18, 20, 20,
  IRMAP(1,42) =  20, 20, 20, 20, 20, 20, 20, 20, 20, 20, 20, 20, 20, 20, 20, 20,
20, 99, 99, 99, 99, 99, 18, 20, 20,
  IRMAP(1,43) =  20, 20, 20, 20, 20, 20, 20, 20, 20, 20, 20, 20, 20, 20, 20, 20,
20, 99, 99, 99, 99, 99, 18, 20, 20,
  IRMAP(1,44) =  20, 20, 20, 20, 20, 20, 20, 20, 20, 20, 20, 20, 20, 20, 20, 20,
20, 99, 99, 99, 99, 99, 18, 20, 20,
  IRMAP(1,45) =  20, 20, 20, 20, 20, 20, 20, 20, 20, 20, 20, 20, 20, 20, 20, 20,
20, 99, 99, 99, 99, 99, 18, 20, 20,
  IRMAP(1,46) =  20, 20, 20, 20, 20, 20, 20, 20, 20, 20, 20, 20, 20, 20, 20, 20,
20, 99, 99, 99, 99, 99, 18, 20, 20,
  IRMAP(1,47) =  20, 20, 20, 20, 20, 20, 20, 20, 20, 20, 20, 20, 20, 20, 20, 20,
20, 20, 20, 20, 20, 20, 20, 20, 20,
  IRMAP(1,48) =  21, 22, 22, 22, 22, 22, 22, 22, 22, 22, 22, 22, 22, 22, 22, 22,
22, 22, 22, 22, 22, 22, 22, 22, 22,
  IRMAP(1,49) =  21, 22, 22, 22, 22, 22, 22, 22, 22, 22, 22, 22, 22, 22, 22, 22,
22, 22, 22, 22, 22, 22, 22, 22, 22,
  IRMAP(1,50) =  21, 22, 22, 22, 22, 22, 22, 22, 22, 22, 22, 22, 22, 22, 22, 22,
22, 22, 22, 22, 22, 22, 22, 22, 22,
  IRMAP(1,51) =  21, 22, 22, 22, 22, 22, 22, 22, 22, 22, 22, 22, 22, 22, 22, 22,
22, 22, 22, 22, 22, 22, 22, 22, 22,
 /
 &XRGN
  LRGN = 18,
  RGNAMB = 'T91 WALL',
  TGINB     = 5.43000E+02, PSFINB    = 5.00000E+05,
  NST1B  = 1,
 /
 &XRGN
  LRGN = 19,
  RGNAMB = 'LBE',
  ALMINB(3) = 1.00000E+00, TLMINB(3) = 5.43000E+02,
  TGINB     = 5.43000E+02, PSFINB    = 1.00000E+06,
 /
 &XRGN
  LRGN = 20,
  RGNAMB = 'AR GAS',
  TGINB     = 5.23000E+02, PSFINB    = 1.20000E+05,
 /
  ALMINB(3) = 0.00000E+00, TLMINB(3) = 5.23000E+02,
 &XRGN
  LRGN = 21,
  RGNAMB = 'Ar gas: safety valve',
  TGINB     = 5.23000E+02, PSFINB    = 6.00000E+05,
 /
 &XRGN
  LRGN = 22,
  RGNAMB = 'UPPER STRUCTURE',
  TGINB     = 2.93000E+02, PSFINB    = 1.00000E+05,
  NST1B  = 1,
 /
 &XEDT
  PRTC = 999999, PPFC = 999999, DMPC = 999999,  BSFC = 999999,
  DTDMP(1) = 1.0E-02,      TCDMP(1) = 2.0E+02,
  DTBSF(1) = 2.0E-02,      TCBSF(1) = 2.0E+02,
  SN(1)  = 'ALPSK1', 'ALPSK2', 'ALPSK3', 'ALPSK4', 'ALPSK5', 'ALPSK6',
           'ALPSK7', 'ALPSK8', 'ALPSK9',
           'ALPLK1', 'ALPLK2', 'ALPLK3', 'ALPLK4', 'ALPLK5', 'ALPLK6',
           'ALPGK',  'PK',
           'RBSK1',  'RBSK2',  'RBSK3',  'RBSK4',  'RBSK5',  'RBSK6',
           'RBSK7',  'RBSK8',  'RBSK9',  'RBSK10', 'RBSK11', 'RBSK12',
           'RBLK1',  'RBLK2',  'RBLK3',  'RBLK4',  'RBLK5',  'RBLK6',
           'RBLK7',  'RBLK8',  'RBLK9',  'RBLK10',
           'RBGK1',  'RBGK2',  'RBGK3',  'RBGK4',  'RBGK5',
           'SIESK1', 'SIESK2', 'SIESK3', 'SIESK4', 'SIESK5', 'SIESK6',
```

```
           'SIESK7', 'SIESK8', 'SIESK9',
           'SIELK1', 'SIELK2', 'SIELK3', 'SIELK4', 'SIELK5', 'SIELK6',
           'SIEGK',
           'TSK1',   'TSK2',   'TSK3',   'TSK4',   'TSK5',   'TSK6',
           'TSK7',   'TSK8',   'TSK9',
           'TLK1',   'TLK2',   'TLK3',   'TLK4',   'TLK5',   'TLK6',
           'TGK',
           'VK1',    'VK2',    'VK3',    'UK1',    'UK2',    'UK3',
           'RBIK1',  'RBIK2',  'EIPINK', 'TIPINK', 'ALPINK',
           'ALPNFK1','ALPNFK2','ALPNFK3',
           'RPINK',  'DHK',
           'AQSTK1', 'AQSTK2', 'BQSTK1', 'BQSTK2',
           'QN1',    'QN2',    'QN3',    'QN4',    'QN5',
           'RGBK',
           'RLMBK1', 'RLMBK2', 'RLMBK3', 'RLMBK4', 'RLMBK5',
           'RLMDK1', 'RLMDK2', 'RLMDK3', 'RLMDK4', 'RLMDK5',
           'ALPGEK', 'ASMZ',
           'CPK',    'DPK',
           'IRGMK',
 /
 &XBND
  NBC = 0,

  LBCSET(1) = 27*0,
              1350*0,
              27*0,
              0, 1, 25*0,
  LVPSET(1) = 27*0,
              432*0,
              11*0, 3, 2*0, 1, 12*0,
              1215*0,
              27*0,
  LVPMP(1) = 3,
  VPMTME(1,1) = 0.0,  60.0,  200.0,
  VPMTAB(1,1) = -2.70e4, -2.70e4 ,-2.70e4,
  LVPMP(3) = 3,
  VPMTME(1,3) = 0.0,  60.0,  200.0,
  VPMTAB(1,3) = 0.0,  0.0,   0.0,
  LWASET(18,18) = 1010, LWASET(19,18) = 0010, LWASET(20,18) = 0010, LWASET(21,18) =
0010, LWASET(22,18) = 0110,
  LWASET(18,19) = 1001, LWASET(19,19) = 0001, LWASET(20,19) = 0001, LWASET(21,19) =
0000, LWASET(22,19) = 0100,

                                                                    LWASET(21,20)  =
1000, LWASET(22,20) = 1100,
                                                                    LWASET(21,21)  =
1000, LWASET(22,21) = 1100,
                                                                    LWASET(21,22)  =
1000, LWASET(22,22) = 1100,
                                                                    LWASET(21,23)  =
1000, LWASET(22,23) = 1100,
                                                                    LWASET(21,24)  =
1000, LWASET(22,24) = 1100,
                                                                    LWASET(21,25)  =
1000, LWASET(22,25) = 1100,
                                                                    LWASET(21,26)  =
1000, LWASET(22,26) = 1100,
                                                                    LWASET(21,27)  =
1000, LWASET(22,27) = 1100,
                                                                    LWASET(21,28)  =
1000, LWASET(22,28) = 1100,
                                                                    LWASET(21,29)  =
1000, LWASET(22,29) = 1100,
                                                                    LWASET(21,30)  =
1000, LWASET(22,30) = 1100,
                                                                    LWASET(21,31)  =
1000, LWASET(22,31) = 1100,
```

```
  LWASET(18,32) = 1010, LWASET(19,32) = 0010, LWASET(20,32) = 0010, LWASET(21,32) =
0000, LWASET(22,32) = 1100,
  LWASET(18,33) = 1000,                                             LWASET(21,33) =
0000, LWASET(22,33) = 1100,
  LWASET(18,34) = 1000,                                             LWASET(21,34) =
0000, LWASET(22,34) = 1100,
  LWASET(18,35) = 1000,                                             LWASET(21,35) =
0000, LWASET(22,35) = 1100,
  LWASET(18,36) = 1000,                                             LWASET(21,36) =
0000, LWASET(22,36) = 1100,
  LWASET(18,37) = 1000,                                             LWASET(21,37) =
0000, LWASET(22,37) = 1100,
  LWASET(18,38) = 1000,                                             LWASET(21,38) =
0000, LWASET(22,38) = 1100,
  LWASET(18,39) = 1000,                                             LWASET(21,39) =
0000, LWASET(22,39) = 1100,
  LWASET(18,40) = 1000,                                             LWASET(21,40) =
0000, LWASET(22,40) = 1100,
  LWASET(18,41) = 1000,                                             LWASET(21,41) =
0000, LWASET(22,41) = 1100,
  LWASET(18,42) = 1000,                                             LWASET(21,42) =
0000, LWASET(22,42) = 1100,
  LWASET(18,43) = 1000,                                             LWASET(21,43) =
0000, LWASET(22,43) = 1100,
  LWASET(18,44) = 1000,                                             LWASET(21,44) =
0000, LWASET(22,44) = 1100,
  LWASET(18,45) = 1000,                                             LWASET(21,45) =
0000, LWASET(22,45) = 1100,
  LWASET(18,46) = 1001, LWASET(19,46) = 0001, LWASET(20,46) = 0001, LWASET(21,46) =
0001, LWASET(22,46) = 1101,
  LWASET(1,48) =  0010,
  LWATME(1,21,26) = 0.0, 5.0 , 200.0,
  LWATME(1,1,48) =  0.0, 120.6 , 200.0,
 /
  LWATME(1,20,19) = 0.0, 1.0 , 90.0,
  VPMTAB(1,1) = -8.00e5, -8.00e5, -8.00e5
 &XBND
  NBC=1,LBCS=2,LBCP=3,
  PTAB(1) = 6.000E+05, 6.000E+05, 6.000E+05,
  PTME(1) = 0.0,         25.0,        200.0,
 /
 &XMXF
  CORFRN(20,26) = 7.0e9,   # Perdita di carico rottura
  CORFRN(11,18) = 5.0,     # Perdita di carico bypass
 /
  CORFRN(17,30) = 10.0     # Ingresso PHX (non usato)
  CORFRN(17,31) = 10.0     # Ingresso PHX (non usato)
 &XSOS
 /
 &XERG
  REGN = 1,
  REGC(1,1) = 1,
  REGC(2,1) = 1,
  REGC(3,1) = 25,
  REGC(4,1) = 51,
  MATEOS(1,1) = 8,
  MATEOS(3,1) = 4,
 /
```

References

[A2.1] W. Maschek, "SIMMER Assessment Work on HLM Flow Problems," KIT, March 2013.

Appendix 3: MATLAB software [A3.1]

MATLAB (matrix laboratory) is a multi-paradigm numerical computing environment. A proprietary programming language developed by MathWorks, MATLAB allows matrix manipulations, plotting of functions and data, implementation of algorithms, creation of user interfaces, and interfacing with programs written in other languages, including C, C++, C#, Java, Fortran and Python.

Although MATLAB is intended primarily for numerical computing, an optional toolbox uses the MuPAD symbolic engine, allowing access to symbolic computing abilities. An additional package, Simulink, adds graphical multi-domain simulation and model-based design for dynamic and embedded systems.

A3.1 MATLAB Script for the PHXTR event evaluation

A sample MATLAB script used for the analysis of the Primary Heat Exchanger tube rupture event is shown hereafter.

```
g = 9.81; % m/s^2 accelarazione gravitazionale
sigma = 5.670373*10^-8; % Stefan-Boltzmann constant
R_g = 8.314;    % J/(mol*K) perfect gas constant

% Variables: H_bub, v_bub, R_bub, p_bub, (rho_vap_bub, T_bub)

equation = zeros(4,1);

H_bub = sol(1);
v_bub = sol(2);
if sol(3) >= 0
    R_bub = sol(3);
else
    R_bub = 0;
end
p_bub = sol(4);

% Proprietà geometriche

H_PHX = 2.1;
H_freelevel = 1.6 + H_PHX;
d_bub = 2*R_bub;
A = (pi/4)*d_bub^2;   % Area sezione della bolla

% Fattori di emissività ed assorbimento per irraggiamento

eps = 0.21;
A_2 = 1;

% Proprietà termofisiche

if H_bub < H_PHX
    T_LBE = (270 + 55*(H_bub/H_PHX)) + 273.15;
else
    T_LBE = 325 + 273.15;
end
T_LBE_1 = T_LBE-273.15;

T_LBE_in_1 = 270;

T_drop = XSteam('Tsat_p',p_bub/10^5) + 273.15;
T_drop_1 = T_drop-273.15;
T_bub = (T_LBE+T_drop)/2;
T_bub_1 = T_bub-273.15;

rho_l = XSteam('rhoL_p',p_bub/10^5);
rho_s = p_bub/(R_g*T_bub);

k_l = XSteam('tcL_p',p_bub/10^5);     % Conducibilità del liquido
k_s = XSteam('tcV_p',p_bub/10^5);     % Conducibilità del vapore

sur_ten = XSteam('st_p',p_bub/10^5);

h_fg = 1000*(XSteam('hV_p',p_bub/10^5)-XSteam('hL_p',p_bub/10^5));    % Latent
enthalpy (J/kg)

% Condizioni al contorno

R_in = radius(caso);
p_in = rho_LBE(T_LBE_in_1)*g*(H_freelevel+1);
```

```
p_LBE = rho_LBE(T_LBE_1)*g*(H_freelevel+1-H_bub);

% Stima della massa e del volume della bolla

V_liq = (4/3)*pi*R_bub^3;
V_vap = (4/3)*pi*(R_in^3-R_bub^3)*(rho_l/rho_s);  % Volume della parte vapore
V_bub = V_liq + V_vap;

alpha = (V_vap/V_bub);

rho_m = (1-alpha)*rho_l + alpha*rho_s;

m_liq = V_liq*rho_l;
m_vap = V_vap*rho_s;
m_bub = (4/3)*pi*(R_in^3)*XSteam('rhoL_p',p_in/10^5);

% LBE velocity evaluation

m_LBE = -13800/4;
A_PHX = 0.357550943090361;
v_LBE = m_LBE/(rho_LBE(T_LBE_1)*A_PHX);

% Calcolo delle grandezze necessarie alla risoluzione del sistema

Re_bub = rho_LBE(T_LBE_1)*abs(v_bub-v_LBE)*d_bub/dyn_vis_LBE(T_LBE_1);

if Re_bub <= 10^3
    C_d = (24/Re_bub)*(1+0.15*(Re_bub^0.687));
else
    C_d = 0.44;
end

% Caratterizzazione delle bolle

% Equazioni risolutive

equation(1) = v_bub;
equation(2) = ((rho_LBE(T_LBE_1) - rho_m)*g*V_bub - C_d*rho_LBE(T_LBE_1)*((v_bub-
v_LBE)^2)*A/2)/m_bub;

equation(3) = (sigma.*(T_LBE^4-T_drop^4)*((1/A_2)+((1/eps)-
1)*(((rho_l/rho_s)+1)*((R_in^3)/(R_bub^3))-(rho_l/rho_s))^(-1/3))^(-1)...
    +0.255*sqrt((k_s*h_fg*(T_LBE-
T_drop))/(2*R_bub))*((R_bub*g*rho_l*rho_s)^(1/4)))/(-h_fg*rho_l);

equation(4) = ((p_bub-p_LBE-(2*sur_ten/R_bub)-
(4*dyn_vis_LBE(T_LBE_1)*equation(3)/R_bub))/rho_LBE(T_LBE_1)) -
(3/2)*(equation(3))^2;

time_period_2 = [0 :0.002:22];
H_0 = 0.0;
v_0 = 0.0000001;
R_in = radius(caso);
p_in = rho_LBE(T_LBE_in_1)*g*(H_freelevel+1);
[t_2,sol]=ode45(@Bubble_superfinal, time_period_2, [H_0; v_0; R_in; p_in]);
```

References

[A3.1] Wikipedia, "https://en.wikipedia.org/wiki/MATLAB," 2018. [Online].